4-13-2017

Characterizing Gross Lesions in Corals on Fringing Reefs of Taiwan and Hainan Island, China

Adrienne George
University of South Florida, adrienneg@mail.usf.edu

Characterizing Gross Lesions in Corals on Fringing Reefs of Taiwan and Hainan Island, China

by

Adrienne George

A dissertation submitted in partial fulfillment
of the requirements for the degree of
Doctor of Philosophy
College of Marine Science
University of South Florida

Major Professor: Pamela Hallock Muller, Ph.D.
Chaloun Allen Chen, Ph.D.
Esther C. Peters, Ph.D.
John Paul, Ph.D.
Kendra Daly, Ph.D.

Date of Approval:
April 13, 2017

Keywords: coral disease, DGGE, Biolog EcoPlate™, coral histology, South China Sea

Acknowledgments

The NSF EAPSI grants (2012 and 2013) provided funds for this research project and travel to international labs. Drs. Karyna Rosario and Maria Vega Rodriguez provided comments and critiques of the grant proposals which improved the proposals. Many thanks goes to Dr. Chaloun Allen Chen (Academia Sinica) and Dr. Kefu Yu (Chinese Academy of Sciences) for allowing me to spend months in their labs processing the data for this project.

I am most grateful to the Florida Education Fund McKnight Fellowship, Alfred P. Sloan Fellowship, and the CMS Bridge to the Doctorate Fellowship. I also am grateful for the initial financial support by the Florida-Georgia LSAMP Bridge to the Doctorate Fellowship funded by National Science Foundation Grant HRD #0929435, with special thanks to Shekhar Bhansali and Bernard Batson in the USF College of Engineering and Dr. Ashanti Johnson, formerly of CMS, for their efforts and leadership in providing this funding to students at USF.

I would like to thank my thesis and dissertation advisor, Dr. Pamela Hallock Muller for providing advice, feedback, constructive criticism, and overall mentorship throughout the years. Additionally, I would like to thank my dissertation committee members Drs. Chaloun Allen Chen, Esther C. Peters, John Paul and Kendra Daly for providing feedback and constructive criticism, which allowed me to complete this project. I am very grateful to Dr. Yoko Nozawa for allowing me to use his lab's histology equipment to process my samples. Stephane DePalmas provided great assistance with DGGE methodology and without him, I would have not been able to complete this project. I am deeply indebted to Dr. David Jones for his assistance in the statistical analyses for this project.

Table of Contents

List of Tables

List of Figures

Abstract

Visible lesions on coral colonies are potential indicators that environmental stressors are influencing a reef. To test this hypothesis, pairs of near-shore reefs on Taiwan were surveyed along an anthropogenically influenced gradient that included locations near the cities of Taipei and Taitung, and more remote reefs off Green Island. Two fringing reefs at Sanya, Hainan Island, a popular Chinese resort area, were also assessed. Field surveys were undertaken to detect, quantify and visually describe the occurrence of lesions at each site. Coral mucus samples were collected from both normal-appearing polyps and lesion-afflicted areas of colonies to assess carbon requirements of associated microbes. Tissue samples were also collected to identify bacterial communities inhabiting healthy tissue for comparison with those associated with lesions; denaturing gradient gel electrophoresis and 16S rRNA sequencing for bacterial identification were utilized in these analyses. In addition, tissue samples were collected in the vicinity of lesions and prepared for histological examination.

At sites in Taiwan, lesions were encountered twice as often at the sites near Taipei and Taitung than at Green Island. The fewest (15/72 sightings) lesions were encountered at the reefs near Sanya, primarily because there has been nearly an 80% loss of coral cover at Sanya in recent decades. Overall, tissue loss was the most common lesion recorded (52%), followed by pink discoloration (27%) and color loss (i.e., bleaching, 15%). *Porites* was the taxon most commonly observed with one or more lesions (45% of sightings). Microbes within mucus from lesioned areas utilized similar carbon sources as microbes from mucus from healthy polyps, but utilized those sources more than twice as often. Examples of carbon sources utilized by microbes in >50% of the

lesion samples were D-cellobiose, D-mannitol, N-acetyl-D-glucosamine, alpha-cyclodextrin, and glycogen. Bacterial assemblages on corals were significantly different between Taiwan and China, among sites, and between water samples and coral samples, but not between healthy samples and lesions. Bacterial sequences identified in tissue samples from lesions revealed the presence of well-known disease-related genera, such as *Clostridium* and *Vibrio*. Microbes specifically indicating anthropogenic sources, included *Bacillus* sp. (sewage sludge) and *Geobacillus thermolevorans* (irritable bowel syndrome). Histological examination of tissue samples, particularly those from lesions characterized as tissue loss, revealed fragmentation and detachment from the mesoglea of gastrodermis and epidermis, as well as brown granular material, and the presence of ciliates and small crustaceans.

Corals are susceptible to a variety of diseases. For reefs in the western Atlantic and Caribbean, occurrences of lesions and characterization of coral diseases have been relatively well documented. In contrast, many areas in the vast Indo-Pacific, including the reefs of Taiwan and China, have received much less attention. This study of lesions and associated microbiomes on nearshore reefs of Taiwan and Hainan Island supports previous research that has revealed higher incidences of coral lesions and disease in reefs near extensive human populations. The results also support the hypothesis that many of the microbes associated with coral lesions are part of the natural coral microbiome and that some microbes can become opportunistic when the host corals are stressed.

1. Introduction and Literature Review

1.1 Organization of the Dissertation

Chapter 1 of this dissertation provides background information and a literature review essential to understanding coral disease in the region of the South China Sea. There is a section in Chapter 1, section 1.5, which is a paper that has been submitted for publication that focuses on ciliates and their relation to coral disease. Chapter 2 focuses on the rationale, objectives, and hypotheses. Chapter 3 discusses the range of methods that were used to conduct this study. Chapter 4 presents the results of this study. The discussion of the results is in Chapter 5. References are presented in Chapter 6.

1.2 Background

Coral reefs are valued at more than $352,000 per hectare per year for the economic and environmental services they provide through shoreline protection, areas of natural beauty, recreation and tourism, and as sources of food, pharmaceuticals, and jobs (Costanza et al., 1997; de Groot et al., 2012). Corals have become increasingly plagued with diseases in both wild populations and captive settings (Sweet and Bythell, 2012; Miller and Richardson, 2015). Common signs include the loss of zooxanthellae, tissue sloughing, abnormal growths, and mortality (Richardson, 1998; Sutherland et al., 2004; Aeby et al. 2011).

For the purpose of this study, disease is defined as a condition of abnormal vital function involving any structure, part, or system of an organism (Mosby's Medical Dictionary, 2009). Apparently healthy is defined as being free of gross lesions. Gross lesions are defined as any

visible, macroscopic abnormality of tissue. This can include discoloration, tissue loss and growth anomalies.

Diseases can be caused by abiotic or biotic factors, or a combination of both. Parasites and pathogens, such as bacteria, fungi, protozoans, and viruses, are considered biotic diseases. Abiotic diseases result from stress due to changes in the physical environment and are non-infectious, but can result in increased susceptibility to biotic diseases (Snieszko, 1974; Vadas, 1979).

Although the coral holobiont is a complex system that harbors microbial communities in its skeleton, tissue, and mucus, one part of my study assessed coral health by focusing on the mucus layer. Ritchie and Smith (2004) postulated that the normal mucus microbial community protects the coral from invasive microbes, and when the normal community changes, this may allow for the development of disease. The resident microbial community, which is critical to the healthy functioning of the coral holobiont, aids in limiting the abundance of pathogenic microbes within coral mucus. Under stressful conditions the resident microbial community is replaced by pathogenic microbes, often *Vibrio,* and this allows for the development of disease (Mao-Jones et al., 2010). Aspects of the metabolic activity of the microbial assemblage of coral mucus can be analyzed using Biolog EcoPlate^{TM} (Gil-Agudelo et al., 2006a), which is a simple, relatively inexpensive technique that analyzes carbon metabolism of a microbial community (Gil-Agudelo et al., 2006a).

In addition to changes in the metabolic potential of microorganisms within the mucus layer, this study examined changes in the microbial community through a molecular fingerprinting method. Because many marine microbes are uncultivable, molecular techniques such as denaturing gradient gel electrophoresis (DGGE) are used to study complex microbial communities. DGGE,

coupled with sequencing, has been used in numerous studies to document microbial communities of healthy and diseased corals (e.g., Chiou et al., 2010; Croquer et al., 2013; Smith et al., 2015; Glasl et al., 2016).

Histological examination is another useful technique to analyze coral afflictions (Sweet and Bythell, 2012; Work and Meteyer, 2014). According to Yevich and Barszcz (1983), histopathology is an important tool in investigating diseases in marine organisms and is useful in correlating physicochemical and physiological changes with those changes seen at the population and community level. Therefore, histological examinations observed in coral tissue can be compared with changes at the biochemical and molecular level in associated microbial communities.

1.3 Mucus, Microbial Associations, and Environmental Stress

Corals have a powerful defense mechanism: mucus (e.g., Ritchie, 2006). Every coral produces insoluble, hydrated glycoproteins, which form a viscoelastic gel that is secreted from the epidermal mucus cells (Ducklow and Mitchell, 1979; Kushmaro and Kramarsky-Winter, 2004; Bythell and Wild, 2011). The purpose of mucus is to aid in heterotrophic feeding (Brown and Bythell, 2005), to provide a physical barrier to pathogens (Ducklow and Mitchell, 1979; Cooney et al., 2002), and to protect the corals from sedimentation (Stafford-Smith, 1993), and desiccation (Meikle et al., 1988). However, too much mucus can allow bacterial blooms within the mucus and kill the coral through oxygen depletion, accumulation of sulfide poisons at the coral surface below the mucus layer, or predation on weakened coral polyps (Ducklow and Mitchell, 1979). Sulfide poisoning, in particular, has been linked to black band disease, where sulfur-cycling bacteria

produce hydrogen sulfide levels and mycrocystins, which create a toxic environment and lead to coral tissue death (Richardson et al., 1997; Stanic et al., 2011). Corals including *Porites* have also been documented to produce the organic sulfur compound dimethylsulfoniopropionate under stress (Frade et al., 2016), and *Vibrio corallilyticus* has been reported to use coral-produced sulfur compounds as a cue to target stressed corals (Garren et al., 2014).

The mucus makes up a surface mucopolysaccharide layer that varies quantitatively and qualitatively with each coral species (Meikle et al., 1988). The thickness of the surface mucopolysaccharide layer can range from less than one millimeter in some scleractinians to as much as a few centimeters in some gorgonians. Zooxanthellae provide most of the fixed carbon that makes up the surface mucopolysaccharide layer (Patton et al., 1977).

Corals can also use the microbial community that inhabits the surface mucopolysaccharide layer as a food source (Sorokin, 1973; Ducklow and Mitchell, 1979). Coral mucus is able to sustain high bacterial growth, possibly through the degradation of the mucus constituents (Ducklow and Mitchell, 1979; Kooperman et al., 2007). The bacteria living in the mucus, the mucus itself, and the mucus degradation products may be used as nutrient sources by the coral (Ducklow and Mitchell, 1979; Kooperman et al., 2007). Kline et al. (2006) found that, when corals were exposed to elevated dissolved organic carbon levels, the microbial community experienced accelerated growth by an order of a magnitude. Furthermore, Nguyen-Kim et al. (2015) found coral mucus to be a highly favorable habitat for viruses on colonies of *Fungia repanda* and *Acropora formosa* and were more abundant than bacteria and *Symbiodinium*. Their results support the hypothesis that viruses might regulate the coral's bacterial community or surrounding pathogens (Bettarel et al., 2015). Correa et al. (2013) showed the first genomic evidence of *Symbiodinium*-infecting viruses in *Orbicella cavernosa*.

Several studies determined that the abundance and community composition of microbes living throughout the water column is significantly different from the community of microbes living in the coral mucus (Rohwer et al., 2002; Ritchie and Smith, 2004). In fact, the culturable bacteria within the surface mucopolysaccharide layer can be two orders of magnitude more abundant than those within the surrounding water column, and they are also many orders of magnitude more metabolically active (Ritchie et al., 1996; Ritchie and Smith, 2004). However, there is usually some overlap between coral microbiota and the surrounding seawater, which indicates that water and mucus interact (Kooperman et al., 2007).

Ritchie and Smith (1995a, 2004) reported that microbial assemblages in coral species within a genus seemed to have similar metabolic characteristics, indicating that there are specific relationships between coral taxa and their bacterial communities in the surface mucopolysaccharide layer. Rohwer et al. (2001) discovered a specific coral-microbial relationship when they found that one species of bacteria was present on all *Orbicella franksi (*previously known as *Montastraea franksi*; Budd et al., 2012) colonies although they were separated up to 10 km. Rohwer et al. (2002) later found, when studying three massive corals (*O. franksi*, *Diploria strigosa*, and *Porites astreoides*), that different coral species had distinct bacterial assemblages even when they were physically adjacent, while corals of the same species had similar microbial communities even when separated by space and time. Daniels et al. (2011) assessed the spatial variability of bacterial communities on three *O. annularis* colonies in the Florida Keys using both culture-based and culture-independent methods. They found that the bacterial communities varied among colonies and even on the same colony, indicating that even within a colony the bacterial community is not homogenous. Daniels and co-authors also reported that the bacterial communities found on the colonies were significantly different than the bacterial community found

within the surrounding water column, an observation that has previously been noted in other studies (Rohwer et al. 2001; Ritchie et al., 1996; Ritchie and Smith, 2004).

Environmental changes can lead to changes in the normal microbial community of healthy corals (Ritchie and Smith, 2004; Rosenberg et al., 2007; Ainsworth and Hoegh-Guldberg, 2009; Miller and Richardson, 2015). The stability and composition of the mucus layer are affected by environmental parameters such as water motion, irradiance, and nutrient availability (Brown and Bythell, 2005; Kline et al., 2006; Kooperman et al., 2007). When corals are stressed, the chemistry and quantity of the mucus changes (Ritchie and Smith, 1995a). Peters and Pilson (1985) found that when colonies of *Astrangia danae* were starved for two weeks and had sediment applied three times per day, there was a reduction of mucocytes, which resulted in less mucus production. Ritchie and Smith (2004) postulated that the normal microbial community protects the coral from invasive microbes; therefore, changes in the normal community provide a chance for the development of disease caused by pathogenic bacteria. Kooperman et al. (2007) noted that it is likely that environmental conditions coupled with the coral's physiological condition determine the microbial community associated with a coral holobiont (the host organism and all of its associated symbiotic microorganisms). Studies by Mitchell and Chet (1975) and Kline et al. (2006) found that elevated levels of dissolved organic carbon triggered microbial blooms that caused coral mortality. Hallock (2000) postulated that fluctuations in the rate of photosynthate release (consisting mainly of carbohydrates and lipids) by zooxanthellae could play a role in disease susceptibility in corals exposed to pulses of excess fixed nitrogen.

1.4 Coral Disease and Parasitism in the Indo-Pacific

Coral cover on Indo-Pacific reefs has declined by an average of 50% in the last 30 years (Bruno and Selig, 2007; Pollock et al., 2011; Hughes et al., 2013). The causes of decline have been linked to anthropogenic activities (Walker and Ormond, 1982; Bellwood et al., 2004; Hughes et al., 2013). One of the main contributors to the significant loss of coral cover is coral disease (Sutherland et al., 2004; Bourne et al., 2009). The first coral disease was described in the 1970s and, since then, field studies documenting disease in organisms associated with coral reefs has increased substantially (Weil, 2004; Willis et al., 2004; Harvell et al., 2007; Miller et al., 2015).

Disease identification for corals can be challenging, particularly because there are at least two criteria that have to be met to classify it as a disease. The criteria include: an identifiable group of signs, a causal agent, and consistent macroscopic/microscopic structural alterations. Coral disease identification is further complicated through these criteria because most coral diseases do not have a known causal agent, and different causal agents can display similar signs. Typically, the first step to identifying coral disease is the documentation of gross lesions on the coral colony.

Scientists have employed a variety of methods to identify coral diseases (Work et al., 2008; Pollock et al., 2011; Work et al., 2015). Methods includes websites and visual guides to aid in identification (i.e., CDHC website; Beeden et al., 2008; Raymundo et al., 2012), visual surveys of coral reefs for gross lesions by scientists (Work and Rameyer, 2005; Work and Aeby, 2006; Pollock et al., 2011; Williams et al., 2011; Bourne et al., 2015), and even visual surveys for signs of disease by volunteer divers (i.e., Reefcheck; Beeden et al., 2012). Because coral diseases, in particular white syndromes and completely bleached colonies, can be confusing to even the most

trained eye, field studies of progression rates and laboratory examination through molecular and histological techniques is crucial (Work and Meteyer, 2014).

The six most common coral diseases found in the Indo-Pacific include black-band disease (Antonius, 1985), skeleton-eroding band (see Appendix 1) (Antonius, 1999), white syndrome (Willis et al., 2004), growth anomalies (Squires, 1965), ulcerative white-spot disease (Raymundo et al., 2003), and brown band disease (see Appendix 1) (Willis et al., 2004). Other diseases include, but are not limited to, color loss (bleaching) (Kushmaro et al., 1996), pink-line syndrome (Ravindran and Raghukumar, 2002), yellow-band disease (Korrubel and Riegl, 1998) and red-band disease (Sussman et al., 2006). The following sections describe the most common coral diseases, including those observed in my study.

1.4.1 Color Loss — A common type of color change is bleaching. Bleaching occurs when corals reduce or completely lose their zooxanthellae through expulsion or when zooxanthellae lose chlorophyll (Glynn, 1991, 1993, 1996; Brown and Dunne, 2016). Although bleaching is commonly associated with high sea water temperatures, it can also be caused by UV radiation (Glynn, 1996), high sedimentation and turbidity (Anthony and Connolly, 2007), and low sea water temperatures (Hoegh-Guldberg and Fine, 2004). Upton and Peters (1986) documented *Gemmocystis cylindrus* (a coccidium) in Caribbean scleractinian colonies, which was associated with the loss of zooxanthellae resulting in patchy bleaching and tissue necrosis. *Vibrio* spp. have been implicated in bleaching in some coral species (Kushmaro et al., 1997, 1998; Banin et al., 2000; Hormansdorfer et al., 2000; Munn, 2015), and *Vibrio* spp. are often spread by amphinomid polychaetes (Goldstein, 2008). Two bacterial pathogens from the genus *Vibrio* that have been associated with bleaching are *V. shiloi* and *V. coralliilyticus* (Kushmaro et al., 1996; Ben-Haim and Rosenberg, 2002; Sutherland et al., 2004). *V. shiloi* adheres to the mucus of the coral and penetrates the epidermis.

Once it has penetrated the coral tissue it multiplies and produces toxins, that inhibit photosynthesis, and bleach and lyse the zooxanthellae (Ben-Haim et al., 1999). It is important to note that adhesion is temperature dependent and does not occur below 16° C. *V. coralliilyticus* causes tissue lysis through the synthesis of a metalloproteinase (Ben-Haim and Rosenberg, 2002). Like *V. shiloi*, this is temperature dependent, and only occurs at temperatures above 26° C.

During histological examination, Work and Rameyer (2005) noted that the most common microscopic change associated with color loss was a depletion of zooxanthellae from the atrophied gastrodermis, which resulted in bleaching. Ainsworth and Hoegh-Guldberg (2009) exposed *Acropora aspera* and *Stylophora pistillata* to thermal stress in aquaria and found that bacteria colonized or overgrew the tissue only after temperature-induced bleaching of the coral tissues. In the bleached coral tissue, there was a mixed bacterial population within the mesentarial filaments and epithelia. They also noted rod-shaped γ-proteobacteria in the gastrodermis of both healthy and bleached corals.

1.4.2 White Syndrome — In the Indo-Pacific, white lesions or white 'diseases' found on corals are collectively termed "white syndrome" (Sweet and Bythell, 2012). The term describes conditions resulting in white bands, spots, or patches as a consequence of tissue loss exposing white skeleton. Because it encompasses all signs of tissue loss, white syndrome is poorly defined for the Indo-Pacific (Bythell et al., 2004; Bourne et al., 2015), although white plague-like disease, which falls under white syndrome, has been characterized. White plague disease and white plague-like disease have been documented since the late 1970s and 1980s affecting Caribbean and Indo-Pacific corals, respectively (Dustan, 1977; Antonius, 1985; Richardson, 1998; Sutherland et al., 2004). White plague is characterized by sharp demarcation between healthy coral tissue and exposed white skeleton (Dustan, 1977; Sutherland et al., 2004). White plague signs have been documented in at

least 38 species of Indo-Pacific scleractinian, including many species from the genus *Acropora* (Antonius, 1985; Coles, 1994; Riegl, 2002). The etiological agents of white syndromes have been debated, and causes and associations have included apoptosis (Ainsworth et al., 2007), bacteria (*Vibrio*–Sussman et al., 2008), virus-like particles (Lawrence et al., 2015) and even parasites (ciliates–Work and Aeby, 2011; Sweet and Bythell, 2012).

1.4.3 Pink-line Syndrome — Ravindran et al. (2001) first characterized pink-line syndrome affecting *Porites compressa* and *P. lutea* on Kavaratti Island, Indian Ocean. Pink-line was described as a band of pink-pigmented tissue separating dead skeleton from apparently healthy tissue, the band may begin as a ring and progress outward horizontally across a coral colony (Ravindran et al., 2001; Sutherland et al., 2004). Ravindran and Raghukumar (2002) previously documented that pink-line syndrome is associated with the cyanobacterium *Phormidium valderianum*, which induces pink coloration to the coral tissue. Other researchers have suggested that pink-line syndrome is not an infectious disease but a physiological reaction to stress (Palmer et al., 2009a, b; Willis et al., 2009; Benzoni et al., 2010). When studying the effects of trematode infections on *Porites compressa*, Palmer et al. (2009a) documented green fluorescence in histological sections of healthy coral tissue and red fluorescence in trematode-compromised tissue. Willis et al. (2009) stated that *Porites* appears to respond to a variety of competitive, invasive and parasitic challenges by producing pink or purple pigmentation in the coenosarc (tissue overlying the skeleton that connects polyps) and in polyps adjacent to sites of competitive interactions and lesions. They further noted that, although most commonly observed on *Porites*, pigmentation responses have been observed on most genera. Most recently, however, pink-line syndrome has been reintroduced into the literature as a coral disease, although the source of the disease is still being debated (Lin et al., 2016; Ravindran et al., 2016).

1.4.4 Brown Band Disease — Willis et al. (2004) first characterized brown band syndrome on the Great Barrier Reef. They described the syndrome as a brown zone of variable width at the interface between healthy coral tissue and recently exposed skeleton. A white zone between the healthy tissue and the brown band was often documented, indicating that zone may be bleached tissue or denuded skeleton. The brown coloration is derived from dense populations of ciliates containing zooxanthellae from the coral tissue consumed. The 'brown' coloration can range from brown to white based on the quantity of ciliates present, which has led to ciliates being implicated in the white syndromes (Randall et al., 2015; Sweet and Bythell, 2015).

Ulstrup et al. (2007), Yarden et al. (2007), and Nugues and Bak (2009) suggested that brown band syndrome may be caused by *Helicostoma nonatum*, a ciliate that is often found within the "brown jelly", a similar condition that has affected aquarium corals, indicating that brown jelly and brown band syndrome may be the same affliction. One possibility is that the "brown jelly" may result from the accumulation of ciliates and their wastes in the absence of predators of the ciliates, a situation that may be more common in aquaria than in nature (George, 2011).

1.4.5 Parasitic Copepods — Riddle (2010) documented approximately 200 parasitic copepods found on corals. Riddle further noted that many hobbyists lump parasitic crustaceans into loose categories called 'red bugs' and 'black bugs'. For example, red bugs are commonly referred to a single species, *Tegastes acroporanus;* however, this species has only officially been described in *Acropora florida.* The genera of parasitic copepods in corals include *Alteuthellopsis, Xarifia, Stockia, Humesiella, Tegastes, Parategastes, Orstomella, Zazaranus,* and many others. Riddle

(2010) noted that many copepods reside within coral polyps, making them hard to detect; however, general signs often include a general lack of wellness, loss of vibrant coloration, poor polyp expansion, and loss of zooxanthellae (perhaps a result of predation by the copepods). Ivanenko and Smurov (1996) suggested that copepods might introduce pathogens to their host, which might explain why some copepod infestations are relatively harmless, while other seemingly mild cases of parasitism can cause rapid decline and mortality of the host. Humes (1985) documented that over 400 species of copepods live in association with scleractinian corals and even have immunity to the coral's nematocyts' toxins.

1.4.6 Growth Anomalies — Growth anomalies have been widely documented in corals both in natural and aquarium environments (Peters et al., 1986; Work and Rameyer, 2005; Domart-Coulon et al., 2006; Weil and Hooten, 2008; Williams et al., 2011; Aeby et al., 2011; Sere et al., 2015). Growth anomalies appear as distinctive protuberant masses on coral, so they are easily recognized. Growth anomalies may also cause some change in coloration. Usually these growths are not only raised areas on the corals, but they also often display fewer polyps and zooxanthellae as compared to adjacent healthy tissue (Domart-Coulon et al., 2006). Fungi, algae, or polychaetes living in or on the coral skeleton can cause the skeletal matrix to encroach around the individual organism, causing growth anomalies (Weil and Hooten, 2008). Thus, there is no single definitive cause for all growth anomalies.

Many coral taxa can be affected by growth anomalies, including *Orbicella*, *Colpophyllia*, *Diploria*, and *Acropora* (Aeby et al., 2011). In wild corals, growth anomalies can be associated with reduced colony growth, partial colony mortality, and decreased reproduction. Aeby et al. (2011) reported that growth anomalies have been recorded in more than 17 *Acropora* spp. and concluded that colonies within this genus appear to be very susceptible. In the survey conducted

by Aeby and colleagues, growth anomalies were much more prevalent on Indo-Pacific acroporids (~16%) than on Atlantic-Caribbean acroporids (0%). Indeed, Aeby et al. (2011) found only two published reports of *Acropora* with growth anomalies in the Atlantic-Caribbean (Bak, 1983; Peters et al., 1986).

Breitbart et al. (2005) documented that microbial communities from coral colonies exhibiting growth anomalies grew faster than microbial communities of healthy coral colonies. However, they found no significant difference between microbial growth rates from mucus from the healthy portion of the colony exhibiting the growth anomaly and the actual growth anomaly. Using Biolog EcoPlate™ techniques, Breitbart et al. (2005) found that microbial communities on coral with the growth anomalies were able to use four more carbon sources than the microbial communities from unaffected colonies.

Histological studies have revealed interesting details of coral tissue associated with growth anomalies. Work and Rameyer (2005) found that growth anomalies were usually manifested as hyperplasia (increase in number of cells). Peters et al. (1986) described proliferated gastrovascular canals and the associated calicoblastic epidermis associated with growth anomalies in *Acropora palmata*. This resulted in the degeneration of normal polyp structures and loss of zooxanthellae in the gastrodermal cells. Peters also noted a lack of mucus secretory cells normally present in the epidermis. Williams et al. (2011) documented hyperplasia of the basal body wall, absence or reduction of polyp structure, which includes mesenteries and filaments, actinopharynx and tentacles, and a depletion of zooxanthellae in the gastrodermis of the upper body wall. They also noted fungi, algae, sponges, and crustaceans in some of their samples exhibiting growth anomalies. Sutherland et al. (2004) concluded that growth anomalies presenting with distinctive protuberant

masses are a result of neoplasia (uncontrolled abnormal cell proliferation), hyperplasia (increase in number of cells), or hypertrophy (increase in size of cells).

1.4.7 Black-band Disease — Rutzler and Santavy (1983) described black-band disease as a dense microbial mat overlying coral tissue, typically dominated by one or two cyanobacteria, sulfate-reducing bacteria, and the sulfur–oxidizing bacteria *Beggiatoa* spp. They found that the band also contained ciliates, fungi and other heterotrophic bacteria. Black-band disease was first identified in the Red Sea off the coast of Saudi Arabia and in the Indo-Pacific (Philippines) in 1981 (Antonius, 1981). In the Indo-Pacific and Red Sea, black-band disease has been reported on 46 species. It also occurs most commonly on faviid corals, including *Favia* (four species), *Favites pentagona*, *Goniastrea* (two species), *Platygyra lamellina*, *Diploastrea heliopora*, *Echinopora* (two species) and *Leptoria phrygia*. Boyett et al. (2007) documented that similar to the Caribbean, in the Indo-Pacific, black-band disease is more abundant during warm water periods; and that elevated temperature and light enhance the progression and transmission of black-band disease. A review found that black-band disease occurs primarily at low levels in the Indo-Pacific (Bruckner, 2016).

1.4.8 Ulcerative White-spot Disease — Raymundo et al. (2003) characterized ulcerative white-spot disease by ovoid bleached lesions, 3–5 mm in diameter that is usually followed by tissue mortality. It primarily affects *Porites*. Ulcerative white-spot disease was first observed in 1996 in the Philippines, and has since been reported from other locations including Indonesia (Haapkylä et al., 2009), Australia (Willis et al., 2004) and Guam (Myers and Raymundo, 2009). The disease

is known to have a high prevalence, but a slow progression. For example, Raymundo et al. (2003) noted that 20% of the *Porites* colonies were affected by ulcerative white-spot disease on 80% of the reefs examined in the Philippines in the mid-1990s, and Kaczmarsky (2006) found that up to 54% of the *Porites* colonies he examined had the disease during 2002–2003 in the Philipines were affected.

1.5 Ciliates and Their Relationship with Coral Health and Disease

A paper has been submitted for publication that focuses on ciliates and their relation to coral disease. See Appendix 1.

1.6 Coral Health and Disease on the Reefs of the South China Sea

Coral reefs in the South China Sea, including China's coastal fringing reefs and on disputed territorial offshore atolls and islands, occupy about 30,000 km^2 and represent important natural assets of high conservation value (Hughes et al., 2013). They support livelihoods and provide ecosystem services, such as fish and areas for aquaculture and reef-based tourism (Morton and Blackmore, 2001; Gu and Wong, 2008). The approximately 130 atolls and platform reefs (Morton and Blackmore, 2001) are claimed by up to six countries: Brunei, China, Malaysia, Taiwan, Philippines, and Vietnam. Climate change is adding to the problems of sustaining the world's coral reefs (Hughes et al., 2003), but ongoing overfishing, pollution, coastal development, and other human activities that affect reefs are much more prevalent in many densely populated regions like China (Hughes et al., 2013). Coral bleaching and outbreaks of disease and crown-of-thorns starfish

have also been reported throughout the South China Sea since the late 1990s, and these events have resulted in substantial loss of coral cover (e.g., Soong et al., 2002; Huang et al., 2009, 2011).

China's fringing reefs are now being degraded, with 30% to 70% loss of live coral coverage in the past few decades (Zhang et al., 2006; Chen et al., 2007; Yu et al., 2010; Zhao et al., 2010; Zhao et al., 2012). Surveys have found that most of the degradation has been the result of human activities, including engineering projects, destructive fishing practices, and pollution (Wang et al., 2006; Zhang et al., 2006; Chen et al., 2007). In recent years, scientists have documented "black" disease and ciliate infections in China (Qui et al., 2010; Shi et al., 2011; Hughes et al., 2013). Yang et al. (2014) published the first report of black band disease in the South China Sea.

In Taiwan, scientists have documented "black" disease, parasitic copepods, and pink line syndrome (Liao et al., 2007; Cheng and Dai, 2009, 2010; Chiou et al., 2010; Lin et al., 2016). In 2004, Dai et al. documented various kinds of tissue and skeleton abnormalities in corals from northeastern, eastern, southern Taiwan, and offshore islands, including Hsiaoliuchiu and Penghu Islands. 'Black disease' has previously been noted at Chaikou (Liao et al., 2007). In 2010, Cheng and Dai documented for the first time in Taiwan two species of poecilostomatoid copepods that induced galls on *Montipora aequituberculata*.

It is important to note that although "black" disease has been documented in the literature as a coral disease, it is no longer classified as a coral disease. It has been identified as an encrusting sponge named *Terpios hoshinota* that has photosynthetic cyanobacteria symbionts (Ruetzler and Muzik 1993; Liao et al. 2007).

2. Study Rationale, Objectives, and Hypotheses

In a previous study (George, 2011), I identified and characterized diseases in captive corals through visual recognition, characterization of carbon utilization by microbial assemblages in coral mucus samples, and histological examination. I surveyed public aquaria throughout the United States that housed corals, acquiring photographs, mucus samples for microbial carbon utilization analysis, and tissue samples for histological examination. The gross lesions from diseased samples fit into six categories: discoloration associated with darkening of the tissue or with color loss (bleaching), growth anomalies, and tissue loss associated with pests, with brown jelly, or with no obvious cause. Possible contributing factors were included: addition of inadequately quarantined corals to a tank, damage during transport, change of location, handling stress, and variations in light, salinity, or temperature. Introduction of inadequately quarantined specimens was the most common possible contributing factor to pest introduction. Significant differences in carbon source utilization were found between tank-water samples and mucus from both apparently healthy and diseased areas of sampled corals. Although bacterial communities associated with mucus samples from apparently healthy and diseased coral samples did not differ in carbon source utilization overall, D-mannitol was used by 52% of microbial assemblages in mucus from diseased areas compared with only 17% of microbial assemblages from apparently healthy mucus samples. Histologically, the most commonly observed features across all samples were changes in zooxanthellae, endolithic organisms, and nematocysts, all of which are normal features that can be influenced by stress factors. Brown granular material and ciliates were found associated with some anomalies, primarily the three categories of tissue loss. The presence of dense aggregates of

zooxanthellate-engorged ciliates in corals afflicted with brown jelly was similar to histological observations of brown band syndrome, previously described from natural coral reefs (Willis et al., 2004; Sweet and Bythell, 2012).

The focus of my dissertation research has been to expand and apply insights gained from my work with aquarium corals to document and characterize diseases in naturally occurring corals using field observations, sample collection and laboratory analyses. During summer 2012, I had the opportunity to survey coral lesions at six reef locations in Taiwan that differed in degree of anthropogenic influence. During summer 2013, I conducted research at two additional fringing-reef locations on Hainan Island, China. Methods included surveys of coral lesions, and collection of samples for histological examination, denaturing gradient gel electrophoresis (DGGE), and analysis of carbon requirements of the microbes in coral mucus.

2.1 Objectives

The objectives of my study were to describe the occurrence and histological features of coral lesions from each study site and to assess the diversity and nutritional requirements of microbiota associated with the lesions. My research strategy was to use in-water surveys to determine if lesions were present on corals, and, when observed, collect mucus samples to analyze the carbon requirements of the microbes in mucus of afflicted corals, and to collect tissue samples for denaturing gradient gel electrophoresis (DGGE) and histological examination. This study provides insight on the morphological, physiological, and microbial characteristics of gross lesions on corals at the locations sampled.

2.2 Research Questions and Hypotheses

Because this research was largely exploratory, questions were straightforward and null hypotheses were basic. Thus, discoveries and further investigations were based on cases in which the null hypotheses were not supported. Assuming that lesions were present in coral colonies living on the reefs surveyed:

a. What are the most frequently observed types of lesions? Based on a literature review and previous research (i.e., George, 2011), I suspected that the coral lesions would fall into the following categories: discoloration associated with color loss, discoloration associated with tissue darkening, growth anomalies, tissue loss associated with parasites, and "black disease" (Liao et al., 2007; Qui et al., 2010; Aeby et al., 2011; Shi et al., 2012).
b. Were lesions more commonly observed in some taxa? *Null hypothesis:* Lesion occurrence is the same among taxa. H_A*:* The lesion occurrence is different among taxa. *Prediction:* Based on previous research, I anticipated that Agariciidae and Pectiniidae would be the most affected coral families (George, 2011).
c. Do types and prevalences of coral lesions differ among sites? *Null hypothesis:* Types and prevalences of coral lesions are similar across sites. H_A*:* Types and prevalences of coral lesions across sites are different. *Prediction:* Based on the literature, I anticipate that I will find the fewest lesions at Green Island sites, Keelung and Taitung sites will have intermediate prevalence, and Sanya sites will have the highest prevalence of coral lesions.
d. Do carbon requirements of microbial assemblages differ: (1) across sites; (2) between healthy corals and water column; (3) between healthy areas and lesions of each identified category? *Null hypothesis:* The carbon requirements of microbial assemblages do not differ: (1) across sites; (2) between healthy corals and water column; (3) between healthy

areas and lesions of each identified category. H_A*:* The carbon requirements of microbial assemblages will differ: (1) across sites; (2) between healthy corals and water column; (3) between healthy areas and lesions of each identified category.

e. Do microbial assemblages differ (using DGGE method): (1) across sites; (2) between apparently healthy corals and water column; (3) between healthy mucus and tissue and lesions of each identified category? *Null hypothesis:* The microbial assemblages do not differ (using DGGE method): (1) across sites; (2) between apparently healthy corals and water column; (3) between healthy mucus and tissue and lesions of each identified category. H_A*:* The microbial assemblages will differ (using DGGE method): (1) across sites; (2) between apparently healthy corals and water column; (3) between healthy mucus and tissue and lesions of each identified category. *Prediction:* The microbial community will most likely vary between apparently healthy areas and lesions on the same coral species (Gil-Agudelo et al., 2006a; Chiou et al., 2010; Daniels et al., 2011; George, 2011).

f. What are the most common microbial assemblages: (1) across sites; (2) between healthy corals and the water column; (3) between healthy and diseased corals of each identified category?

g. Do histological features differ among identified affliction categories? *Null hypothesis:* Histological features do not differ by lesion type. H_A*:* Histological features differ among lesion types.

Based on data collected from the reefs and corals of Taiwan and Hainan, when significant differences were found after applying statistical tests to the above hypotheses, the following comparisons were made based on the results:

a. Are kinds of lesions and their prevalences similar between the two areas? *Null hypothesis:* Signs and prevalences of coral disease show no difference between areas. H_A*:* Signs and prevalences of coral disease differ between areas.
b. Are microbial assemblage responses in water column, in healthy coral taxa and in lesion-afflicted taxa consistent between areas? *Null hypothesis:* Microbial assemblage responses in water column, in healthy coral taxa and in lesion taxa are consistent between areas. H_A*:* Microbial assemblages' responses in water column, in healthy coral taxa and in lesion taxa differ between areas.
c. Are histological features in transitional areas of the coral lesion consistent with the histological features of corals exhibiting the same signs in the literature? *Null hypothesis:* Histological features in this study do not differ from the histological features from published studies. H_A*:* Histological features in this study differ from the histological features from published studies.

3. Methods

3.1 Background Information on Methods Used

3.1.1 Carbon-Source Utilization

Aspects of the metabolic activity of the microbial community in coral mucus can be observed and analyzed using Biolog EcoPlate™ assessment (Biolog Inc., Hayward, CA) (Biolog, 2004b; Gil-Agudelo et al., 2006a). Techniques such as culturing and molecular genetics require a large amount of effort, time, and money. The Biolog EcoPlate™ is a simple, inexpensive technique to perform a microbial community analysis based on carbon metabolism. This technique is sometimes referred to as community-level physiological processing and is effective in demonstrating spatial and temporal changes in microbial communities (Biolog, 2004a).

The Biolog EcoPlate™ contains 31 carbon sources (Figure 1) with three replicates per source (Biolog, 2004a). When inoculated with a microbial sample and incubated, a pattern will develop on the plates, providing what is called a metabolic fingerprint. That pattern can be assessed for the following key characteristics: pattern development (similarity), rate of color change in each well, and richness of well response (diversity) (Biolog, 2004a). In 1991, Garland and Mills originated the concept of community analysis by applying samples from water, the rhizosphere, and soil to Biolog GN Microplates. They found that each sample source (water, rhizosphere, soil) had a distinct pattern of carbon source utilization. Ritchie and Smith (1995b) applied this concept to bacterial isolates from healthy *Acropora cervicornis*, as well as specimens exhibiting signs of white-band disease. This technique proved to be very useful in distinguishing healthy coral

samples from diseased coral samples. Their study showed that the white-band isolates preferentially metabolized more carbon sugars, organic acids, and amino acids than isolates from the "normal" coral.

To demonstrate what they considered the most simple, reliable method of characterizing the metabolic diversity of the mucosal microbial community, Gil-Agudelo et al. (2006b) used Biolog EcoPlate™. Their study indicated that vortexing coral fragments followed by 72 hours of incubation provided the most reliable assay method. In another study, Gil-Agudelo et al. (2006a) found that microbial communities from the water column were significantly different from microbial communities of healthy and diseased (*Aspergillosis*) colonies of *Gorgonia ventalina* and there were differences between the microbial communities of healthy and diseased samples. Nine carbon sources were responsible for the differences between the seawater and the coral samples. The biggest difference between coral samples was the metabolic profile between completely healthy colonies and diseased colonies, though the metabolic profiles of the microbial communities on healthy areas of diseased colonies and diseased areas of the colony were very similar. This indicates that the coral microbial community as a whole, not just in lesion areas, can be affected by disease. Pantos et al. (2003) observed shifts in the microbial community of *Orbicella annularis* exhibiting a white plague-like disease, even on healthy looking tissue.

A1 Water	A2 β-Methyl-D-Glucoside	A3 D-Galactonic Acid γ-Lactone	A4 L-Arginine	A1 Water	A2 β-Methyl-D-Glucoside	A3 D-Galactonic Acid γ-Lactone	A4 L-Arginine	A1 Water	A2 β-Methyl-D-Glucoside	A3 D-Galactonic Acid γ-Lactone	A4 L-Arginine
B1 Pyruvic Acid Methyl Ester	B2 D-Xylose	B3 D-Galacturonic Acid	B4 L-Asparagine	B1 Pyruvic Acid Methyl Ester	B2 D-Xylose	B3 D-Galacturonic Acid	B4 L-Asparagine	B1 Pyruvic Acid Methyl Ester	B2 D-Xylose	B3 D-Galacturonic Acid	B4 L-Asparagine
C1 Tween 40	C2 I-Erythritol	C3 2-Hydroxy Benzoic Acid	C4 L-Phenylalanine	C1 Tween 40	C2 I-Erythritol	C3 2-Hydroxy Benzoic Acid	C4 L-Phenylalanine	C1 Tween 40	C2 I-Erythritol	C3 2-Hydroxy Benzoic Acid	C4 L-Phenylalanine
D1 Tween 80	D2 D-Mannitol	D3 4-Hydroxy Benzoic Acid	D4 L-Serine	D1 Tween 80	D2 D-Mannitol	D3 4-Hydroxy Benzoic Acid	D4 L-Serine	D1 Tween 80	D2 D-Mannitol	D3 4-Hydroxy Benzoic Acid	D4 L-Serine
E1 α-Cyclodextrin	E2 N-Acetyl-D-Glucosamine	E3 γ-Hydroxybutyric Acid	E4 L-Threonine	E1 α-Cyclodextrin	E2 N-Acetyl-D-Glucosamine	E3 γ-Hydroxybutyric Acid	E4 L-Threonine	E1 α-Cyclodextrin	E2 N-Acetyl-D-Glucosamine	E3 γ-Hydroxybutyric Acid	E4 L-Threonine
F1 Glycogen	F2 D-Glucosaminic Acid	F3 Itaconic Acid	F4 Glycyl-L-Glutamic Acid	F1 Glycogen	F2 D-Glucosaminic Acid	F3 Itaconic Acid	F4 Glycyl-L-Glutamic Acid	F1 Glycogen	F2 D-Glucosaminic Acid	F3 Itaconic Acid	F4 Glycyl-L-Glutamic Acid
G1 D-Cellobiose	G2 Glucose-1-Phosphate	G3 α-Ketobutyric Acid	G4 Phenylethyl-amine	G1 D-Cellobiose	G2 Glucose-1-Phosphate	G3 α-Ketobutyric Acid	G4 Phenylethyl-amine	G1 D-Cellobiose	G2 Glucose-1-Phosphate	G3 α-Ketobutyric Acid	G4 Phenylethyl-amine
H1 α-D-Lactose	H2 D,L-α-Glycerol Phosphate	H3 D-Malic Acid	H4 Putrescine	H1 α-D-Lactose	H2 D,L-α-Glycerol Phosphate	H3 D-Malic Acid	H4 Putrescine	H1 α-D-Lactose	H2 D,L-α-Glycerol Phosphate	H3 D-Malic Acid	H4 Putrescine

Figure 1. Carbon Sources in EcoPlate™. (Figure from Biolog, 2004a)

3.1.2 DGGE

Muyzer et al. (1993) first used DGGE analysis of 16S rRNA sequences obtained after amplification of genomic DNA isolated from complex microbial populations to assess microbial communities from various environments including microbial mats from Wadden Sea sediment and bacterial biofilms obtained from wastewater treatment reactors. DGGE provides a banding-pattern profile of the assemblages in that the relative intensity of each band and its position most likely represent the relative abundance of a particular species in the population. Muyzer et al. (1993) used DGGE analysis of 16S rRNA PCR products from various microbial communities, finding many distinguishable bands, and concluded that this was most likely from the many different bacterial species within the microbial communities.

DGGE has also been used to assess the microbial communities in corals (Chiou et al., 2010; Meron et al., 2011; Sweet and Bythell, 2012; Smith et al., 2015; Lin et al., 2016). Chiou et al. (2010) used DGGE to assess healthy and diseased coral colonies from three locations off the coast of southern Taiwan: a nuclear power plant III water outlet, Green Island, and Liuqiu. Results from this study showed that microbial communities varied between healthy and diseased sections of the same coral, and that microbial communities varied on healthy areas of colonies from the same species at different geographic locations. Chiou et al. (2010) analyzed the microbial diversity of *Acropora hyacinthus* in healthy and diseased tissue, and the transition between the healthy and diseased zones. They found that the microbial community within the transition zone was more diverse than either the healthy or diseased zones, suggesting that, as the organism deteriorates, opportunistic bacteria feast on the released nutrients of the failing organism.

Meron et al. (2011) observed the effects of pH (7.3 and 8.2) after a 10-week exposure on the microbial communities of *Acropora eurystoma* and found that the microbial community was

more diverse at pH 7.3. The authors speculated that the lower pH triggered an intermediate disturbance, which led to an increase in microbial diversity. Meron et al. (2011) also found that corals maintained at the lower pH revealed an increase in bacteria such as *Vibrionaceae* and *Alteromonadaceae*, which have previously been found to be associated with diseased and stressed corals.

Sweet and Bythell (2012) documented microbial and ciliate communities on *Acropora muricata* and *A. aspera* colonies at Heron Island, Great Barrier Reef, and in the Solomon Islands, exhibiting signs of white syndrome and brown-band syndrome. Results of their study showed that four bacterial and nine ciliate ribotypes were found within both diseases, but not within the healthy areas of the coral, indicating highly similar bacterial and ciliate communities between the two diseases. Furthermore, some of the ciliates contained zooxanthellae, indicating the ingestion of coral tissue. Sweet and Bythell (2012) then suggested, based on the highly similar bacterial and ciliate community coupled with ciliates containing ingested zooxanthellae, that white syndrome and brown-band syndrome are actually the same syndrome. Smith et al. (2015) also used DGGE to identify ciliate communities on coral colonies exhibiting white syndrome.

3.1.3 Histology

While visual identification is useful to identify signs of disease, histological examination is a useful descriptive tool to analyze coral afflictions microscopically (Peters et al., 1986; Santavy and Peters, 1997; Domart-Coulon et al., 2006; Ainsworth and Hoegh-Guldberg, 2009; Aeby et al., 2011; Work and Meteyer, 2014). Histology is the study of the structure of cells, tissues, organs, and organ systems. Histopathology is the study of cytological and histological structure of abnormal tissues. Histology is useful because it gives a visual record of the cells and tissues of an

organism and allows comparisons between healthy and diseased tissue and cells. However, histology cannot completely identify a pathogen and, because it is a destructive methodology, it does not allow testing the same lesion over time.

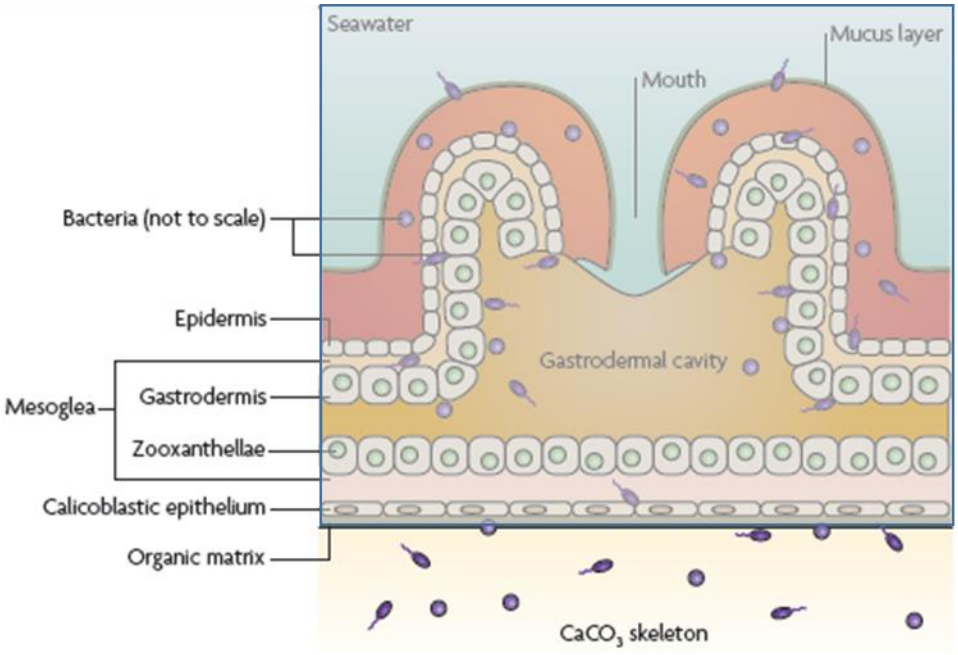

Figure 2. The structure of coral tissue. (Modified from Rosenberg et al., 2007)

Corals are made up of two layers of cells, the epidermis and the gastrodermis (Figure 2), which are separated by the mesoglea (Borneman, 2001; Peters, 2004; Rosenberg et al., 2007). The epidermis covers the coral surface and the gastrodermal cavity is lined by the gastrodermis. Zooxanthellae are located in the gastrodermis. The mesoglea maintains the arrangement of cells and cell layers. The calicoblastic epithelium (now referred to as the calicodermis) lines the basal surface of the coral and lays down calcium carbonate. Any histological changes to the structure of the coral tissue are important and should be documented when corals exhibit disease.

According to Yevich and Barszcz (1983), histopathology is an important tool in investigating diseases in marine organisms and is useful in comparing physicochemical and

physiological changes with changes seen at the population and community level. Histopathology provides the first step in identifying microbial agents associated with gross and microscopic lesions; however, it provides few clues on the temporal process of the disease (Work and Rameyer, 2005; Work and Meteyer, 2015).

3.2 Study Sites

During summer 2012, coral-lesion surveys were carried out at six sites around Taiwan (Figure 3). Two sites, Kihau and Shanyuang, are located on the southeastern coast of Taiwan. They are located in the waters off Taitung, a city with a population of approximately 106,929. The Chaikou and Gonguan sites are located off the coast of the remote volcanic island of Green Island, approximately 33 km off the eastern coast of Taiwan. With a population of only 2,634, Green Island is considered to be one of the best places to dive in Taiwan and Chaikou is one of two major diving sites on the island (Cheng et al., 2005). Approximately 168 scleractinian coral species have been recorded at Green Island (Chang et al., 1992). The other two sites are Bitou and Yeliu. These are primarily subtropical non-reefal habitats, located off the northeastern coast of Taiwan near the city of Keelung. Keelung has a population of 373,077 and borders New Taipei (population 3.9 million). The Taipei-Keelung metropolitan area, which includes Taipei city (population 2.7 million) has an estimated population of 6.9 million.

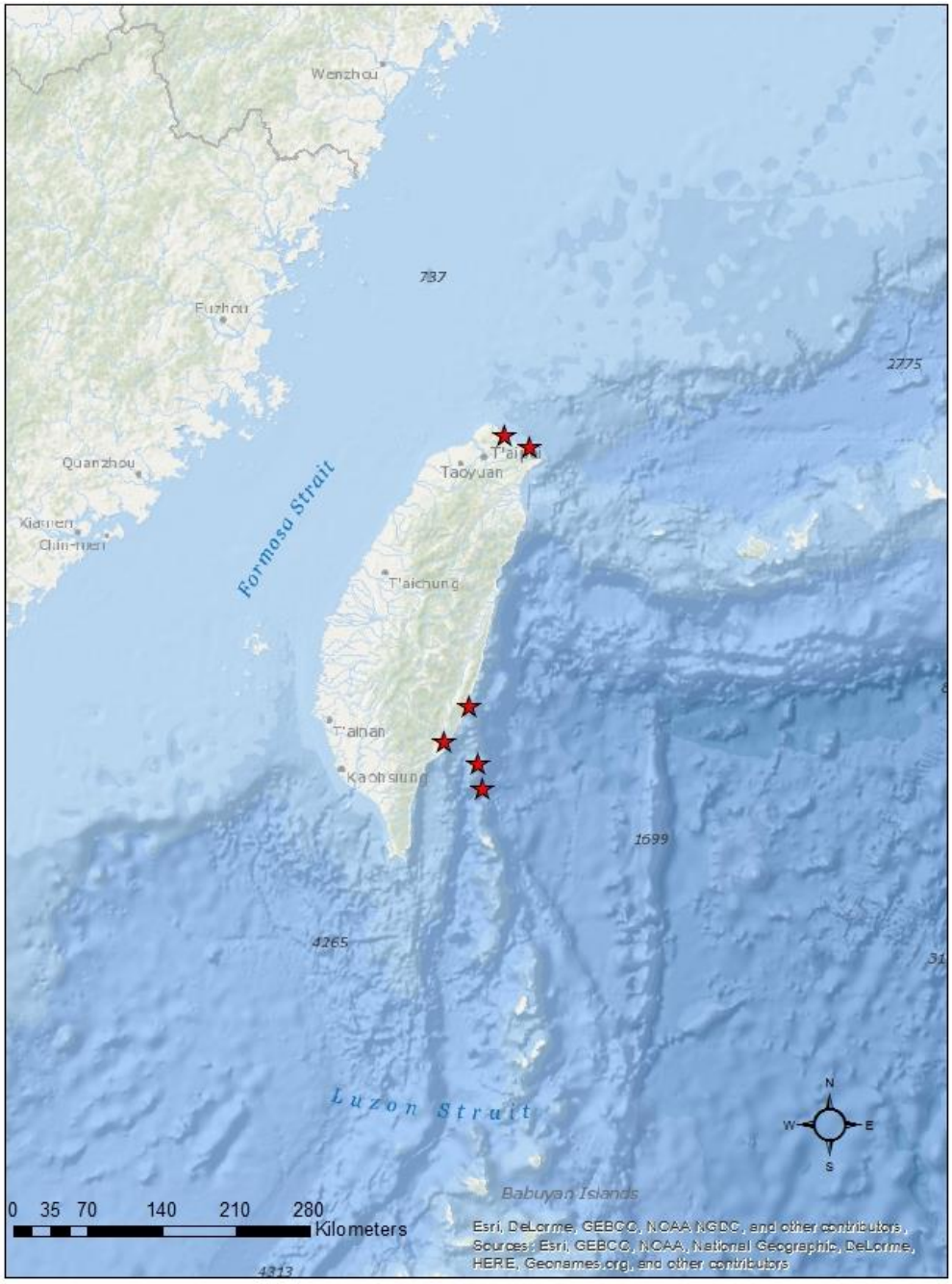

Figure 3. Map of study sites including North Taiwan, Taitung, and Green Island. Map was generated in ArcGIS.

In summer 2013, a similar coral lesion survey was conducted at two sites off Sanya, Hainan Island (Figure 4). The Luhuitou fringing reef, which is approximately 3 km long and 250-500 m

wide, is located along the southern coast of the Hainan Island adjacent to Sanya urban area (Zhao et al., 2012). Historically Luhuitou reef had high biodiversity, with 12 families, 24 genera, and 81 corals species recorded in 1975 (Zou et al., 1975). More recent surveys indicate a significant decline; for example *Goniastrea* and *Montipora,* which previously prevailed on the reef flats during the 1960s, have now disappeared and have been replaced with *Porites lutea* (Zhao et al., 2012). The mean coral cover has dropped from 80–90% in the 1960s to 12% in 2009 (Hughes et al., 2013). Anthropogenic activities such as coral-block mining, overfishing, blast fishing, cyanide fishing, electric fishing, anchoring, and recreational activities including scuba diving have been documented as playing a large role in mass coral mortality and damage to the reef's structure (Pan et al., 1983; Hutchings and Wu, 1987; Lui, 1998).

The Dadonghai fringing reef is approximately 60–150 m wide and is located within a small bay near Sanya City, southern Hainan Island, in the northern South China Sea (Yu et al., 2010). Xiaodonghai reef is approximately 100–300 m wide with a reef flat that is 1.5 km long (Nie et al., 1997). The fringing reef is located along the southeast (windward) coast of Luhuitou Peninsula in Sanya City, southern Hainan Island (Zhang, 2004). Xiaodonghai reef has been affected less by human activities and has apparently healthy corals (Li et al., 2008).

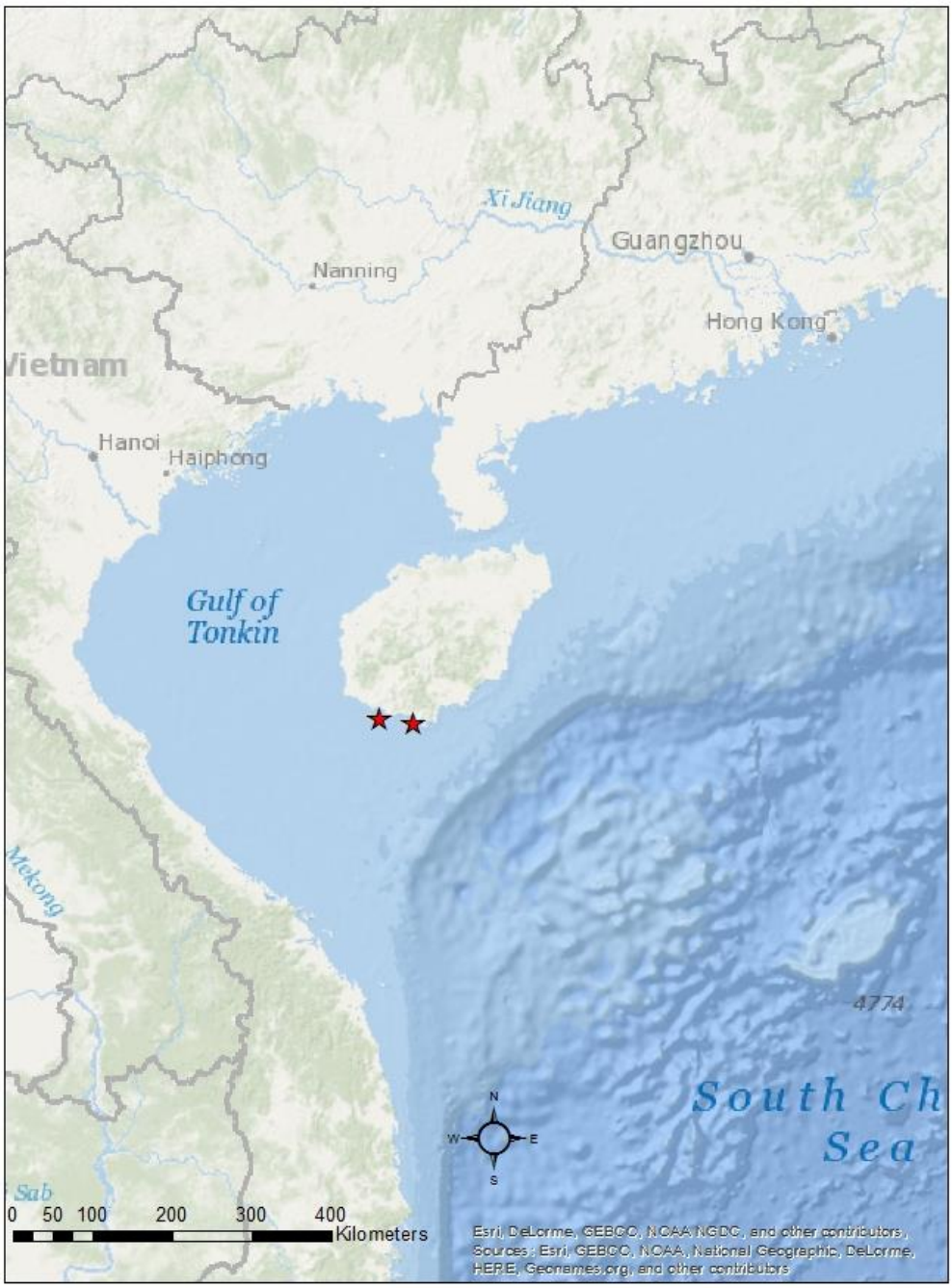

Figure 4. Map of study sites in China at three reef sites (Luhuitou and Xiaodonghai fringing reefs) at Sanya, Hainan Island.

3.3 Field Methods

At each reef site, divers using SCUBA assessed incidences of coral disease by counting colonies exhibiting signs of disease or parasitism, recording the coral taxon affected, a visual description of the disease, and the time spent conducting the survey. Sightings per minute then were calculated to allow comparison among sites. Each diseased coral was photographed to capture the transition between healthy and unhealthy tissue from several angles and as close to the sample as possible. Then each coral was sampled for microbiological and histological analyses. Water temperature and depth also were recorded for each site.

At two sites in Taiwan, Bitou and Yeliu, 14 sets of samples were collected for analysis of carbon-source utilization using Biolog EcoPlate^{TM} methodology. Each sample set included a mucus sample from a lesion and a mucus sample from an apparently healthy region of the coral, as well as water samples near coral colonies from each site. Similarly, at Luhuitou and Xiaodonghai in China, 13 sets of mucus samples (lesion and apparently healthy areas on the same colony) were collected, along with a water sample from each site. Unfortunately, environmental conditions precluded successful analyses of the Luhuitou and Xiaodonghai samples.

For analysis of carbon utilization by microbial assemblages, samples of mucus from an apparently healthy and a diseased section from the same coral, from a nearby healthy coral of the same species (when possible), and from the water column near coral colonies were collected using methods described by Ritchie and Smith (1995a). A 20 ml syringe was lightly tapped against the surface of the coral colony to agitate it enough to release mucus. As the mucus was released, the syringe was drawn until full and then capped.

Samples for DGGE analysis of coral mucus, tissue, and skeleton were taken from apparently healthy and lesioned sections from the same coral, and from the water column, At all sites, pairs of samples (apparently healthy coral tissue and lesion), as well as a water sample, were collected, including 38 pairs from Taiwan sites, and 13 pairs of samples from Hainan. Samples for DGGE analysis were fixed in 70% ethanol. Each sample was collected using a hammer and chisel, transported to shore in its own sample bag, and taken to a laboratory for further processing. For water samples, two liters of water were collected near coral colonies and filtered on site and the filter was fixed in 70% ethanol in sterile containers.

Sixteen samples from Taiwan sites and eight from sites in China were collected and processed for histological examination. Coral tissue samples that included the transition from apparently healthy tissue into the lesion were obtained and fixed in 10% neutral buffered formalin (formaldehyde diluted with freshwater). The ratio of fixative to the sample was 10:1. Each sample was collected using a hammer and chisel, transported to shore in its own sample bag, and then taken to a laboratory for further processing.

3.4 Laboratory Methods

Coral mucus samples, to assess carbon-source utilization, were processed within 5 hours of collection. Sample vials were vortexed using the Fisher Vortex Genie 2 (Fisher Scientific, Pittsburgh, PA) for 30 sec on a medium setting. Then each sample was poured into a 25 mL sterile Biolog Reagent Reservoir (Biolog, 2004a,b). A multi-tip pipetter was used to inoculate each Biolog Ecoplate^{TM} with 150 µl per well. On each Ecoplate^{TM}, the following was recorded: date, sample number, and sample type (i.e., water, or mucus from healthy or diseased tissue). The plates

were scored after 96 hours of incubation at 28° C. In each individual well containing a different carbon source, if microbes used that carbon source then, microbial respiration reduced the tetrazolium dye, resulting in the change of the well color to purple (Biolog, 2004a). Color development in the well, was scored (by eye) as either positive or negative (Frette et al., 2010). A carbon source was determined positive if at least two replicates on the triplicate plate had purple coloration. A carbon source was determined negative if none or one of the replicates of the triplicate had purple coloration. Comparisons were made between: (1) water column samples between sites; (2) apparently healthy individuals of the same taxon, same sites, and between sites; (3) diseased individuals (by disease) from the same taxon, same sites and between sites; and (4) apparently healthy and diseased samples from each coral taxon, each disease sign between individuals, and among sites.

For DGGE, DNA was extracted using the phenol/chloroform method as described by Chiou et al. (2010). DNA and PCR products were verified by agarose gel electrophoresis. The DNA extracted from seawater and coral was amplified by a nested PCR using two pairs of universal bacterial 16S rRNA primers, forward and reverse – 341F and 907R (see Garren et al., 2009 and Kellogg et al., 2012 for actual sequences), and forward and reverse – 27F and 1494R (see Muyzer et al., 1995 and Kellogg et al., 2012 for actual sequences). A GC-clamp was added to primer 341F to increase the separation of DNA bands in DGGE gel (Muzyer et al., 1993). The thermal PCR profile was as follows: initial denaturation at 95° C for 5 min followed by 30 cycles of primer annealing at 55° C for 30 seconds, chain extension for 30 seconds at 72° C, denaturation for 30 seconds at 94° C and a final extension at 72° C for 10 minutes. DGGE was performed using the DGGE System (C.B.S. Scientific Company, Inc.), resolved on 8% (w/v) polyacrylamide gels that contained a 45–80% denaturant gradient at 60° C for 830 minutes with a constant voltage

(115V). Gels were stained with SYBR green (Molecular Probes, Eugene, OR, USA) for 20 min, and photographed for further analysis. Bands were excised from the gel, reamplified, and then sent for direct sequencing. Comparisons were made between: (1) water column samples between sites; (2) apparently healthy individuals of the same taxon, same sites, and between sites; (3) diseased individuals (by disease) from the same taxon, same sites and between sites; and (4) apparently healthy and diseased samples from each coral taxon, each disease sign between individuals, and among sites.

For histological preparation, the specimens were processed in Dr. Yoko Nozawa's lab at Academia Sinica, Biodiversity Research Center, including decalcification, tissue processing, and staining of tissue samples. Coral tissue samples were decalcified using 10% formic acid. All fragments were carefully removed from the decalcifying solution as soon as decalcification was complete to prevent overexposure, which can interfere with staining. The coral tissue was processed on Thermo EXCELSIOP ES automated processor and the protocol for dehydration, clearing, and infiltration is shown in Table 1.

Table 1. Coral tissue processing protocol.

Solution	Time
70% alcohol	30 mins
90% alcohol	30 mins
Absolute alcohol	30 mins
Absolute alcohol	30 mins
Absolute alcohol	30 mins
Xylene	30 mins
Xylene	30 mins
Xylene	30 mins
Paraffin Wax	30 mins
Paraffin Wax	30 mins
Paraffin Wax	30 mins

Tissues were cut at 6 µm using Thermo Fitness 325 rotary microtome. The coral tissue was stained using Thermo VARISTAIN 24-4 automated staining machine and the protocol for staining is shown in Table 2.

Table 2. Coral tissue staining protocol for Gill 2 hematoxylin and eosin y. DW = Deionized water.

Process	Time
1. Xylene Ⅰ	5min
2. Xylene Ⅱ	3min
3. Xylene Ⅲ	3min
4. EtOH 100%	5min
5. EtOH 99.5%	5min
6. EtOH 95%	5min
7. EtOH 70%	5min
8. DW	5min
9. Hematoxy	3:50min
10. Running water	20min
11. <Skip>	<Skip>
12. Running water	15:30min
13. Eosin	1:20min
14. EtOH 70%	10sec
15. EtOH 95%	10sec
16. EtOH 99.5%	10sec
17. EtOH 100%	5min
18. Xylene	5min
19. Xylene	5min
20. Xylene	5min
21. End	----------
	Total time:1hr20min

After staining, coverslips were placed over the tissue samples using Permount (Fisher Scientific) and dried overnight under a hood. The comparison of histological features of healthy and diseased corals was based on features documented by Peters (2016). Comparisons were made between the transitional area (healthy to lesioned) samples from each coral taxon and each disease sign between individuals.

3.5 Data Analysis and Statistical Methods

The survey data were analyzed by summing the number of lesions recorded, then calculating the percent of corals affected by each documented affliction by site and by taxon. A visual description was recorded for each affliction, including pictures with gross descriptions using terminology of Work and Aeby (2006).

Biolog data can be analyzed both descriptively and statistically (Garland and Mills, 1991; Ritchie and Smith, 1995b; Breitbart et al., 2005; Gil-Agudelo et al., 2006a, b). After 96 hours of incubation, I scored each Biolog plate for presence or absence of utilization of each carbon source. Non-parametric multivariate analysis of variance (np-MANOVA) was performed on the presence/absence data to compare results from the water, and the healthy and lesioned coral-mucus samples. All statistical analyses were performed in MATLAB® with the fathom toolbox.

The DGGE data were analyzed by comparing profiles within each lane for each set of samples analyzed, following Chiou et al. (2010) and Meron et al. (2011). Specific bands were then selected for sequencing. Sequence data were assembled using the program SeqMan (DNASTAR, Inc.). The 16S rRNA gene sequences were submitted to NCBI/GenBank databases. The sequences were then compared to those in the GenBank database using the basic local alignment search tool (BLAST) network service (www.ncbi.nlm.nih.gov). Non-parametric multivariate analysis of variance (np-MANOVA) was performed on the presence/absence data of sequences, which were identified in the water, apparently healthy and diseased samples, using MATLAB® with the fathom toolbox. Sequence data were entered as presence or absence and because some sequences were present on more than one gel, that allowed for comparisons between the gels.

Histological data can be analyzed three ways: descriptive, semi-quantitative, or quantitative (Peters, 2004). A descriptive analysis was the best option for this study because

sample quality was variable and numbers of samples were limited. Histological features were categorized and their presence or absence was compared among lesion types, afflicted taxon and site.

4. Results for Coral Disease on Six Reefs in Taiwan and Two Reefs in China

4.1 Survey and Sightings

During coral-lesion surveys around Taiwan in the summer 2012, 57 sightings of coral lesions were recorded (Table 3). Water temperature and depth also were recorded for each site. Roughly half as many sightings per minute were made in the Green Island sites, Chaikou (0.9/min) and Gonguan (0.13/min), in comparison to the four sites in closer proximity to major human populations centers (0.17–0.26/min). Analysis of variance was performed on lesion sightings, which determined that there was no significant difference between sites (Table 4). Lesion categories recorded included discoloration associated with color loss (bleaching), pink discoloration, growth anomalies, and general tissue loss. The latter was the most common coral lesion found (33 sightings). Coral lesions were observed on 12 different taxa, most commonly the genus *Porites* (Figure 5).

Table 3. Sightings of lesions, sightings per effort, and temperature and depth by location. Dis-Pink = Discoloration-Pink Line Syndrome; Dis-Bleach = Discoloration-Bleaching; GA = Growth Anomalies; TL = Tissue Loss.

Site	Dis-Pink	Dis-Bleach	GA	TL	Sightings (#)	Sightings per Minute	Temp (°C)	Depth (m)
Chaikou	0	1	1	3	5	0.09	28	2-5
Gonguan	1	0	1	6	8	0.13	28	2-5
Kihau	4	1	0	5	10	0.17	29	2-4
Shanyuang	0	1	0	6	7	0.26	28	2-3
Bitou	6	2	1	3	12	0.18	29	1-5
Yeliu	5	0	0	10	15	0.25	28	1-4
Luhuitou	0	3	0	5	8	0.12	30.5	2-7
Xiaodonghai	5	0	0	2	7	0.11	30	2-5

Table 4. Analysis of Variance (ANOVA) on sightings of lesions by location.

ANOVA

Source of Variation	*SS*	*df*	*MS*	*F*	*P-value*	*F crit*
Rows	18	7	2.571429	0.644776	0.7145	2.487578

In summer 2013, during a similar coral-lesion survey at sites off Sanya, Hainan Island, 15 coral lesions were recorded (Table 2). Lesion categories noted included discoloration associated with color loss (bleaching), pink discoloration, and general tissue loss. Tissue loss and bleaching were the most common coral lesions observed (7 and 5 sightings, respectively) and were recorded from only four taxa. The most common genera observed to have coral lesions were *Porites* sp. and *Platygyra* sp. (Figure 6).

4.2 Lesion Descriptions

For the purposes of this study, discoloration associated with color loss was characterized as normal tissue bereft of pigmentation overlying normal skeleton (Figures 7A, 8B). The distribution of the lesions varied between focal and diffuse. Pink discoloration was characterized as pink pigmentation of tissue overlying skeleton (Figures 7C, 8A). The distribution of the lesions was focal or multifocal depending on the sample. Edges were annular. Pink discoloration lesions were located centrally or peripherally on the colonies. Growth anomalies were characterized by focal areas of umbonate growths of tissue and/or skeleton (Figure 7B). Lesions were located centrally on the colonies. Tissue loss was characterized by areas bereft of coral tissue leaving recently exposed white skeleton (Figure 7D), with some colonies having algal growth on the skeleton (Figure 8C).

Porites was the most common genus sampled and it was sampled from all sites except Shanyuang (Taiwan) and Xiaodonghai (Hainan) (Figures 5 and 6). Genera sampled at Xiaodonghai were not observed at any of the other sites. The Hainan sites had the least amount of diversity of samples collected with only two genera per site. Three to five genera were sampled per site in Taiwan.

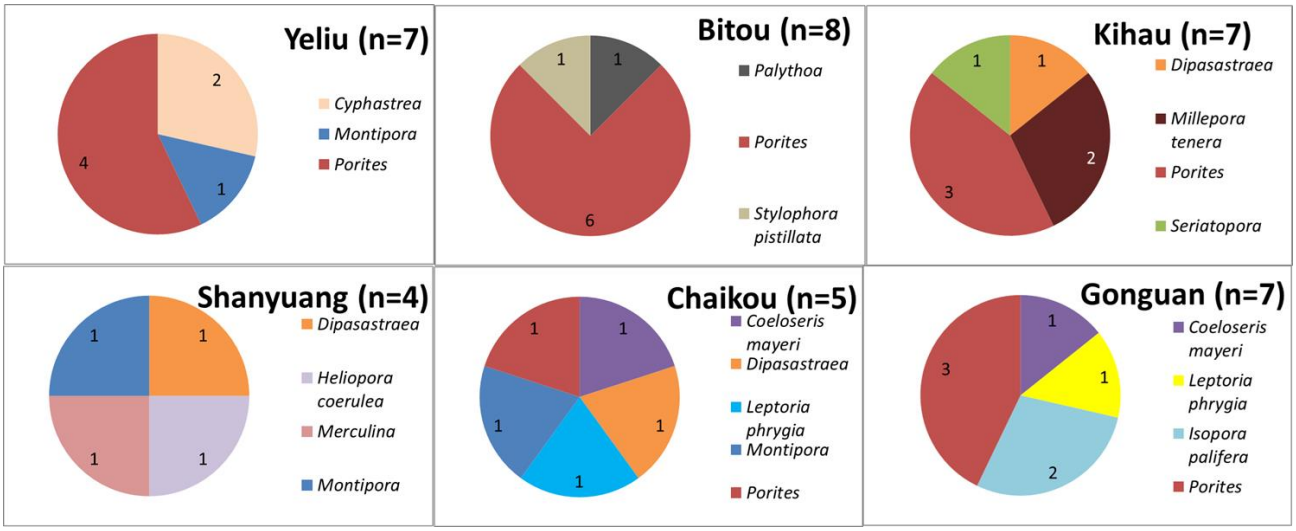

Figure 5. Samples by taxa at each study site in Taiwan. *Favia* in the Indo-Pacific is now referred to as *Dipsastraea* (Budd et al., 2012).

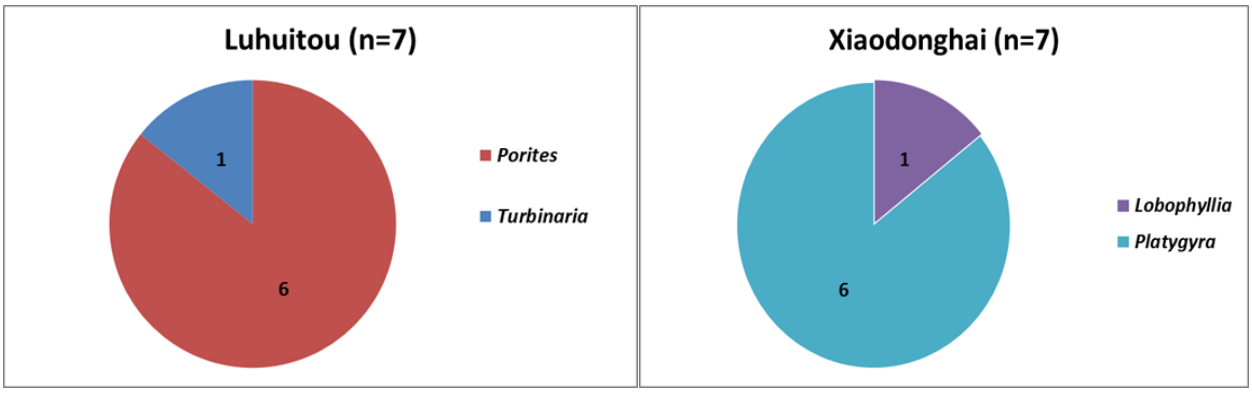

Figure 6. Samples by taxa at each study site in Hainan.

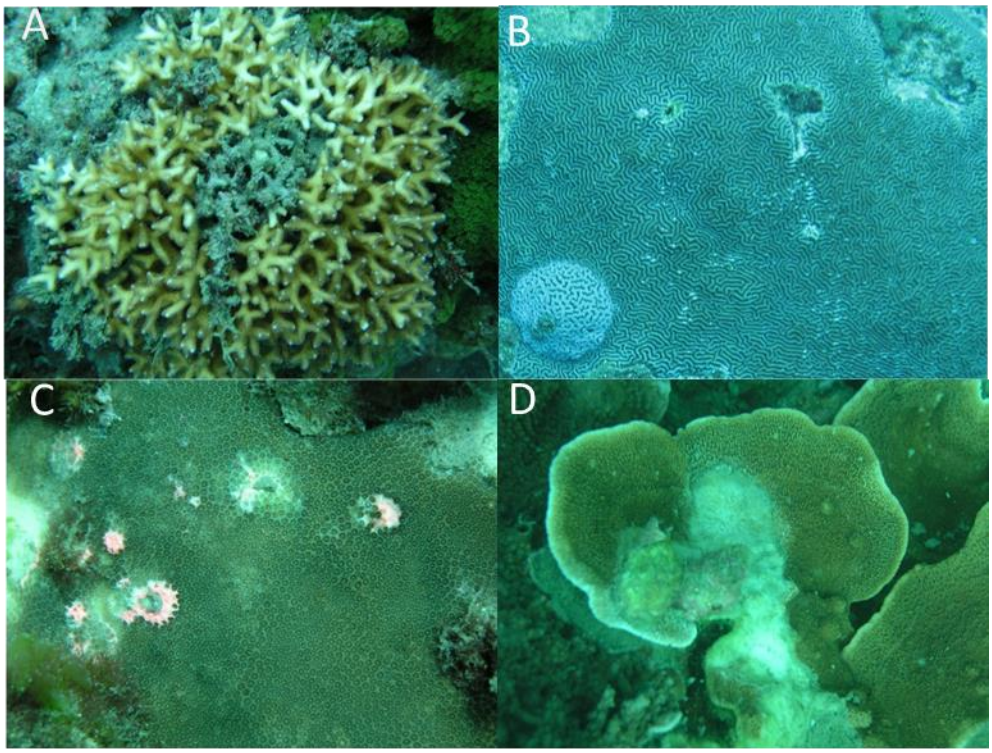

Figure 7. Examples of lesions seen on corals surveyed in Taiwan in 2012: (A) *Seriatopora* colony exhibiting color loss. (B) *Leptoria* colony exhibiting growth anomalies. (C) *Porites* colony exhibiting pink lines. (D) *Montipora* colony exhibiting tissue loss.

Figure 8. Examples of lesions seen on corals surveyed in Hainan in 2013: (A) *Porites* colony exhibiting pink discoloration. (B) *Platygyra* colony exhibiting color loss. (C) *Turbinaria* colony exhibiting tissue loss with algae colonizing the skeleton.

4.3 Carbon-Source Utilization

In Taiwan, two water samples and 14 sets of mucus samples were collected at two sites, Bitou and Yeliu, and analyzed for carbon-source utilization. Eleven of the 14 sets had positive carbon utilization. The number of positive records for each carbon source under each set of conditions (water, mucus from healthy tissue and mucus from lesion-afflicted tissue) was tallied and reported as percent of total possible (Tables 5 and 6). A significant difference was found between the carbon utilization by the microbial community within the water column, and the microbial community from healthy and lesion-afflicted areas on the coral ($p = 0.002$). Water samples utilized the fewest carbon sources. The four most used carbon sources within a lesion were glycogen (79%), D-mannitol (64%), alpha-cyclodextrin (57%), and N-acetyl-D-glucosamine (57%) (Table 5). Microbes in the mucus from lesioned areas utilized 22 out of 26 carbon sources (106 positive records) more than twice as often (Figure 9) as microbes from mucus from healthy polyps (23 out of 26 carbon sources; 50 positive records).

Non-parametric multivariate analysis of variance (NP-MANOVA) and pair-wise NP-MANOVA tests were performed to determine if significant differences could be identified based on the site (Table 7), sample type (water, apparently healthy, lesion) (Table 8, 9), and affliction (Table 10, 11). NP-MANOVA showed that between sites carbon source usage was not significantly different ($p = 0.138$) (Table 7), while carbon source usage was significantly different ($p = 0.002$) between sample types (Table 8). ANOVA showed significant differences between samples from apparently healthy and lesion-afflicted corals ($p = 1.32E-11$) (Table 9). Among afflictions, no differences in carbon source usage were detected (Table 10, 11).

Canonical analyses of principal coordinates (CAPs) were performed to visualize dissimilarity based on site (Figure 10), sample type (water, apparently healthy, lesion) (Figure 11),

and affliction (Figure 12). SIMPER was performed to determine what sequences were contributing the most to differences (Table 12).

Table 5. Percent of positive records for each carbon source under each set of conditions (water N = 6, apparently healthy mucus N = 14, or lesion mucus N = 14). Orange = amines/amides, Blue = Amino acids, Green = carbohydrates, Pink = Carboxylic Acids, Yellow = Polymers, Burgundy = Miscellaneous.

Carbon Sources	Water Total %	Healthy Total %	Disease Total %
phenylethylamine	0	7	0
putrescine	0	7	7
glycyl-L-glutamic acid	0	21	36
L-arginine	0	7	0
L-asparagine	0	14	43
L-phenylalanine	0	7	21
L-serine	0	0	21
L-threonine	0	21	21
alpha-D-lactose	0	14	0
B-methyl-D-glucoside	0	7	21
D-cellobiose	0	28	50
D-mannitol	0	36	64
i-erythritol	0	7	0
N-acetyl-D-glucosamine	17	21	57
gamma-hydroxybutryic acid	0	7	14
D-galactonic acid/gamma lactone	0	0	7
D-galacturonic acid	0	7	7
D-glucosaminic acid	0	7	21
itaconic acid	0	0	14
alpha-cyclodextrin	0	36	57
glycogen	33	36	79
Tween 40	0	7	42
Tween 80	0	21	50
D,L-alpha-glycerol phosphate	0	14	36
glucose-1-phosphate	0	7	43
Pyruvic acid methyl ester	17	21	43

Table 6. Summary of carbon source utilization by site, sample type (water, apparently healthy, diseased), and affliction type. Site: B = Bitou Y = Yeliu. HDW: H = healthy, D = diseased, W = water. AFF: W = water, P = pink discoloration, G = growth anomalies, T = tissue loss. Black rectangle indicates that the carbon source was utilized.

B-methyl-D-glucoside																											
D-galctonic acid/gamma lactone																											
L-arginine																											
Pyruvic acid methyl ester																											
D-galacturonic acid																											
L-asparagine																											
Tween 40																											
i-erythritol																											
L-phenylalanine																											
Tween 80																											
D-mannitol																											
L-serine																											
alpha-cyclodextrin																											
N-acetyl-D-glucosamine																											
gamma-hydroxybutryic acid																											
L-threonine																											
glycogen																											
D-glucosaminic acid																											
itaconic acid																											
glycyl-L-glutamic acid																											
D-cellobiose																											
glucose-1-phosphate																											
phenylethylamine																											
alpha-D-lactose																											
D,L-alpha-glycerol phosphate																											
putrescine																											
Site	B	B	B	Y	Y	Y	B	B	B	B	B	Y	Y	Y	Y	Y	Y	B	B	B	B	B	Y	Y	Y	Y	Y	Y
HDW	W	W	W	W	W	W	H	H	H	H	H	H	H	H	H	H	H	D	D	D	D	D	D	D	D	D	D	D
AFF	W	W	W	W	W	W	P	G	T	P	T	T	T	P	T	P	T	P	G	T	P	P	P	T	P	T	P	T

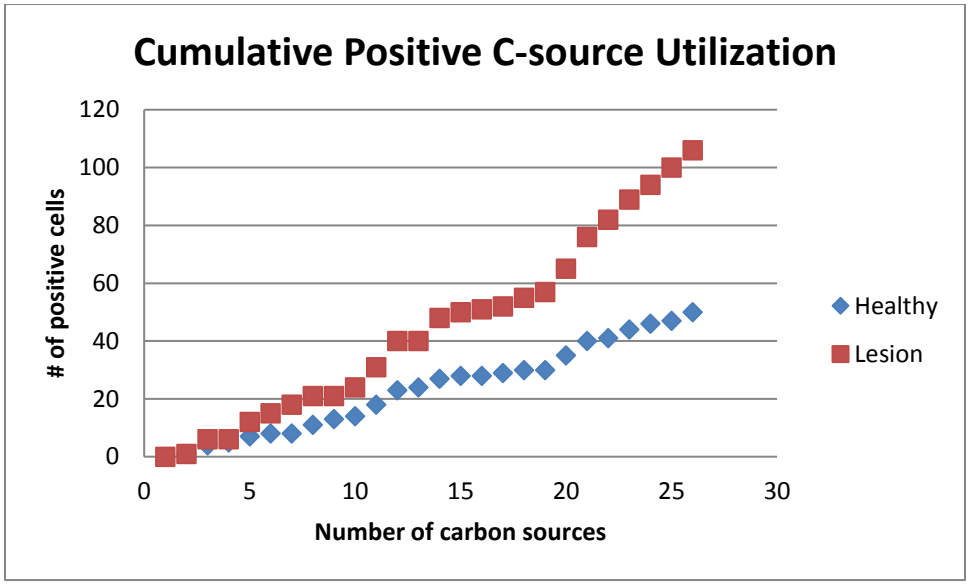

Figure 9. Cumulative positive carbon source utilization of microbial assemblages in healthy and lesioned areas.

Table 7. Non-parametric multivariate analysis of variance (NP_MANOVA) on the basis of Bray-Curtis dissimilarities for carbon-source utilization based on site.

```
================================================
    Nonparametric (Permutation-based) MANOVA:
------------------------------------------------
    'Source'      'df'    'SS'         'MS'         'F'        'p'
    'factor 1'    [ 1]    [0.44]       [0.44]       [1.76]     [0.14]
    'residual'    [26]    [ 6.5]       [0.25]       [ NaN]     [  NaN]
    'total'       [27]    [ 6.9]       [ NaN]       [ NaN]     [  NaN]
```

Table 8. Non-parametric multivariate analysis of variance (NP_MANOVA) on the basis of Bray-Curtis dissimilarities for carbon-source utilization based on sample type (water, healthy, disease).

```
================================================
    Nonparametric (Permutation-based) MANOVA:
------------------------------------------------
    'Source'      'df'    'SS'         'MS'        'F'         'p'
    'factor 1'    [ 2]    [2.008]      [1.004]     [5.04]      [0.002]
    'residual'    [25]    [4.9]        [ 0.19]     [   NaN]    [  NaN]
    'total'       [27]    [6.9]        [   NaN]    [   NaN]    [  NaN]
```

Table 9. Analysis of variance (ANOVA) of carbon utilization by healthy and diseased samples.

ANOVA

	df	*SS*	*MS*	*F*	*Significance F*
Regression	1	577	577	143	1.32E-11
Residual	25	101	4.03		
Total	26	678			

Table 10. Non-parametric multivariate analysis of variance (NP_MANOVA) on the basis of Bray-Curtis dissimilarities for carbon-source utilization based on lesion (pink discoloration, growth anomalies, tissue loss, and water samples).

```
================================================
    Nonparametric (Permutation-based) MANOVA:
------------------------------------------------
    'Source'      'df'    'SS'         'MS'         'F'         'p'
    'factor 1'    [ 3]    [2.2]        [0.72]       [3.6]       [0.001]
    'residual'    [24]    [4.8]        [0.201]      [   NaN]    [  NaN]
    'total'       [27]    [6.9]        [    NaN]    [   NaN]    [  NaN]
```

Table 11. Pair-wise multivariate analysis of variance (PW_MANOVA) on the basis of Bray-Curtis dissimilarities for carbon-source utilization based on lesion (pink discoloration=1, growth anomalies=2, tissue loss=3, and water samples=4). Bold= significant.

Results of pair-wise comparisons between each factor level:

	t:	p:	p_bon:	p_ds:	p_holm:
1 vs. 2:	1.248	0.058	0.348	0.301	0.174
1 vs. 3:	0.824	0.675	1.000	0.999	0.675
1 vs. 4:	**2.549**	**0.004**	**0.024**	**0.024**	**0.024**
2 vs. 3:	1.079	0.296	1.000	0.878	0.592
2 vs. 4:	**5.419**	**0.028**	**0.168**	**0.157**	**0.112**
3 vs. 4:	**2.782**	**0.006**	**0.036**	**0.036**	**0.030**

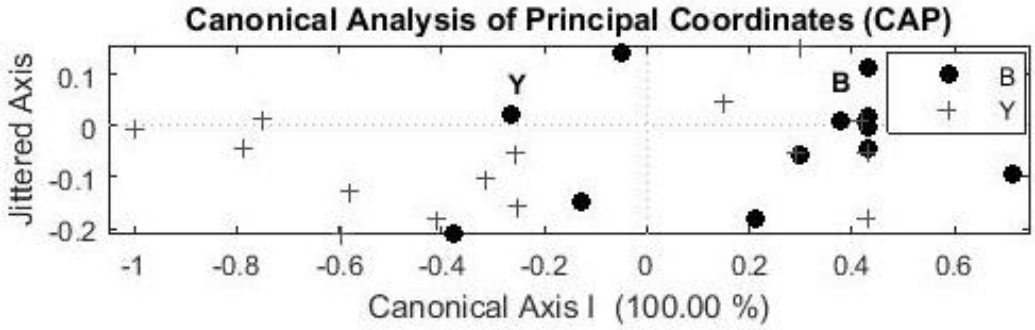

Figure 10. Canonical analysis of principal coordinates location on the basis of Bray-Curtis dissimilarities for carbon-source utilization based on site. B=Bitou and Y=Yeliu.

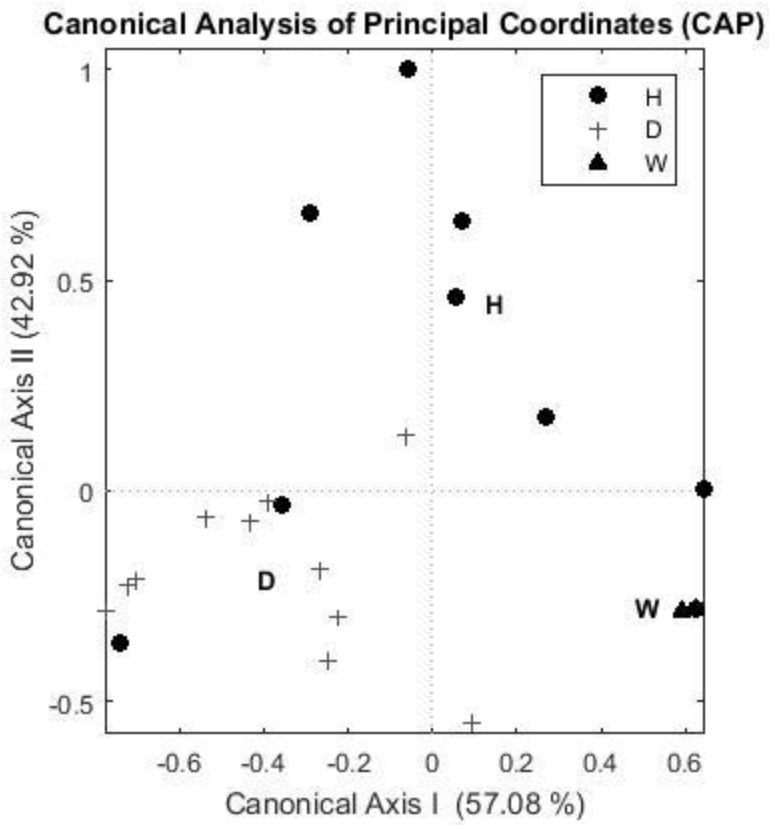

Figure 11. Canonical analysis of principal coordinates location on the basis of Bray-Curtis dissimilarities for carbon-source utilization based on sample type. H = apparently healthy D = disease W = water.

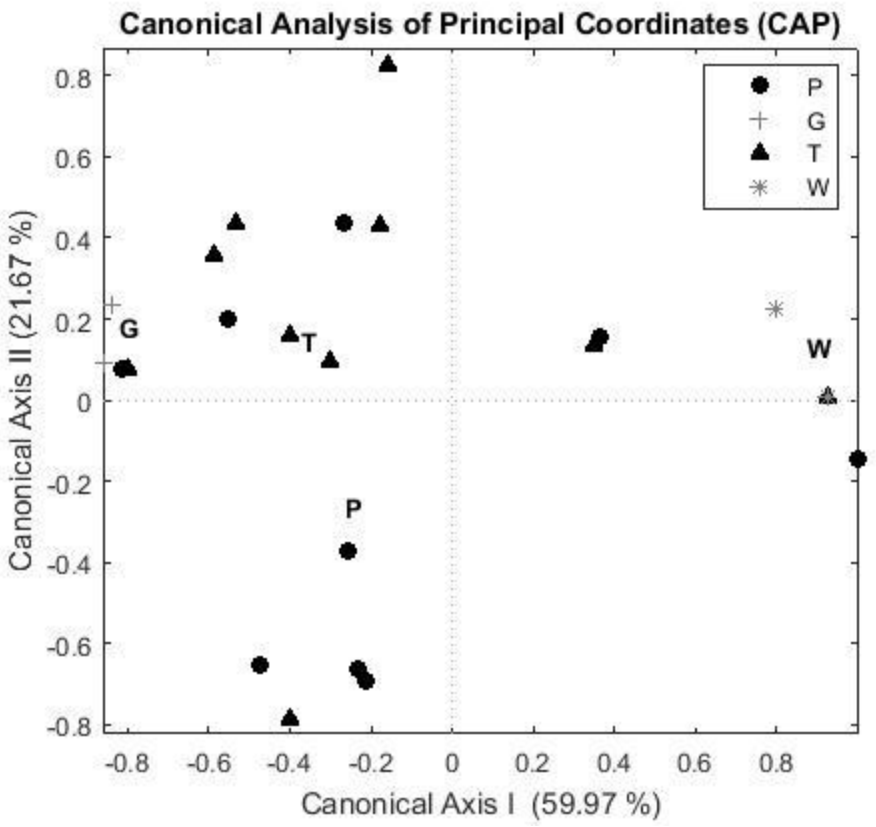

Figure 12. Canonical analysis of principal coordinates location on the basis of Bray-Curtis dissimilarities for carbon utilization based on lesion. P = pink discoloration, G = growth anomalies, T = tissue loss, and W = water.

Table 12. SIMPER results on Biolog EcoPlate™ displaying the different tests, average dissimilarity, the top three carbon sources, and their cumulative percentage. B = Bitou, Y = Yeliu, H = apparently healthy, D = diseased, W = water, P = pink discoloration, G = growth anomalies, T = tissue loss.

			Top 3 Carbon Sources			
	Tests	Average Dissimilarity	1	2	3	Cum. %
Sites	B v. Y	0.68	D-mannitol	Glycogen	Alpha-cyclodextrin	28.95
Sample	H v. D	0.68	Glycogen	Alpha-cyclodextrin	N-acetyl-D-glucosamine	22.79
	H v. W	0.76	Glycogen	D-mannitol	Alpha-cyclodextrin	49.08
	D v. W	0.73	D-mannitol	Alpha-cyclodextrin	L-asparagine	30.61
Affliction	P v. G	0.64	D-galacturonic acid	Gamma-hydroxybutric acid	L-serine	19.84
	P v. T	0.67	Alpha-cyclodextrin	D-mannitol	Glycogen	27.71
	P v. W	0.72	Alpha-cyclodextrin	D-mannitol	Glycogen	43.85
	G v. T	0.58	D-galacturonic acid	L-serine	Gamma-hydroxybutric acid	19.61
	G v. W	0.87	D-galacturonic acid	L-asparagine	Tween 40	17.15
	T v. W	0.74	D-mannitol	Glycogen	Tween 80	36.22

4.4 DGGE Analysis

In data from Taiwan, the DGGE ribotypes showed a distinct difference in the bacterial profiles in the water column, compared to the apparently healthy and lesioned areas of the corals sampled (Figure 13 and Appendix 3). Bacterial communities differed among water samples, despite the close proximity of some sites. Bacterial communities also differed among apparently healthy areas of corals from the same species. The numbers of bacterial ribotypes from the seawater sample at each site were slightly higher compared to the samples collected from apparently healthy and lesioned corals (Table 13), and the ribotypes were different between samples collected from apparently healthy and lesioned corals. There was no significant difference between the number of ribotypes between the water column, apparently healthy, and lesioned corals (Table 14). Bacterial communities also differed in samples from apparently healthy and abnormal areas of coral from the same colony. A table was generated for each gel to show the ribotypes sequenced to identify bacteria present in samples (Table 15 and Appendix 3).

In data from the Hainan sites, the DGGE ribotypes also showed very similar patterns to those found in the DGGE data from Taiwan reefs (See Appendix 3). A table was generated for each gel to show the ribotypes sequenced to identify bacteria present in samples (Appendix 3).

Table 13. Summary data from bacterial ribotypes counted in the water column, apparently healthy, and lesioned corals from all sites.

SUMMARY

Groups	*Count*	*Sum*	*Average*	*Variance*
Water	14	114	8.1	12.1
Healthy	34	249	7.3	16.3
Lesion	36	259	7.2	10.6

Table 14. Analysis of variance (ANOVA) on bacterial ribotypes counted in the water column, apparently healthy, and lesioned corals from all sites.

ANOVA

Source of Variation	*SS*	*df*	*MS*	*F*	*P-value*	*F crit*
Between Groups	9.4	2	4.7	0.4	0.7	3.1
Within Groups	1068.8	81	13.2			
Total	1078.2	83				

4.5 Sequence Analysis

In the samples from Taiwan, 85 sequences were analyzed from 42 samples. The DGGE ribotypes showed distinct bacterial communities among water samples, apparently healthy tissue and lesions. The most common sequences identified were uncultured bacteria, although information on their sources and most related bacteria could be obtained. Slightly more bacteria were identified in water samples than in the coral samples. Several sequences were identified that were closely related to environmental and human factors, including *Microbacterium* sp., *Bacillus* sp., and *Geobacillus thermolevorans*, which have been found in sewage sludge (the first two) and irritable bowel syndrome within humans. Four sequences were noted to be highly related (>91%) to *Vibrio* spp., a genus of bacteria that has long been associated with coral diseases, in particular bleaching and the white syndromes. Five sequences were closely related (>99%) to *Clostridium* sp., which has also been associated with coral diseases, including white plague and black band disease.

In the samples from Hainan, 24 sequences were analyzed from 13 samples. Although there was some variation of the DGGE ribotypes, many appeared to be shared between water samples,

apparently healthy tissue and lesions. Again, the most common sequences identified were uncultured bacteria. Two of the uncultured bacterial ribotypes identified have been found in a human gastrointestinal tract with irritable bowel syndrome. One of the ribotypes was highly related to a bacterium found in white patch syndrome in *Porites* sp. in the Western Indian Ocean. Some other sequences were identified as being closely related to environmental and human factors including *Bacillus* sp., which have been found in sludge, and uncultured bacteria found in shrimp ponds.

NP-MANOVA (Tables 16, 17, 19, 21, 23, 25) pair-wise MANOVA (Tables 18, 20, 22, 24, 26) and CAP (Figures 14-17) were performed to determine if differences were significant based on the location, site, affliction, sample type (water, apparently healthy, diseased), affliction and taxa. SIMPER analyses (Table 27) was performed to determine what sequences were contributing the most to the significant difference and the nearest phylogenetic relative of the accession number is presented in Table 28.

The NP-MANOVA showed that there was a significant difference ($p = 0.001$) between the bacterial assemblages in samples from Taiwan and Hainan (Table 16). The NP-MANOVA also showed a significant difference ($p = 0.001$) between the bacterial assemblages in samples from all eight sites (Table 17) and each site was significantly different from all others (Table 18). The NP-MANOVA shows that there was a significant difference in the bacterial assemblages ($p = 0.019$) between sample types (water, apparently healthy, and lesioned) (Table 19); however, the pair-wise MANOVA showed that the water sample was significantly different from the apparently healthy (0.006) and lesioned ($p = 0.003$) samples, but the apparently healthy and lesioned samples were not significantly different ($p = 0.831$) from each other (Table 20). The NP-MANOVA revealed a significant difference in the bacterial assemblages ($p = 0.001$) between afflictions (tissue loss, pink

discoloration, color loss, growth anomalies, and water) (Table 21); however, the pair-wise MANOVA showed that only the pink discoloration assemblages were significantly different from bacteria found inthe other afflictions (tissue loss p = 0.001; color loss p = 0.012; growth anomalies p = 0.001, p = 0.009) (Table 22). The NP-MANOVA showed that there was a significant difference in the bacterial assemblages (p = 0.001) among taxa (Table 25); however, the pair-wise MANOVA showed that only *Porites* (vs. *Millepora* p = 0.03, *Lobophilla* p = 0.001, *Turbinaria* p = 0.047, *Stylophora* p = 0.005, *Heliopora* p = 0.003*), Millepora* (vs. *Lobophilla* p = 0.028, *Turbinaria* p = 0.011, *Heliopora* p = 0.015), *Lobophyllia* (*vs. Turbinaria* p = 0.004, *Montipora* p = 0.017, *Coeloseris* p = 0.012, *Isopora* p = 0.031, *Cyphastrea* p = 0.031, *Palythoa* p = 0.029, *Stylophora* p = 0.017, *Heliopora* p = 0.001*)* were significantly different from some of the other taxa (Table 26). It is also important to note that *Millepora, Palythoa,* and *Heliopora* are not true corals; however they were included in the study because sequences were successfully collected from them, were shared with coral species, and contributed to the bacterial assemblage analyses of this project.

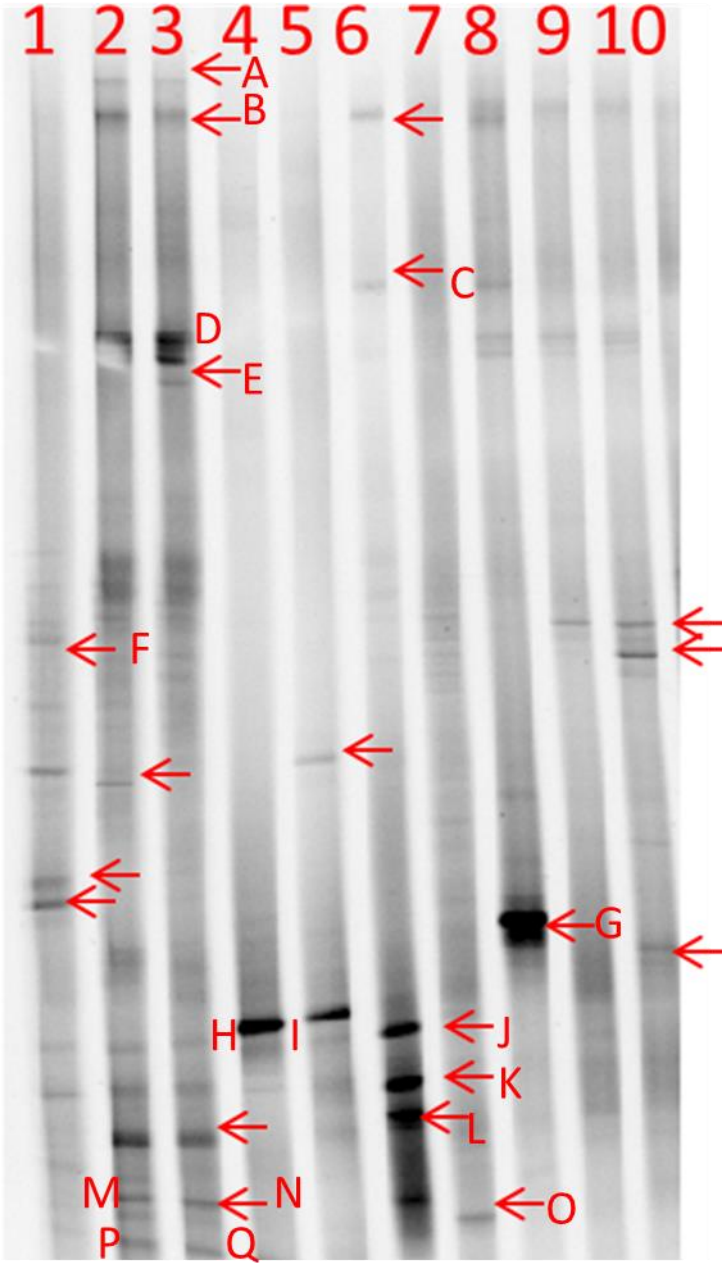

Figure 13. Denaturing gradient gel electrophoresis (DGGE) (45-80% gradient at 60° C for 830 minutes with a constant voltage (115V)) profiles of 16S rRNA gene showing that coral associated bacteria vary between coral tissue in an apparently healthy area and abnormal area and their surrounding water column. Lane 1: Yeliu water sample. Lane 2 and 3: *Porites* sp. exhibiting pink discoloration (apparently healthy and Abnormal) Lane 4 and 5: *Cyphastrea* sp. (Both apparently healthy but from a colony exhibiting tissue loss). Lane 6: *Montipora* sp. (apparently healthy but from a colony exhibiting tissue loss). Lane 7 and 8: *Porite*s sp. Exhibiting tissue loss (apparently healthy and abnormal). Lane 9 and 10: *Porite*s sp. Exhibiting pink discoloration (apparently healthy and abnormal). Red arrows indicate DGGE bands that were cut and sent for sequencing, red letters indicate positive sequences.

Table 15. BLAST analysis of the 16S rRNA bands from Figure 13.

Band Letter	Accession no.	Nearest phylogenetic relative	% similarity
A	FJ463701.1	Ruegeria sp. HDEN30 16S ribosomal RNA gene, partial sequence	79
B	FJ463701.1	Ruegeria sp. HDEN30 16S ribosomal RNA gene, partial sequence	78
C	AB470961.1	Clostridium sp. r53 gene for 16S rRNA, partial sequence	99
D	KJ616372.1	Ruegeria sp. BC13-4 16S ribosomal RNA gene, partial sequence	99
E	HQ439523.1	Ruegeria sp. MR31c 16S ribosomal RNA gene, partial sequence	97
F	KM218876.1	Leptolyngbya sp. UMPCCC 1239 16S ribosomal RNA gene, partial sequence	83
G	KC527502.1	Uncultured bacterium clone Thai14_H04 16S ribosomal RNA gene, partial sequence	100
H	KF465059.1	Uncultured Methylophilus sp. clone DVBSD_M101 16S ribosomal RNA gene, partial sequence	99
I	KM083548.1	Methylophilus sp. R-NB-8 16S ribosomal RNA gene, partial sequence	99
J	AB470961.1	Clostridium sp. r53 gene for 16S rRNA, partial sequence	99
K	AB470961.2	Clostridium sp. r53 gene for 16S rRNA, partial sequence	100
L	AB470961.1	Clostridium sp. r53 gene for 16S rRNA, partial sequence	99
M	KC429860.1	Ruegeria sp. JZ08ML53 16S ribosomal RNA gene, partial sequence	98
N	KC429860.1	Ruegeria sp. JZ08ML53 16S ribosomal RNA gene, partial sequence	98
O	KF180030.1	Uncultured bacterium clone RSAE3C49 16S ribosomal RNA gene, partial sequence	99
P	KF786699.1	Uncultured Rhodobacteraceae bacterium clone S1-7-18 16S ribosomal RNA gene, partial sequence	95
Q	KF179796.1	Uncultured bacterium clone REU1C12 16S ribosomal RNA gene, partial sequence	99

Table 16. Non-parametric multivariate analysis of variance (NP_MANOVA) on the basis of Bray-Curtis dissimilarities for bacterial assemblages based on location (Taiwan and Hainan).

```
================================================

     Nonparametric (Permutation-based) MANOVA:
 --------------------------------------------------
     'Source'      'df'    'SS'         'MS'          'F'          'p'
     'factor 1'    [ 1]    [3.4272]     [ 3.4272]     [8.3854]     [0.001]
     'residual'    [66]    [26.975]     [0.40871]     [   NaN]     [  NaN]
     'total'       [67]    [30.402]     [    NaN]     [   NaN]     [  NaN]
```

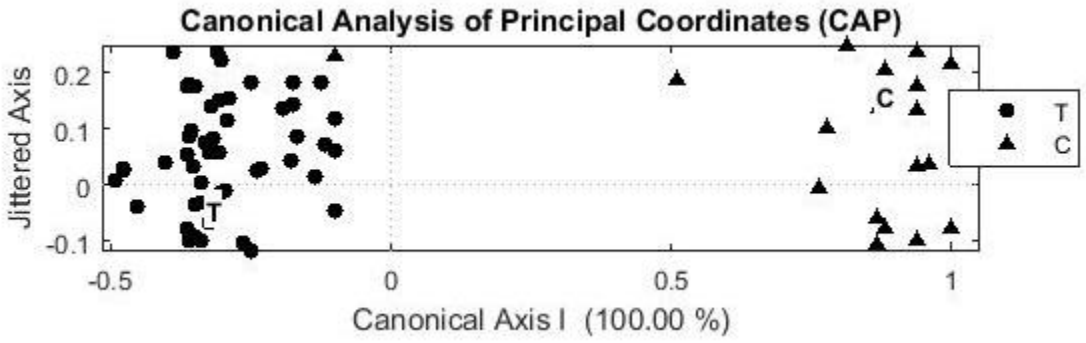

Figure 14. Canonical Analysis of Principal Coordinates Location on the basis of Bray-Curtis dissimilarities for bacterial assemblages based on location from Yeliu. T=Taiwan and C=Hainan.

Table 17. Non-parametric multivariate analysis of variance (NP_MANOVA) on the basis of Bray-Curtis dissimilarities for bacterial assemblages based on site.

```
================================================

    Nonparametric (Permutation-based) MANOVA:
 ------------------------------------------------
    'Source'      'df'    'SS'        'MS'         'F'         'p'
    'factor 1'    [ 7]    [16.6]      [ 2.36]      [  10.2]    [0.001]
    'residual'    [60]    [13.9]      [0.231]      [   NaN]    [  NaN]
    'total'       [67]    [30.4]      [  NaN]      [   NaN]    [  NaN]
 ---------------------------------------------------------------------------
```

Table 18. Pair-wise multivariate analysis of variance (PW_MANOVA) on the basis of Bray-Curtis dissimilarities for bacterial assemblages based on site. (1= Kihau, 2=Chaikou, 3=Shanyuang, 4= Yeliu, 5= Bitou, 6=Gonguan, 7=Luhuitou, 8=Xiaodonghai). Bold= significant.

```
 ----------------------------------------------------------
 Results of pair-wise comparisons between each factor level:
 ==========================================================
          t:     p:     p_bon: p_ds:  p_holm:
 1 vs. 2: 2.2027 0.0020 0.0560 0.0545 0.0280
 1 vs. 3: 3.1844 0.0060 0.1680 0.1551 0.0280
 1 vs. 4: 2.1499 0.0020 0.0560 0.0545 0.0280
 1 vs. 5: 4.4464 0.0010 0.0280 0.0276 0.0280
 1 vs. 6: 2.0552 0.0020 0.0560 0.0545 0.0280
 1 vs. 7: 4.4164 0.0010 0.0280 0.0276 0.0280
 1 vs. 8: 3.4446 0.0010 0.0280 0.0276 0.0280
 2 vs. 3: 2.2028 0.0010 0.0280 0.0276 0.0280
 2 vs. 4: 1.5532 0.0020 0.0560 0.0545 0.0280
 2 vs. 5: 3.4326 0.0010 0.0280 0.0276 0.0280
 2 vs. 6: 1.4042 0.0150 0.4200 0.3450 0.0300
 2 vs. 7: 3.1454 0.0010 0.0280 0.0276 0.0280
 2 vs. 8: 2.5984 0.0010 0.0280 0.0276 0.0280
 3 vs. 4: 2.1917 0.0010 0.0280 0.0276 0.0280
 3 vs. 5: 4.7043 0.0010 0.0280 0.0276 0.0280
 3 vs. 6: 1.5769 0.0250 0.7000 0.5078 0.0300
 3 vs. 7: 5.7916 0.0010 0.0280 0.0276 0.0280
 3 vs. 8: 3.7746 0.0010 0.0280 0.0276 0.0280
 4 vs. 5: 3.4121 0.0010 0.0280 0.0276 0.0280
 4 vs. 6: 1.4659 0.0040 0.1120 0.1062 0.0280
 4 vs. 7: 3.0395 0.0010 0.0280 0.0276 0.0280
 4 vs. 8: 2.5590 0.0010 0.0280 0.0276 0.0280
 5 vs. 6: 3.2762 0.0010 0.0280 0.0276 0.0280
 5 vs. 7: 6.0827 0.0010 0.0280 0.0276 0.0280
 5 vs. 8: 5.1196 0.0010 0.0280 0.0276 0.0280
 6 vs. 7: 3.1228 0.0020 0.0560 0.0545 0.0280
 6 vs. 8: 2.5258 0.0010 0.0280 0.0276 0.0280
 7 vs. 8: 4.8473 0.0010 0.0280 0.0276 0.0280
 ----------------------------------------------------------
 t      = t-statistic
 p      = unadjusted p-value
 p_bon  = Bonferroni adjusted p-value
 p_ds   = Dunn-Sidak adjusted p-value
 p_holm = Holms adjusted p-value
```

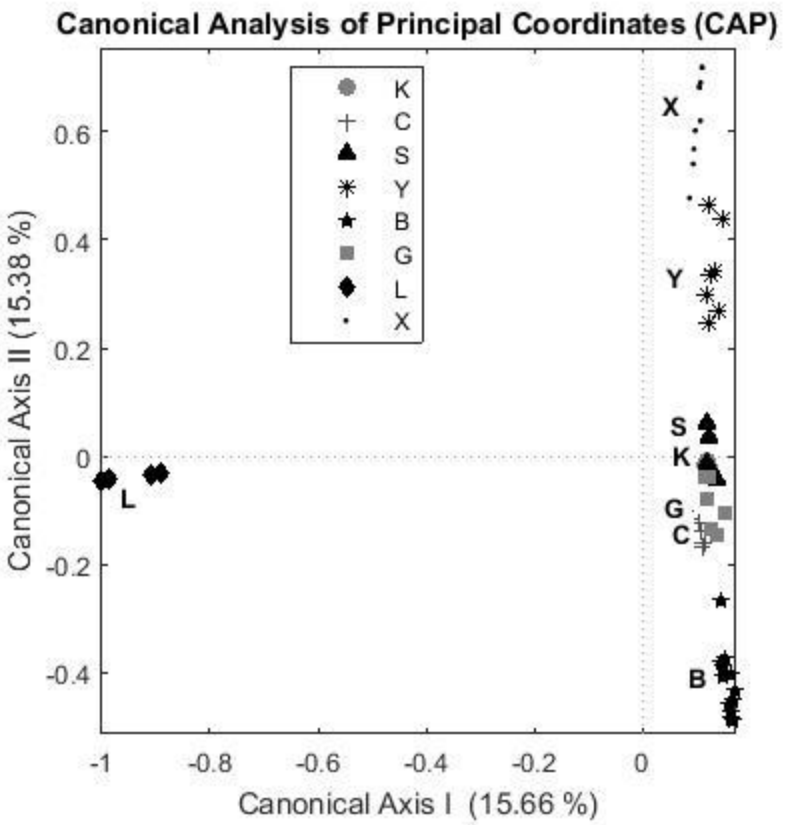

Figure 15. Canonical Analysis of Principal Coordinates Location on the basis of Bray-Curtis dissimilarities for bacterial assemblages based on site. (K= Kihau, C=Chaikou, S=Shanyuang, Y= Yeliu, B= Bitou, G=Gonguan, L=Luhuitou, X=Xiaodonghai).

Table 19. Non-parametric multivariate analysis of variance (NP_MANOVA) on the basis of Bray-Curtis dissimilarities for bacterial assemblages based on sample type. (Water, apparently healthy, disease).

```
================================================
    Nonparametric (Permutation-based) MANOVA:
------------------------------------------------
    'Source'      'df'    'SS'        'MS'         'F'          'p'
    'factor 1'    [ 2]    [1.51]      [0.753]      [1.69]       [0.019]
    'residual'    [65]    [28.9]      [0.444]      [   NaN]     [  NaN]
    'total'       [67]    [30.4]      [  NaN]      [   NaN]     [  NaN]
```

Table 20. Pair-wise multivariate analysis of variance (PW_MANOVA) on the basis of Bray-Curtis dissimilarities for bacterial assemblages based on sample type. (1 = apparently healthy, 2 = disease, 3 = water). Bold= significant.

Results of pair-wise comparisons between each factor level:					
	t:	p:	p_bon:	p_ds:	p_holm:
1 vs. 2:	0.804	0.831	1.000	0.995	0.831
1 vs. 3:	**1.58**	**0.006**	**0.018**	**0.018**	**0.012**
2 vs. 3:	**1.63**	**0.003**	**0.009**	**0.009**	**0.009**

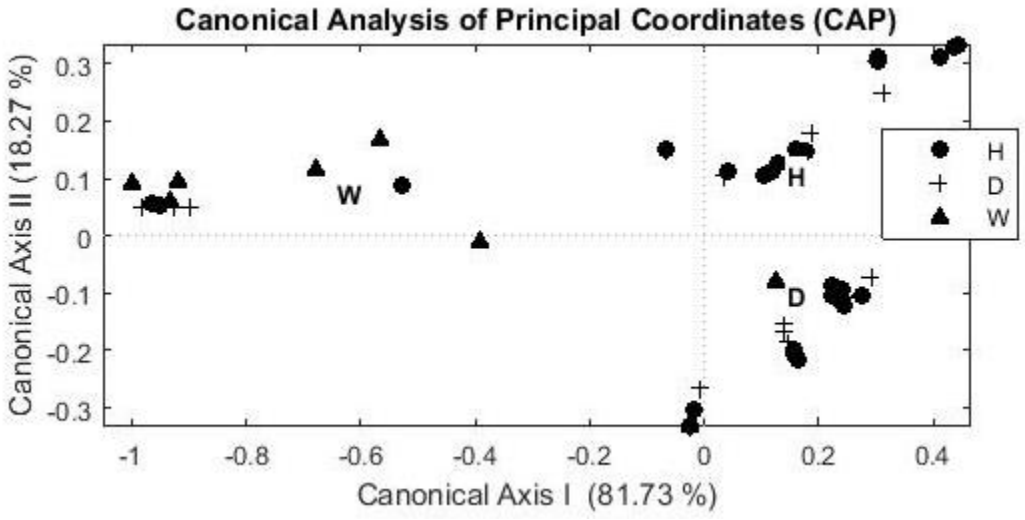

Figure 16. Canonical Analysis of Principal Coordinates Location on the basis of Bray-Curtis dissimilarities for bacterial assemblages based on sample type. (Apparently healthy, diseased, water).

Table 21. Non-parametric multivariate analysis of variance (NP_MANOVA) on the basis of Bray-Curtis dissimilarities for bacterial assemblages based on lesion. (Tissue loss, pink discoloration, color loss, and growth anomalies.

Nonparametric (Permutation-based) MANOVA:					
'Source'	'df'	'SS'	'MS'	'F'	'p'
'factor 1'	[4]	[4.52]	[1.13]	[2.75]	[0.001]
'residual'	[63]	[25.9]	[0.412]	[NaN]	[NaN]
'total'	[67]	[30.4]	[NaN]	[NaN]	[NaN]

Table 22. Pair-wise multivariate analysis of variance (PW_MANOVA) on the basis of Bray-Curtis dissimilarities for bacterial assemblages based on lesion and surrounding water. (1 = tissue loss, 2 = pink discoloration, 3 = color loss, 4 = growth anomalies, 5 = water). Bold= significant.

Results of pair-wise comparisons between each factor level:

	t:	p:	p_bon:	p_ds:	p_holm:
1 vs. 2:	**2.20**	**0.001**	**0.010**	**0.010**	**0.010**
1 vs. 3:	0.987	0.324	1.000	0.980	0.324
1 vs. 4:	1.29	0.064	0.640	0.484	0.192
1 vs. 5:	**1.94**	**0.001**	**0.010**	**0.010**	**0.010**
2 vs. 3:	**1.76**	**0.012**	**0.120**	**0.114**	**0.060**
2 vs. 4:	**1.92**	**0.001**	**0.010**	**0.010**	**0.010**
2 vs. 5:	**1.91**	**0.005**	**0.050**	**0.049**	**0.035**
3 vs. 4:	1.23	0.070	0.700	0.516	0.192
3 vs. 5:	**1.80**	**0.025**	**0.250**	**0.224**	**0.100**
4 vs. 5:	**1.45**	**0.009**	**0.09Z**	**0.086**	**0.054**

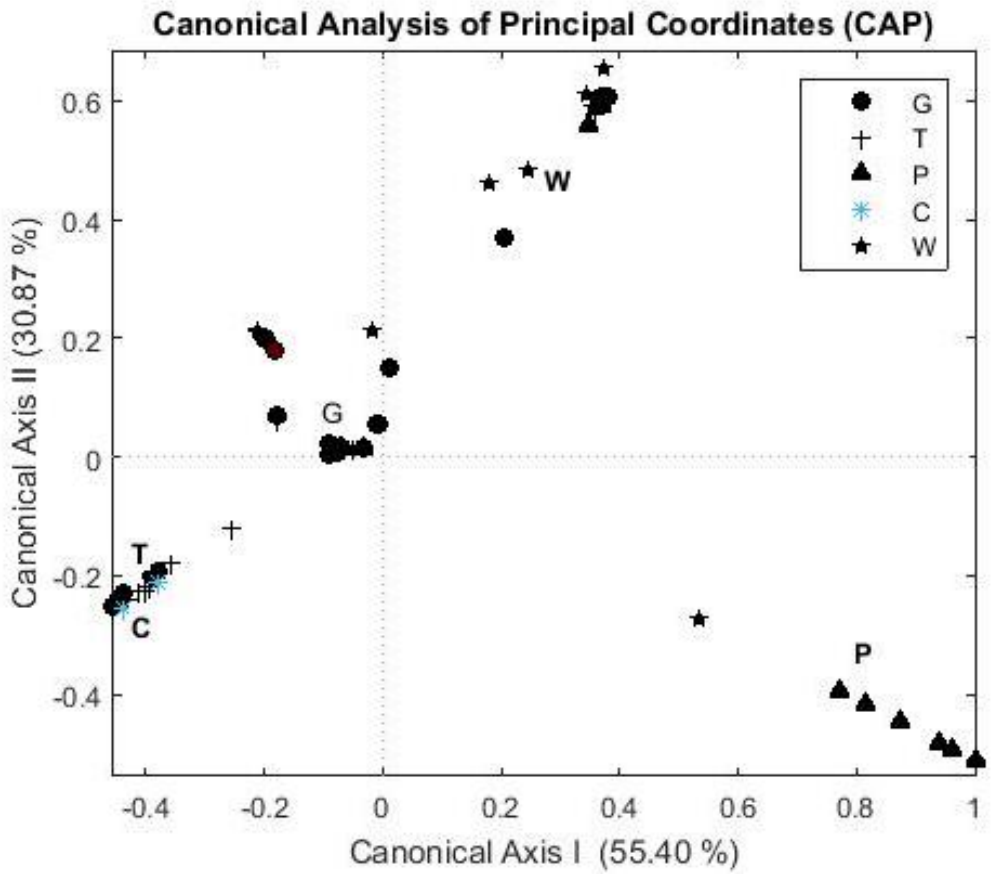

Figure 17. Canonical Analysis of Principal Coordinates Location on the basis of Bray-Curtis dissimilarities for bacterial assemblages based on lesion and surrounding water. (T = tissue loss, P = pink discoloration, C = color loss, G = growth anomalies, W = water).

Table 23. Non-parametric multivariate analysis of variance (NP_MANOVA) on the basis of Bray-Curtis dissimilarities for bacterial assemblages based on these lesions: tissue loss, pink discoloration, and color loss.

```
================================================
    Nonparametric (Permutation-based) MANOVA:
------------------------------------------------
    'Source'      'df'    'SS'        'MS'         'F'         'p'
    'factor 1'    [ 2]    [ 2.69]     [ 1.35]      [3.16]      [0.001]
    'residual'    [55]    [23.39]     [0.425]      [ NaN]      [  NaN]
    'total'       [57]    [26.09]     [  NaN]      [ NaN]      [  NaN]
```

Table 24. Pair-wise multivariate analysis of variance (PW_MANOVA) on the basis of Bray-Curtis dissimilarities for bacterial assemblages based on lesion. (1 = tissue loss, 2 = pink discoloration, 3 = color loss). Bold= significant.

```
----------------------------------------------------------
Results of pair-wise comparisons between each factor level:
==========================================================
         t:     p:     p_bon: p_ds:  p_holm:
1 vs. 2: 2.202  0.001  0.003  0.003  0.003
1 vs. 3: 1.29   0.076  0.228  0.211  0.076
2 vs. 3: 1.93   0.001  0.003  0.003  0.003
----------------------------------------------------------
t      = t-statistic
p      = unadjusted p-value
p_bon  = Bonferroni adjusted p-value
p_ds   = Dunn-Sidak adjusted p-value
p_holm = Holms adjusted p-value
```

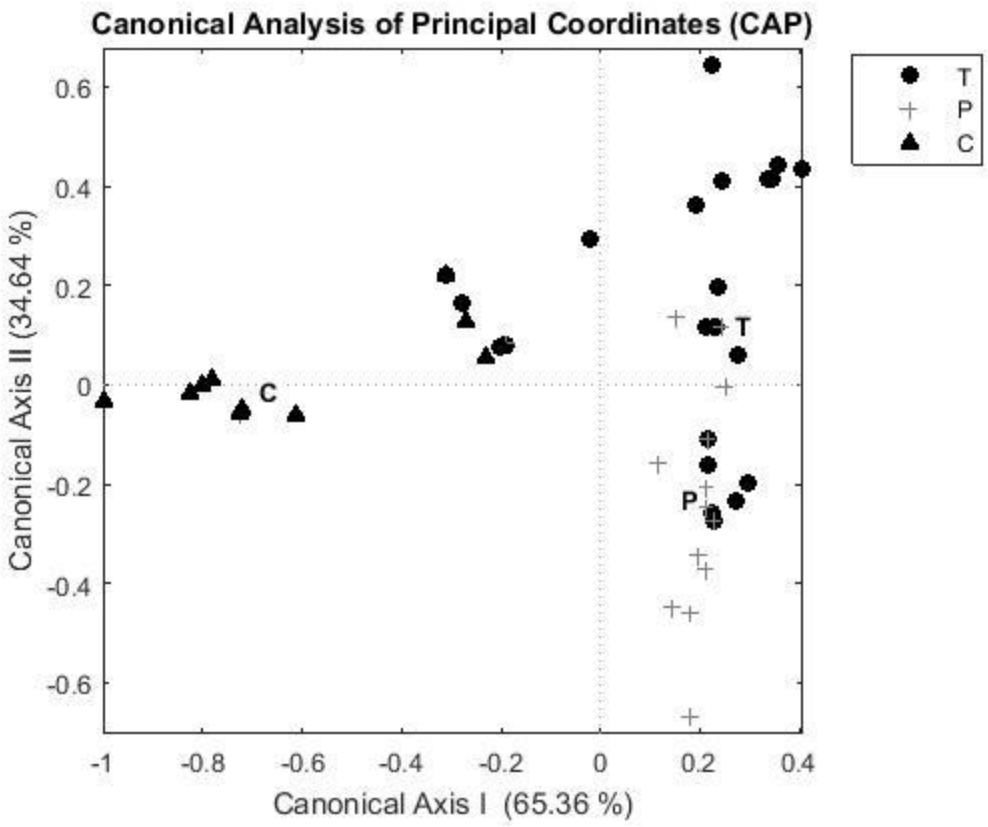

Figure 18. Canonical Analysis of Principal Coordinates Location on the basis of Bray-Curtis dissimilarities for bacterial assemblages based on lesion. (T = tissue loss, P = pink discoloration, C = color loss).

Table 25. Non-parametric multivariate analysis of variance (NP_MANOVA) on the basis of Bray-Curtis dissimilarities for bacterial assemblages based on taxa.

```
================================================
    Nonparametric (Permutation-based) MANOVA:
------------------------------------------------
    'Source'      'df'    'SS'        'MS'         'F'         'p'
    'factor 1'    [11]    [9.7723]    [0.88839]    [2.4115]    [0.001]
    'residual'    [56]    [ 20.63]    [0.36839]    [   NaN]    [  NaN]
    'total'       [67]    [30.402]    [    NaN]    [   NaN]    [  NaN]
```

Table 26. Pair-wise multivariate analysis of variance (PW_MANOVA) on the basis of Bray-Curtis dissimilarities for bacterial assemblages based on taxa. (1 = *Porites*, 2 = *Millepora*, 3 = *Lobophyllia*, 4 = *Platygyra*, 5 = *Turbinaria*, 6 = *Montipora*, 7 = *Coeloseris*, 8 = *Isopora*, 9 = *Cyphastrea*, 10 = *Palythoa*, 11 = *Stylophora*, 12 = *Heliopora*). Only significant differences are shown. See appendix 2 for full table.

```
------------------------------------------------------------
Results of pair-wise comparisons between each factor level:
============================================================
          t:     p:     p_bon: p_ds:  p_holm:
1 vs. 2: 1.4507 0.0300 1.0000 0.8661 1.0000
1 vs. 3: 2.4813 0.0010 0.0660 0.0639 0.0660
1 vs. 5: 1.3791 0.0470 1.0000 0.9583 1.0000
1 vs. 11: 1.5750 0.0050 0.3300 0.2817 0.3100
1 vs. 12: 1.8127 0.0030 0.1980 0.1799 0.1920
2 vs. 3: 4.4467 0.0280 1.0000 0.8465 1.0000
2 vs. 5: 1.5457 0.0110 0.7260 0.5181 0.6710
2 vs. 12: 1.8998 0.0150 0.9900 0.6312 0.8850
3 vs. 5: 2.5185 0.0040 0.2640 0.2324 0.2520
3 vs. 6: 2.4649 0.0170 1.0000 0.6775 0.9860
3 vs. 7: 2.4649 0.0120 0.7920 0.5492 0.7200
3 vs. 8: 2.6366 0.0310 1.0000 0.8749 1.0000
3 vs. 9: 4.0871 0.0310 1.0000 0.8749 1.0000
3 vs. 10: 4.6319 0.0290 1.0000 0.8566 1.0000
3 vs. 11: 4.5633 0.0170 1.0000 0.6775 0.9860
3 vs. 12: 2.9278 0.0010 0.0660 0.0639 0.0660
------------------------------------------------------------
```

Table 27. SIMPER results on DGGE displaying the different tests, average dissimilarity, the top three accession numbers, and their cumulative percentage. B = Bitou, Y = Yeliu, H = Healthy, D = Diseased, W = Water, P = Pink discoloration, G = Growth Anomalies, T = Tissue Loss.

			Top 3 Accession Numbers			
	Tests	Average Dissimilarity	1	2	3	Cum. %
Location	T v. C	1	KF180115.1	HM598135.1	KF373144.1	22.95
Site	K v. C	0.99	KF180115.1	JX173559.1	KC668734.1	34.24
	K v. S	0.94	JF344173.1	JN672323.1	KF180115.1	31.33
	K v. Y	0.99	KF180115.1	JX173559.1	KC668734.1	30.59
	K v. B	1	KF180115.1	HQ290092.1	LN832981.1	31.75
	K v. G	0.97	KF180115.1	JX173559.1	KC668734.1	30.62
	K v. L	1	KF180115.1	HQ754673.1	JX173559.1	44.26
	K v. X	1	KF180115.1	HM598135.1	KF373144.1	39.06
	C v. S	0.94	JF344173.1	JN672323.1	AM913948.1	37.45
	C v. Y	1	KT266806.1	AB470961.2	GU118822.1	22.46
	C v. B	1	HQ290092.1	LN832981.1	KT626460.1	36.24
	C v. G	0.97	KF180034.1	JF344173.1	KT266806.1	25.69
	C v. L	1	KF180115.1	HQ754673.1	KT266806.1	49.46
	C v. X	1	HM598135.1	KF373144.1	KT266806.1	41.69
	S v. Y	0.96	JF344173.1	JN672323.1	AM913948.1	33.54
	S v. B	0.99	JF344173.1	JN672323.1	HQ290092.1	30.23
	S v. G	0.78	JN672323.1	AM913948.1	JF344173.1	30.94
	S v. L	1	JF344173.1	JN672323.1	KF180115.1	42.83
	S v. X	1	JF344173.1	JN672323.1	HM598135.1	39.15
	Y v. B	1	HQ290092.1	LN832981.1	KT626460.1	32.41
	Y v. G	0.99	KF180034.1	JF344173.1	EU372890.1	21.86
	Y v. L	1	KF180115.1	HQ754673.1	AB470961.2	42.99
	Y v. X	1	HM598135.1	KF373144.1	AB470961.2	36.35
	B v. G	0.99	HQ290092.1	LN832981.1	KT626460.1	32.03
	B v. L	1	KF180115.1	HQ290092.1	LN832981.1	43.58
	B v. X	1	HQ290092.1	HM598135.1	LN832981.1	39.07
	G v. L	1	KF180115.1	HQ754673.1	KF180034.1	43.96
	G v. X	1	HM598135.1	KF373144.1	KF180034.1	37.29
	L v. X	1	KF180115.1	HM598135.1	HQ754673.1	60.56
Sample	H v. D	0.92	HQ290092.1	LN832981.1	HM598135.1	16.68
	H v. W	0.95	JN672323.1	KT266806.1	JF344173.1	20.58
	D v. W	0.94	JN672323.1	KT266806.1	JF344173.1	21.22
Affliction	P v. C	0.97	HM598135.1	HQ290092.1	LN832981.1	24.57
	P v. T	0.92	HQ290092.1	LN832981.1	KF180115.1	20.12
	C v. T	0.99	HM598135.1	KF373144.1	KF180115.1	24.14

Table 28. Top SIMPER results on DGGE displaying the accession number, nearest phylogenetic relative, and the source of the sample.

Accession Number	Nearest phylogenetic relative	Source
KF180115.1	Uncultured bacterium clone RSAE6C25 16S ribosomal RNA gene, partial sequence	Healthy tissue *Porites lutea*
JF344173.1	Uncultured alpha proteobacterium clone PET-049 16S ribosomal RNA gene	Petroleum spot over marine sediments
KT266806.1	Geobacillus thermoparaffinivorans strain TH1 16S ribosomal RNA gene, partial sequence	Pig manure (China)
HQ290092.1	Vibrio sp. GHt1-4 16S ribosomal RNA gene, partial sequence	Intertidal zone South China Sea
KF180034.1	Uncultured bacterium clone RSAE3C53 16S ribosomal RNA gene, partial	PWSP infected tissue
HM598135.1	Uncultured bacterium clone SCS_HX21_57 16S ribosomal RNA gene, partial sequence	Surface sediment sample (South China Sea)
JN672323.1	Uncultured bacterium clone GBL1046d01 16S ribosomal RNA gene, partial sequence	Tan microbial mat from lava tube wall

Table 29. (*following 2 pages*) Summary of BLAST analysis of the 16S rRNA bands by location, site, sample type (water, healthy, disease), taxa and affliction type. LOC: T = Taiwan, C = China. Site: K = Kihau, C = Chaikou, S = Shanyuang, Y = Yeliu, B = Bitou, G = Gonguan, L = Luhuitou, X = Xiaodonghai. HDW: H = healthy, D = diseased, W = water. AFF: W = water, P = pink discoloration, G = growth anomalies, T = tissue loss. Black rectangle indicates that the ribotype (nearest phylogenetic relative) was present in the sample.

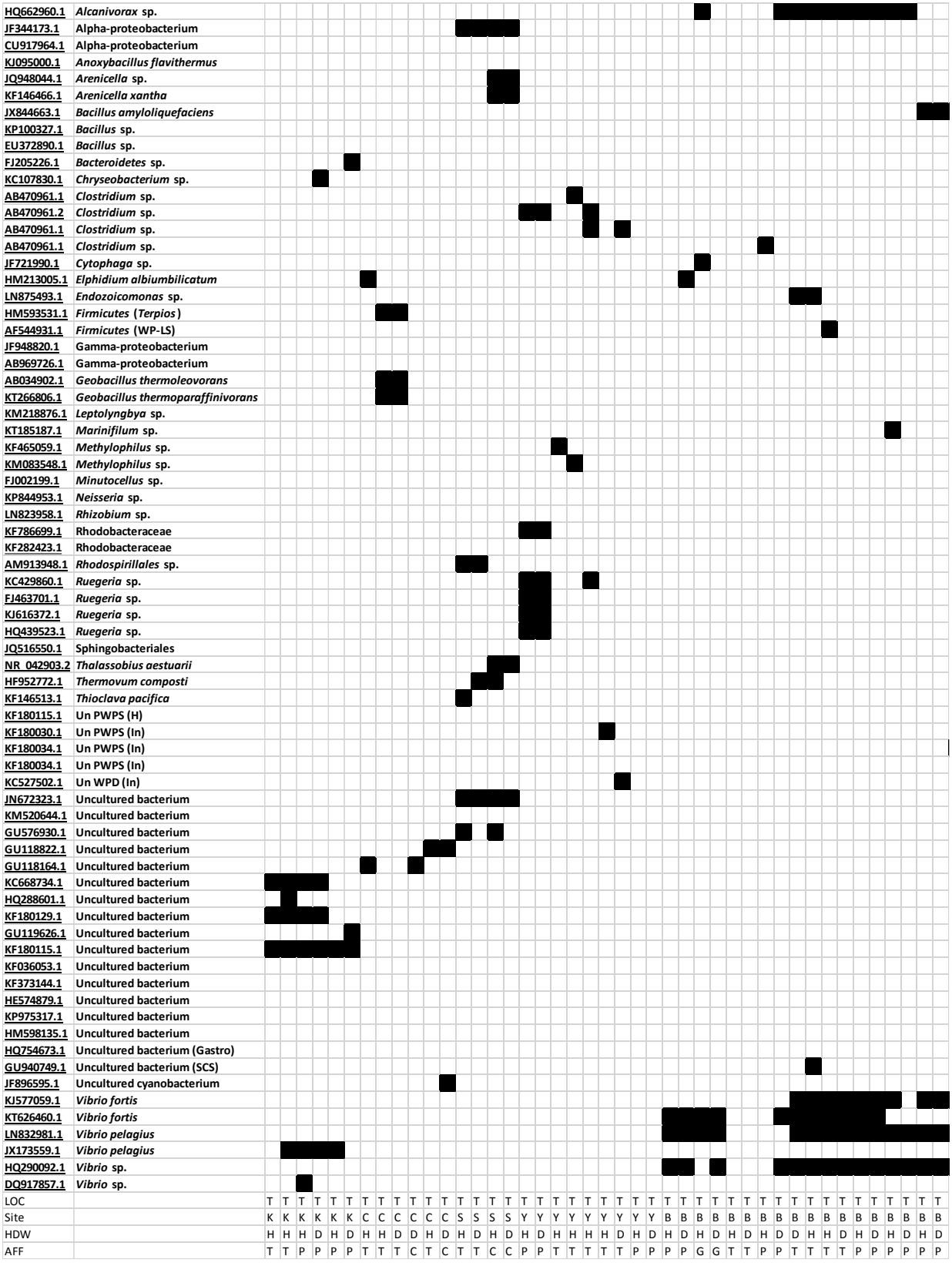
HQ662960.1 Alcanivorax sp.
JF344173.1 Alpha-proteobacterium
CU917964.1 Alpha-proteobacterium
KJ095000.1 Anoxybacillus flavithermus
JQ948044.1 Arenicella sp.
KF146466.1 Arenicella xantha
JX844663.1 Bacillus amyloliquefaciens
KP100327.1 Bacillus sp.
EU372890.1 Bacillus sp.
FJ205226.1 Bacteroidetes sp.
KC107830.1 Chryseobacterium sp.
AB470961.1 Clostridium sp.
AB470961.2 Clostridium sp.
AB470961.1 Clostridium sp.
AB470961.1 Clostridium sp.
JF721990.1 Cytophaga sp.
HM213005.1 Elphidium albiumbilicatum
LN875493.1 Endozoicomonas sp.
HM593531.1 Firmicutes (Terpios)
AF544931.1 Firmicutes (WP-LS)
JF948820.1 Gamma-proteobacterium
AB969726.1 Gamma-proteobacterium
AB034902.1 Geobacillus thermoleovorans
KT266806.1 Geobacillus thermoparaffinivorans
KM218876.1 Leptolyngbya sp.
KT185187.1 Marinifilum sp.
KF465059.1 Methylophilus sp.
KM083548.1 Methylophilus sp.
FJ002199.1 Minutocellus sp.
KP844953.1 Neisseria sp.
LN823958.1 Rhizobium sp.
KF786699.1 Rhodobacteraceae
KF282423.1 Rhodobacteraceae
AM913948.1 Rhodospirillales sp.
KC429860.1 Ruegeria sp.
FJ463701.1 Ruegeria sp.
KJ616372.1 Ruegeria sp.
HQ439523.1 Ruegeria sp.
JQ516550.1 Sphingobacteriales
NR_042903.2 Thalassobius aestuarii
HF952772.1 Thermovum composti
KF146513.1 Thioclava pacifica
KF180115.1 Un PWPS (H)
KF180030.1 Un PWPS (In)
KF180034.1 Un PWPS (In)
KF180034.1 Un PWPS (In)
KC527502.1 Un WPD (In)
JN672323.1 Uncultured bacterium
KM520644.1 Uncultured bacterium
GU576930.1 Uncultured bacterium
GU118822.1 Uncultured bacterium
GU118164.1 Uncultured bacterium
KC668734.1 Uncultured bacterium
HQ288601.1 Uncultured bacterium
KF180129.1 Uncultured bacterium
GU119626.1 Uncultured bacterium
KF180115.1 Uncultured bacterium
KF036053.1 Uncultured bacterium
KF373144.1 Uncultured bacterium
HE574879.1 Uncultured bacterium
KP975317.1 Uncultured bacterium
HM598135.1 Uncultured bacterium
HQ754673.1 Uncultured bacterium (Gastro)
GU940749.1 Uncultured bacterium (SCS)
JF896595.1 Uncultured cyanobacterium
KJ577059.1 Vibrio fortis
KT626460.1 Vibrio fortis
LN832981.1 Vibrio pelagius
JX173559.1 Vibrio pelagius
HQ290092.1 Vibrio sp.
DQ917857.1 Vibrio sp.
LOC T T T T T T T T T T T T T T T T T T T T T T T T T T T T T T T T T T T T T T T T T T T T T T
Site K K K K K K C C C C C C C S S S S S Y Y Y Y Y Y Y Y Y B B B B B B B B B B B B B B B B B B B
HDW H H H D H D H H D D D H D H D H D H D H D H H H H D H D H D D H D H D H D H D H D H D H D
AFF T T P P P P T T T C T C T T C C P P T T T T T P P P G G T T P P T T T T P P P P P P

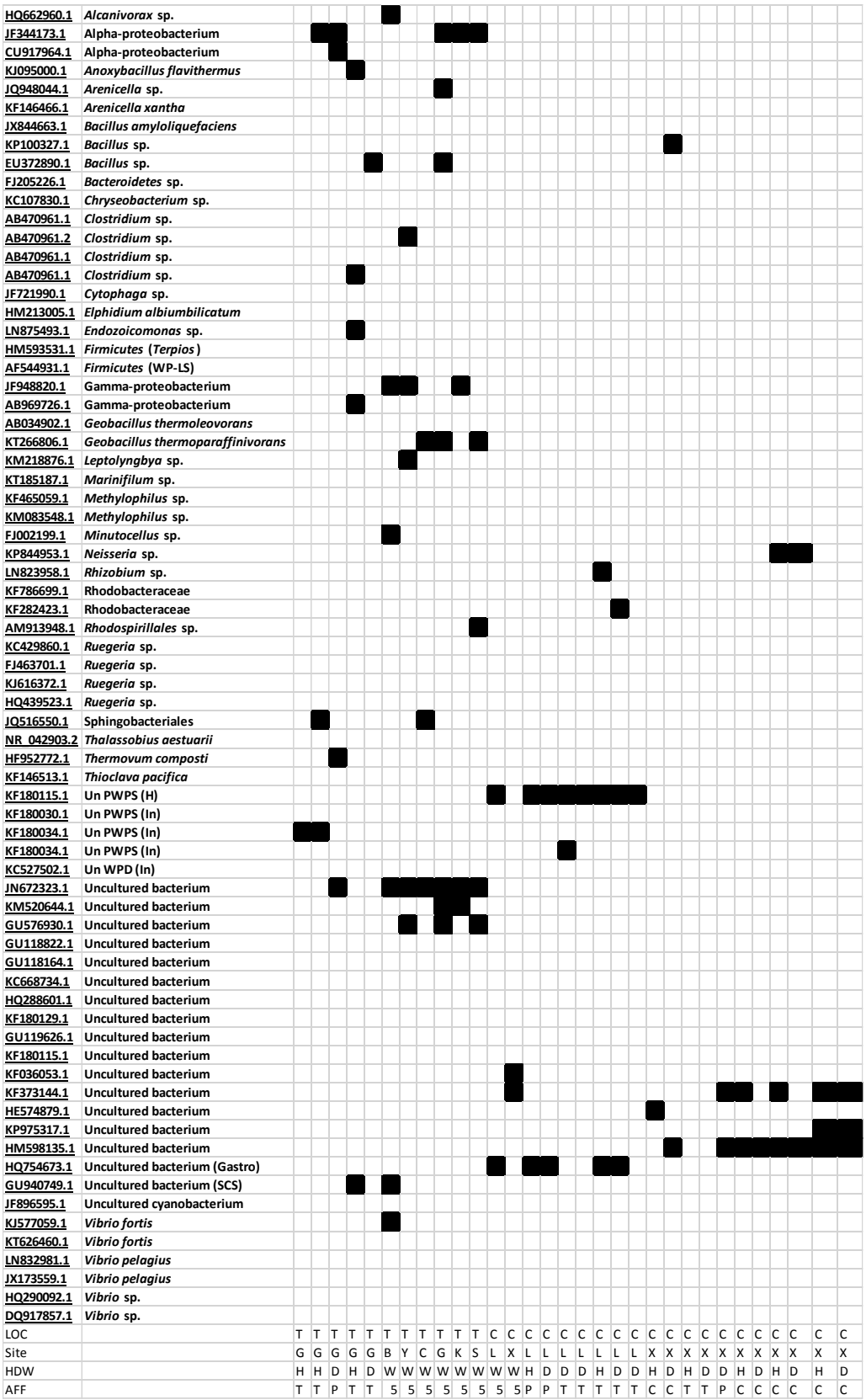

HQ662960.1	*Alcanivorax* sp.																																
JF344173.1	Alpha-proteobacterium																																
CU917964.1	Alpha-proteobacterium																																
KJ095000.1	*Anoxybacillus flavithermus*																																
JQ948044.1	*Arenicella* sp.																																
KF146466.1	*Arenicella xantha*																																
JX844663.1	*Bacillus amyloliquefaciens*																																
KP100327.1	*Bacillus* sp.																																
EU372890.1	*Bacillus* sp.																																
FJ205226.1	*Bacteroidetes* sp.																																
KC107830.1	*Chryseobacterium* sp.																																
AB470961.1	*Clostridium* sp.																																
AB470961.2	*Clostridium* sp.																																
AB470961.1	*Clostridium* sp.																																
AB470961.1	*Clostridium* sp.																																
JF721990.1	*Cytophaga* sp.																																
HM213005.1	*Elphidium albiumbilicatum*																																
LN875493.1	*Endozoicomonas* sp.																																
HM593531.1	*Firmicutes* (*Terpios*)																																
AF544931.1	*Firmicutes* (WP-LS)																																
JF948820.1	Gamma-proteobacterium																																
AB969726.1	Gamma-proteobacterium																																
AB034902.1	*Geobacillus thermoleovorans*																																
KT266806.1	*Geobacillus thermoparaffinivorans*																																
KM218876.1	*Leptolyngbya* sp.																																
KT185187.1	*Marinifilum* sp.																																
KF465059.1	*Methylophilus* sp.																																
KM083548.1	*Methylophilus* sp.																																
FJ002199.1	*Minutocellus* sp.																																
KP844953.1	*Neisseria* sp.																																
LN823958.1	*Rhizobium* sp.																																
KF786699.1	Rhodobacteraceae																																
KF282423.1	Rhodobacteraceae																																
AM913948.1	*Rhodospirillales* sp.																																
KC429860.1	*Ruegeria* sp.																																
FJ463701.1	*Ruegeria* sp.																																
KJ616372.1	*Ruegeria* sp.																																
HQ439523.1	*Ruegeria* sp.																																
JQ516550.1	Sphingobacteriales																																
NR_042903.2	*Thalassobius aestuarii*																																
HF952772.1	*Thermovum composti*																																
KF146513.1	*Thioclava pacifica*																																
KF180115.1	Un PWPS (H)																																
KF180030.1	Un PWPS (In)																																
KF180034.1	Un PWPS (In)																																
KF180034.1	Un PWPS (In)																																
KC527502.1	Un WPD (In)																																
JN672323.1	Uncultured bacterium																																
KM520644.1	Uncultured bacterium																																
GU576930.1	Uncultured bacterium																																
GU118822.1	Uncultured bacterium																																
GU118164.1	Uncultured bacterium																																
KC668734.1	Uncultured bacterium																																
HQ288601.1	Uncultured bacterium																																
KF180129.1	Uncultured bacterium																																
GU119626.1	Uncultured bacterium																																
KF180115.1	Uncultured bacterium																																
KF036053.1	Uncultured bacterium																																
KF373144.1	Uncultured bacterium																																
HE574879.1	Uncultured bacterium																																
KP975317.1	Uncultured bacterium																																
HM598135.1	Uncultured bacterium																																
HQ754673.1	Uncultured bacterium (Gastro)																																
GU940749.1	Uncultured bacterium (SCS)																																
JF896595.1	Uncultured cyanobacterium																																
KJ577059.1	*Vibrio fortis*																																
KT626460.1	*Vibrio fortis*																																
LN832981.1	*Vibrio pelagius*																																
JX173559.1	*Vibrio pelagius*																																
HQ290092.1	*Vibrio* sp.																																
DQ917857.1	*Vibrio* sp.																																
LOC		T	T	T	T	T	T	T	T	T	T	C	C	C	C	C	C	C	C	C	C	C	C	C	C	C	C	C	C	C	C	C	C
Site		G	G	G	G	G	B	Y	C	G	K	S	L	X	L	L	L	L	L	L	L	X	X	X	X	X	X	X	X	X	X	X	X
HDW		H	H	D	H	D	W	W	W	W	W	W	W	W	H	D	D	D	H	D	D	H	D	H	D	D	H	D	H	D	H	D	D
AFF		T	T	P	T	T	5	5	5	5	5	5	5	5	P	P	T	T	T	T	T	C	C	T	T	P	C	C	C	C	C	C	C

4.6 Histological Observations

In total, 24 samples were prepared for histological examination (Table 30). Of those, 16 were from Taiwan and eight were from China. The samples examined were from the three main groups of commonly observed lesions: color loss, pink discoloration, and tissue loss. It is important to note that the original tissue sections and blocks were lost when the author's home flooded, and descriptions are based on original micrographs and notes of the slides. Unfortunately, this prevents the ability to recut and stain more sections. Eleven different taxa were represented in the samples. Table 31 summarizes the notable features across all histological samples. Zooxanthellae released from the gastrodermis and brown granular material were found in 16 histological samples each, representing two-thirds of the specimens; gastrodermis lacking zooxanthellae was also very common (15 samples). Fragmented epidermis and endolithic organisms were identified in 10 samples each. Fragmented gastrodermis was identified in nine samples, and variable mesoglea in 8 samples.

Seventeen histological samples of coral colonies exhibiting tissue loss were examined. Common features in these samples were discharged spirocysts (Figure 19) in five samples, atrophied gastrodermis (Figure 20), and zooxanthellae released from the gastrodermis (Figure 21) in 10 samples each, fragmentation of the epidermis and gastrodermis (Figure 22) in nine and seven samples, respectively, endolithic organisms (Figure 24) in 10 samples, and brown granular material throughout the tissue (Figures 25 and 26) in 11 samples.

Most sections of tissue were from transitional areas between apparently healthy and lesioned areas, so it was difficult to compare between apparently healthy and diseased tissue. However, Figures 21 and 22 were two separate samples (apparently healthy and diseased) of a

Dipastraea colony exhibiting tissue loss. In the apparently healthy section of the coral, the tissues of the gastrodermis, epidermis and mesoglea were clearly intact (Figure 21). In the lesioned section of the coral, the zooxanthellae were released and the gastrodermis was atrophied, with cells detaching from the mesoglea (Figure 22). There were also suspected ciliates in four of the tissue-loss samples (Figures 28, 29, 32) and a possible copepod in one of the tissue-loss samples (Figure 33). Mesoglea with varying thicknesses was also observed in some of the coral samples exhibiting tissue loss. For example, the thickness of the mesoglea in a *Dipastraea* colony ranged from 6 to 43 µm (Figure 27).

Five histological samples of coral colonies exhibiting pink discoloration were examined (Table 33). The most common histological feature in these samples was brown granular material, which was found in all five samples, and gastrodermis lacking zooxanthellae and released zooxanthellae as shown in Figures 30 and 34.

Two histological samples of coral colonies exhibiting color loss were examined. The most common histological features in these samples were fragmented gastrodermis, zooxanthellae being released from the gastrodermis, and lack of zooxanthellae in the gastrodermis (Figures 20, 30, 34). For example, a coral colony of *Coeloseris mayeri* exhibiting color loss showed an atrophied gastrodermis, with parts of the gastrodermis missing because gastrodermal cells were necrotic and had sloughed off the mesoglea (Figure 30). In comparison, the apparently healthy section of the same *Coeloseris mayeri* colony showed the gastrodermis with zooxanthellae present attached to the mesoglea, along with the epidermis. Mesoglea of varying thickness was also observed in one of the coral samples exhibiting color loss. For example, the thickness of the mesoglea in a *Playgyra* colony ranged from 3 to 53 µm (Figure 34).

Table 30. Summary of histological samples analyzed including the site from which they were collected, site location, taxa, and disease. T= Taiwan; C=China; Pink= pink discoloration; CL= color loss; TL= tissue loss.

Site	Location	Taxa	Disease
Bitou	T	*Porites*	Pink
Bitou	T	*Stylophora*	TL
Chaikou	T	*Coeloseris*	CL
Chaikou	T	*Dipastraea*	TL
Chaikou	T	*Montipora*	TL
Chaikou	T	*Porites*	TL
Gonguan	T	*Isopora*	TL
Gonguan	T	*Isopora*	TL
Kihau	T	*Dipastraea*	TL
Kihau	T	*Porites*	Pink
Kihau	T	*Porites*	Pink
Luhuitou	C	*Porites*	Pink
Luhuitou	C	*Porites*	TL
Luhuitou	C	*Porites*	TL
Luhuitou	C	*Porites*	TL
Luhuitou	C	*Porites*	TL
Luhuitou	C	*Turbinaria*	TL
Shanyuang	T	*Favia*	TL
Shanyuang	T	*Merulina*	TL
Shanyuang	T	*Montipora*	TL
Yeliu	T	*Cyphastrea*	TL
Yeliu	T	*Montipora*	TL
Yeliu	T	*Porites*	Pink
Xiaodonghai	C	*Lobophyllia*	TL
Xiaodonghai	C	*Platygyra*	CL
Xiaodonghai	C	*Platygyra*	CL

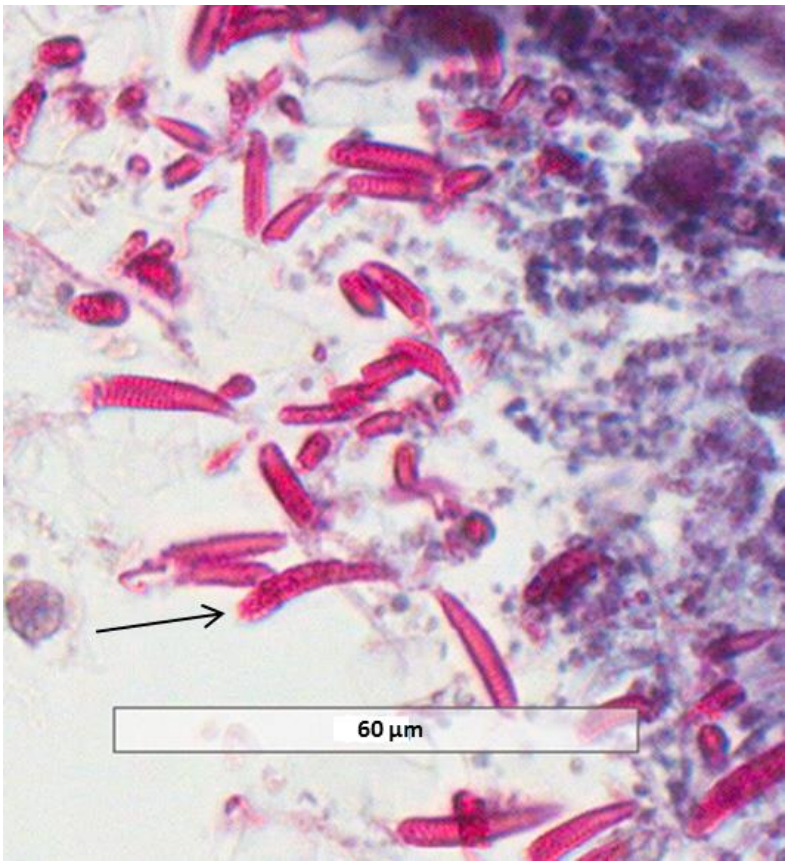

Figure 19. Micrograph showing discharged spirocysts from the epidermis (black arrow) of a *Stylophora* colony exhibiting tissue loss.

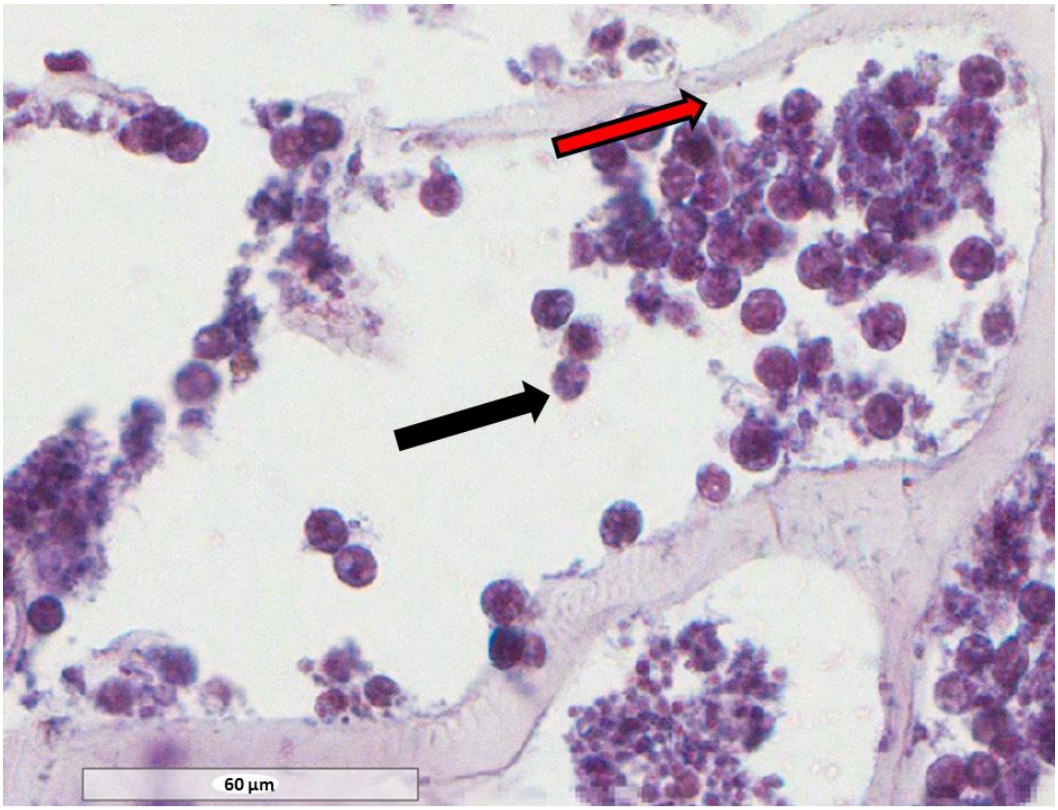

Figure 20. Micrograph showing released zooxanthellae (black arrow) and gastrodermal cells lysed and necrotic (red arrow) of a *Stylophora* colony exhibiting tissue loss.

Figure 21. Micrograph of a *Dipastraea* colony exhibiting tissue loss showing a sloughing epidermis (black arrows), possibly because of necrosis, attached to the mesoglea with the gastrodermis completely missing.

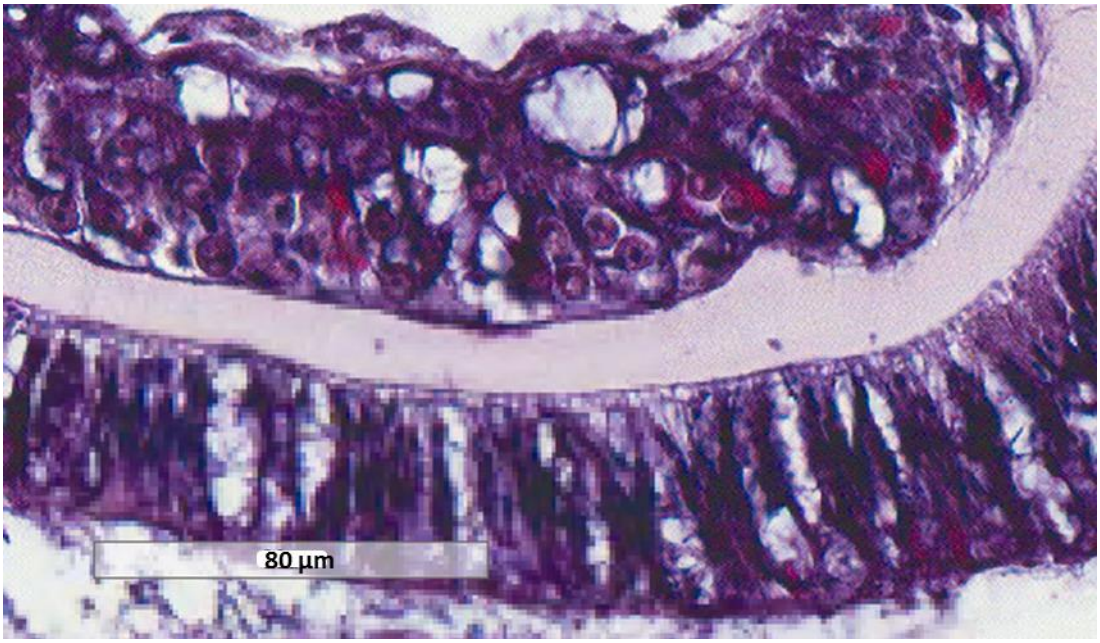

Figure 22. Micrograph from an apparently healthy area of a *Dipastraea* colony exhibiting tissue loss; the epidermis attached to the mesoglea with the gastrodermis present.

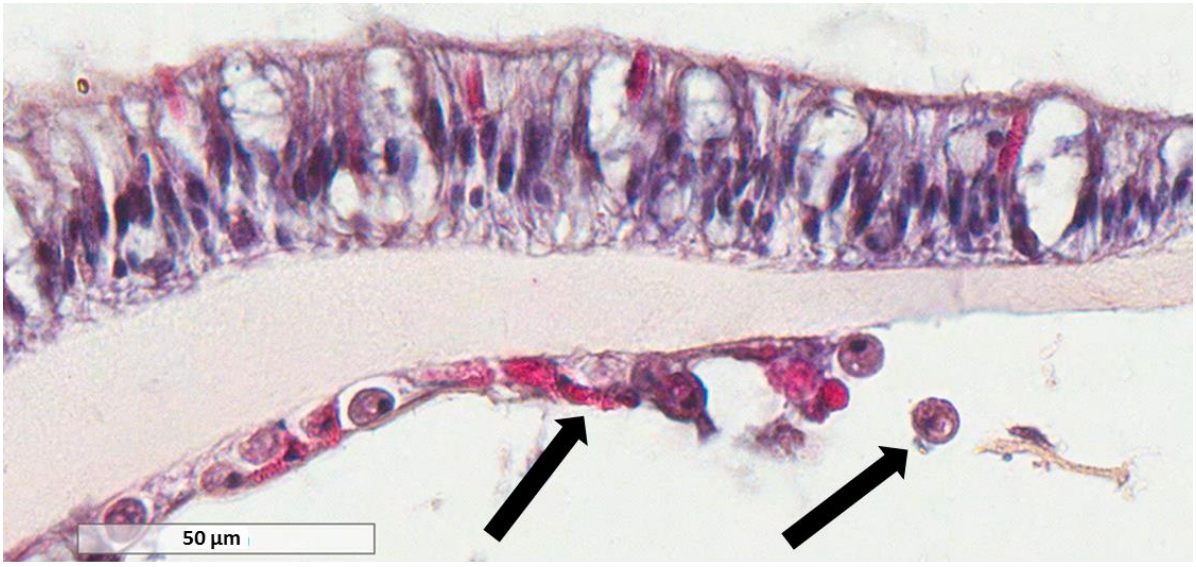

Figure 23. Micrograph showing released zooxanthellae (black arrow) and atrophied gastrodermal cells dying and sloughing from the mesoglea (black arrow) of a *Dipastraea* colony exhibiting tissue loss.

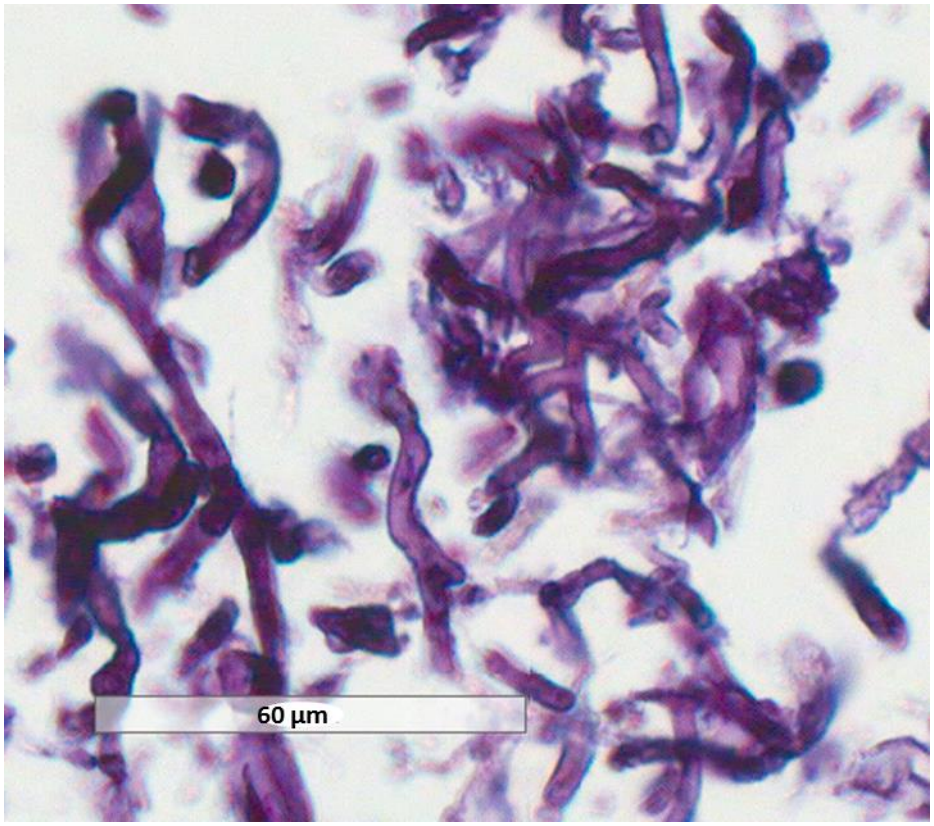

Figure 24. Micrograph showing endolithic organisms in *Isopora palifera* exhibiting tissue loss.

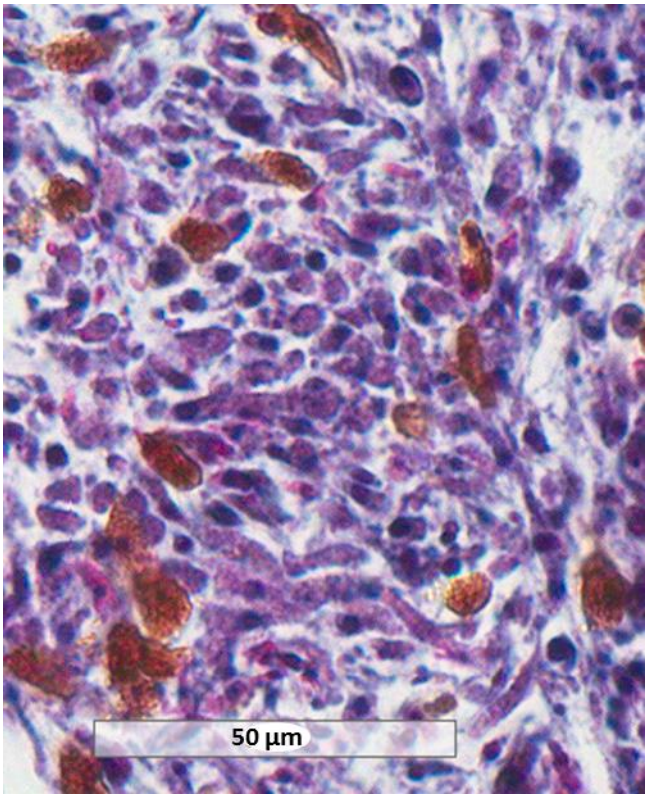

Figure 25. Micrographs showing amoebocytes that contain melanin-like pigment granules in *Isopora palifera* exhibiting tissue loss.

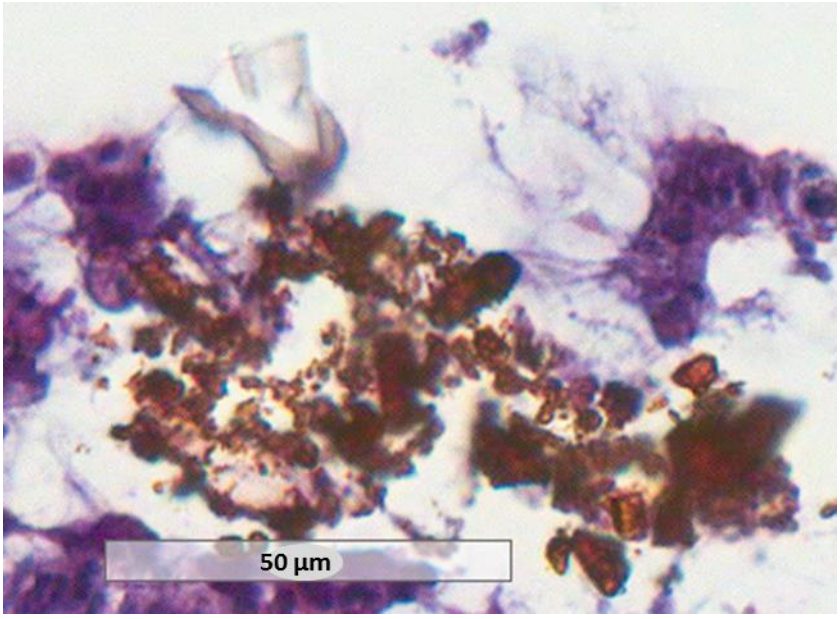

Figure 26. Micrographs showing extracellular brown granular material within *Merulina* sp. exhibiting tissue loss.

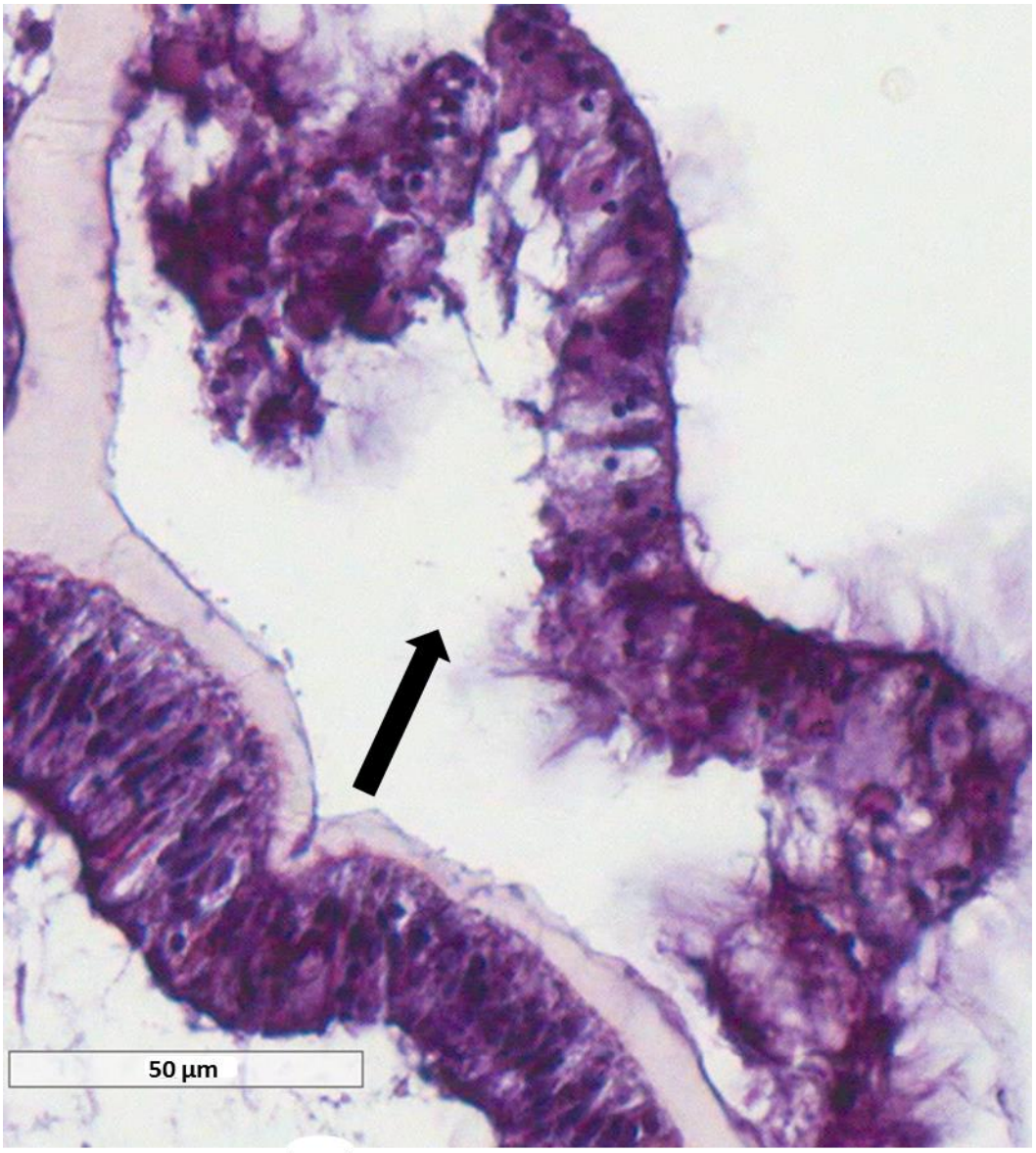

Figure 27. Micrograph showing the gastrodermis detaching from the mesoglea (black arrow) of a *Merulina* sp. colony exhibiting tissue loss.

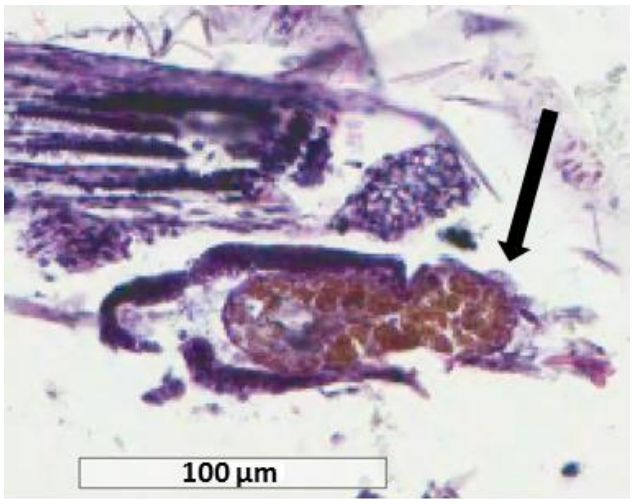

Figure 28. Micrograph of possible ciliate (arrow) on *Montipora* exhibiting tissue loss.

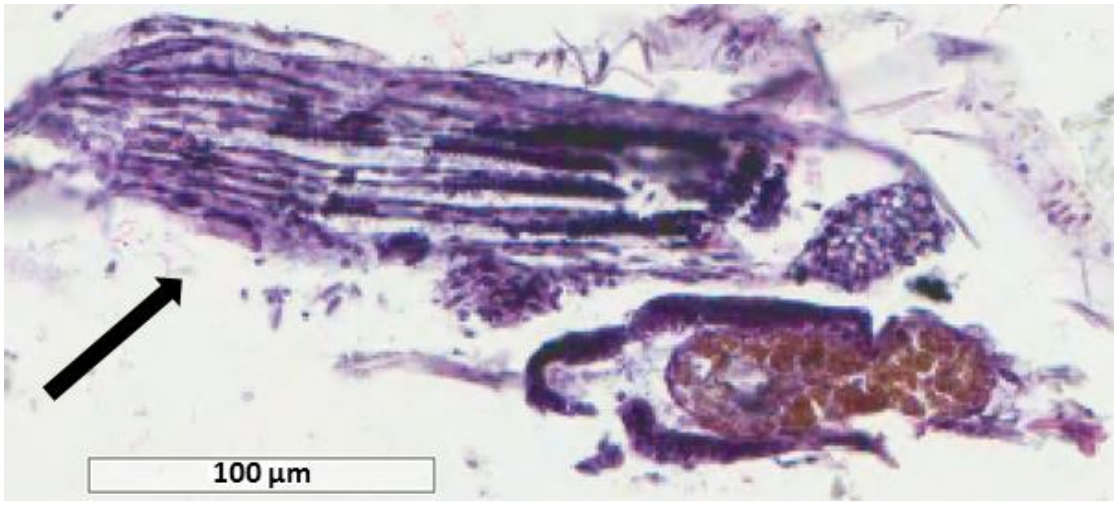

Figure 29. Micrograph of possible ciliate with another unidentified organism (arrow) on *Montipora* sp. colony exhibiting tissue loss.

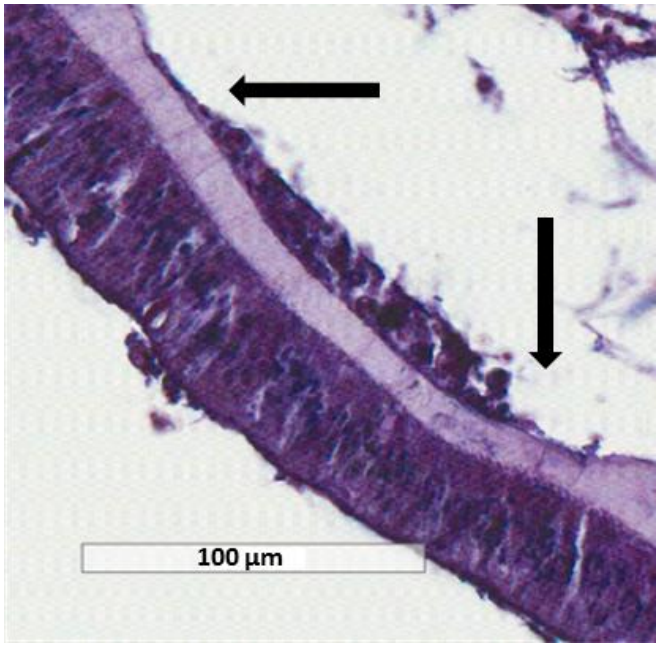

Figure 30. Micrograph showing atrophied and necrotic gastrodermis with parts of the gastrodermis missing, because the gastrodermal cells have lysed and detached from the mesoglea (arrows) from *Coeloseris mayeri* exhibiting color loss in another area of the colony.

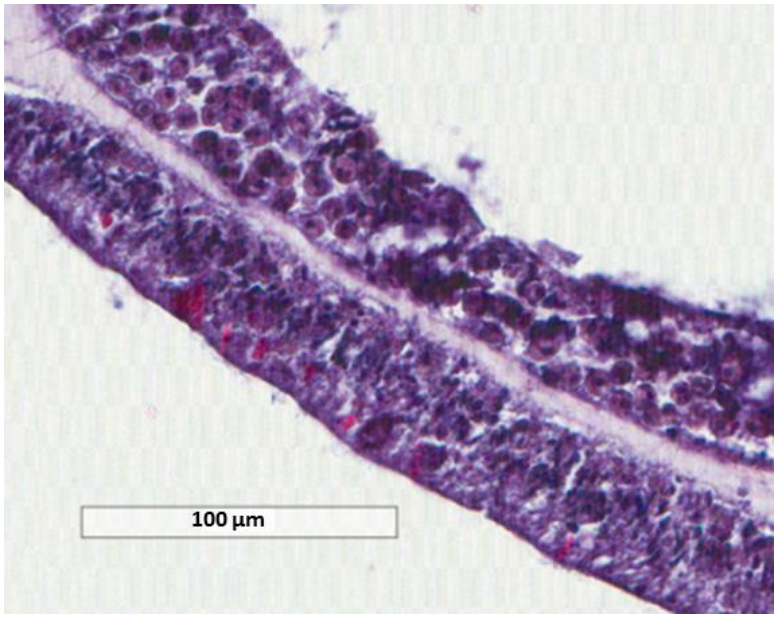

Figure 31. Micrograph showing the gastrodermis attached to the mesoglea along with the epidermis on an apparently healthy section of *Coeloseris mayeri* exhibiting color loss in another area on the colony.

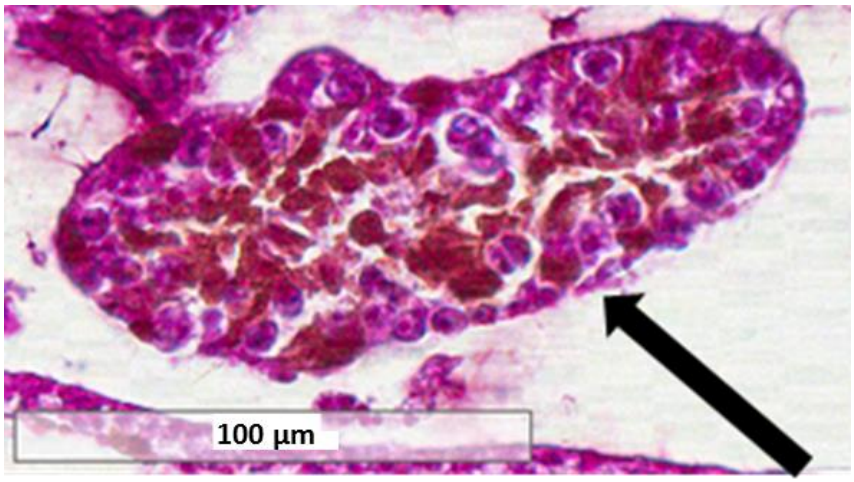

Figure 32. Micrograph of zooxanthellae-engorged ciliate (arrow) on *Turbinaria* exhibiting tissue loss.

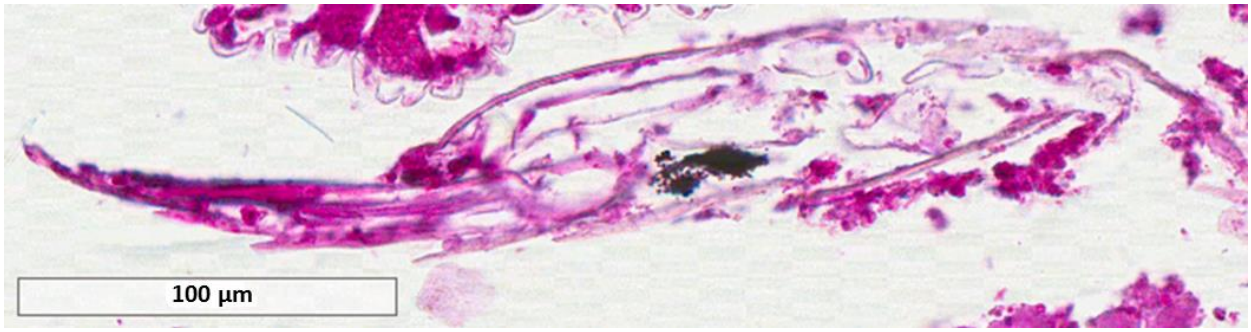

Figure 33. Micrograph of a possible copepod found on *Turbinaria* exhibiting tissue loss.

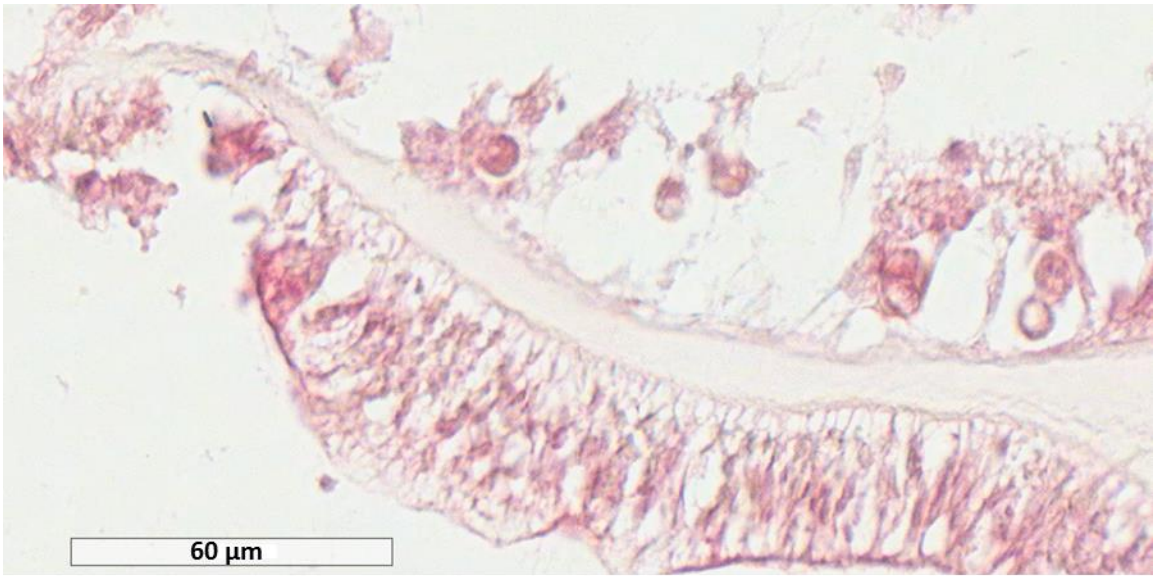

Figure 34. Micrograph of a vacuolated and lysing gastrodermis and atrophied epidermis and mesoglea (far left) on *Platygyra* sp. colony exhibiting color loss.

Table 31. Summary of notable features in histological samples, expressed as presence or absence of each condition. X = present. Pink = pink discoloration; CL = color loss; TL = tissue loss. FG = fragmented gastrodermis; GD = gastrodermis detached; GM = gastrodermis missing; GLZ = gastrodermis lacked zooxanthellae; GNL = gastrodermal cells necrotic and lysing; MVM = mesoglea with varying widths; ED = epidermis detached; EF = sloughing and/or fragmented epidermis; NP = nematocysts present; SD = spirocysts discharged; MP = mucocytes present; EO = endolithic organisms; BGM = brown granular material; AM = amoebocytes containing melanin-like granules; PCS = possible ciliate sighting(s).

Site	Taxa	Affliction	FG	GD	GM	GLZ	GNL	MVW	ED	ESF	SD	EO	BGM	AM	PCS
Bitou	*Porites*	Pink				X							X		
Bitou	*Stylophora*	TL	X			X	X	X		X	X	X			
Chaikou	*Coeloseris*	CL	X			X	X								
Chaikou	*Dipastraea*	TL			X		X	X	X	X		X			
Chaikou	*Montipora*	TL	X	X				X							
Chaikou	*Porites*	TL				X				X		X	X		
Gonguan	*Isopora*	TL							X			X			
Gonguan	*Isopora*	TL										X		X	X
Kihau	*Dipastraea*	TL					X	X	X						
Kihau	*Porites*	Pink												X	
Kihau	*Porites*	Pink				X							X	X	
Luhuitou	*Porites*	Pink				X								X	
Luhuitou	*Porites*	TL	X			X				X				X	
Luhuitou	*Porites*	TL	X			X				X	X			X	
Luhuitou	*Porites*	TL	X			X				X	X			X	
Luhuitou	*Porites*	TL	X			X				X	X			X	
Luhuitou	*Turbinaria*	TL				X						X	X		X
Shanyuang	*Merculina*	TL		X				X				X	X		
Shanyuang	*Montipora*	TL				X									
Yeliu	*Cyphastrea*	TL										X	X		X
Yeliu	*Montipora*	TL				X		X		X		X	X		X
Yeliu	*Porites*	Pink				X							X	X	
Xiaodonghai	*Lobophyllia*	TL	X			X		X		X	X	X	X		
Xiaodonghai	*Platygyra*	CL	X			X	X	X		X					

The most common features across lesions and methods are noted in Table 32. Tissue loss and pink discoloration utilized similar carbon sources, as well as the microbial communities within the apparently healthy areas. The microbial community from the water column primarily utilized glycogen. The bacterial community varied by lesion and apparently healthy and within the water column. The number of ribotypes per sample were equal between tissue loss and the water column. The gastrodermis lacking zooxanthellae was common in all lesion types.

Table 32. Summary of notable features across samples and methods. PD = pink discoloration; CL = color loss; TL = tissue loss; GA = growth anomalies; H = apparently healthy; W = water. Overall # = number of samples in the study. DGGE # = average numbers of bands present. ESF = sloughing and/or fragmented epidermis; FG = fragmented gastrodermis; GLZ = gastrodermis lacks zooxanthellae; ZDG= zooxanthellae detached from gastrodermis; GNL = gastrodermal cells necrotic and lysing; BGM = brown granular material; AM = amoebocytes containing melanin-like granules; PCS = possible ciliate sighting(s). - = no data.

	TL	PD	CL	GA	H	W
Overall #	27	14	8	3	52	8
Biolog	alpha-cylodextrin, d-mannitol, glycogen	alpha-cylodextrin, d-mannitol, glycogen	-	-	alpha-cylodextrin, d-mannitol, glycogen, d-cellobiose	glycogen
DGGE #	8.1	7.3	5.4	5	7.3	8.1
Sequence	*Geobacillus* spp., *Vibrio fortis*, *Vibrio pelagius*, *Vibrio* sp.	*Ruegeria*, *Vibrio fortis*, *Vibrio pelagius*, *Vibrio* sp.	*Ruegeria*, *Neisseria*	*Vibrio fortis*, *Vibrio pelagius*	*Vibrio* spp., *Ruegeria*, *Acanivorax* sp.	*Alpha-proteobacterium*, *Geobacillus thermoparaffinivorans*, *Uncultured bacteria*
Histology	PCS, BGR, ESF, GLZ, FG	AM, BGM, GLZ	GNL, ZDG, FG	-	-	-

5. Discussion

The original impetus for this study of coral diseases in Taiwan and Hainan was the recognition from several papers (e.g., Chiou et al., 2010; Hughes et al., 2013) that coral diseases in recent years have been increasing in this region, but there were no survey data available on what diseases were present. Coral cover has decreased significantly in some reef areas of Taiwan and the South China Sea, and coral disease has been a main contributor to the decline (Chiou et al., 2010; Hughes et al., 2013). Coral disease studies have typically focused on characterizing a particular disease present on the reef and not on all diseases present (Liao et al., 2007; Chiou et al., 2010; Zhenyu et al., 2013; Lin et al., 2016). Additionally, studies generally focused on characterizing one particular aspect of a disease, primarily microbial, with little to no discussion of the disease prevalence, lesion description, or histological description (Zhenyu et al., 2013; Ng et al., 2015; Miller et al., 2015).

In the South China Sea, documented diseases have included white syndrome, coral black disease, yellow inflammatory-like syndrome, pink disease and brown band disease, which contributed to the decline of live coral cover by more than 30% during the past few decades (Qui et al., 2010; Shi et al., 2012; Zhenyu et al., 2013; Lin et al., 2016). However, little information is available regarding the species identities of the microbial pathogens of coral diseases (Zhenyu et al., 2013). Many of the emerging coral diseases around the world have been characterized through visual descriptions, but few pathogens have been identified and even fewer have been tested and

shown to fulfill Koch's postulate, which are used to identify a causative agent of a disease (Zhenyu et al., 2013).

5.1 Survey, Sites, and Sightings

The survey results revealed that the most common type of lesion present on corals on patch reefs along Taiwan and China was tissue loss, which was found at every site. Tissue loss has become a common affliction among corals in the Indo-Pacific (Sweet and Bythell, 2012; Zhenyu et al., 2013) and has been documented as a main indicator of disease throughout the region (Work and Rameyer, 2005; Aeby, 2009; Bourne et al., 2015; Work et al., 2014; Aeby et al., 2016). Any coral disease that results in tissue loss in the Indo-Pacific is typically considered a "white syndrome", which means that multiple pathogens and causes of the syndrome can be involved. Because the main sign of white syndromes is tissue loss on the coral, it has been deemed the most serious disease and is believed to be one of the principal factors in the decline of what were once the dominant corals in the Caribbean and the Indo-Pacific (Sussman et al., 2008; Work and Aeby, 2011; Zhenyu et al., 2013). White syndrome has been documented in the South China Sea previously (Miller et al., 2015) and has been known to affect *Porites andrewsi* (Zhenyu et al., 2013). In my histological samples of corals exhibiting tissue loss, fragmentation of the gastrodermal and epidermal tissues was very common, as were endolithic organisms and brown granular material.

The second most common affliction noted was pink discoloration on *Porites*, which was found at every site except Chaikou, Shanyuang, and Luhuitou. The lesions observed seemed consistent with a disease that was previously known as pink line or pink spot syndrome. Pink

syndrome has been attributed to a variety of causes through the years. First, its pathogen was identified as the cyanobacterium *Phormidium valderianum* (Ravindran et al., 2001; Ravindran and Raghukumar, 2002), then, as the trematode *Odocotyloides stenometra*, which leads to swollen pink nodules on a coral colony (Aeby, 2003). Later, another study claimed the discoloration was from the mechanical/chemical stress caused by the settling of barnacle larvae on living *Porites* (Benzoni et al. 2010), and then not as a disease but a physiological reaction to stress (Palmer et al., 2009a; Willis et al., 2009; Benzoni et al., 2010). Because the pink discoloration appeared as a lesion on the corals, it was still counted as a potential sighting of disease; although, the etiology of the pink lines and pink spots may vary (Ravindran and Raghukumar, 2002; Aeby, 2003; Lin et al., 2016). Most recently, pink-line syndrome has been reintroduced into the literature as a coral disease (Lin et al., 2016; Ravindran et al., 2016). In my histological sections from pink lesions, brown granular material was found in all sections, and in my sequence data, *Vibrio* spp. were commonly found associated with the pink lesions.

Bleaching was noted in a few corals at Chaikou, Kihau, Shanyuang, Bitou, and Luhuitou. Based on other reports of coral-disease surveys in the Indo-Pacific, it may be surprising to see that so few cases of bleaching were noted (Work and Rameyer, 2005; Aeby, 2009; Work et al., 2014). However, water temperatures recorded during surveys in Taiwan were ~28° C (3° C below bleaching threshold), which is not a temperature that normally induces bleaching (Bellantuono et al., 2011). Bleaching was more common at the sites in Hainan, where temperatures were ~30° C. The most common histological findings in my samples exhibiting color loss were fragmented gastrodermis, and zooxanthellae either lacking or being released from the gastrodermis. Although bleaching and tissue loss can be confused in the field, the histological differences that I observed

are consistent with my field assessments. Interestingly, I did not detect *Vibrio* spp. in lesions associated with color loss.

Sites off the coast of Taiwan that are adjacent to substantial human populations typically showed more lesions. Yeliu and Shanyuang had the highest sightings per effort (Table 3). Chaikou and Gonguan, which were off the coast of Green Island, had the fewest sightings, which was not surprising because they were the most remote sites sampled. Previous studies have found a positive association between high human populations and coral lesions (Aeby et al., 2011; Becker et al., 2013).

Although the survey data from the reefs off Hainan revealed even fewer sightings per minute of diver observation, that result can be attributed to the very sparse numbers of corals on the two reefs that were sampled. Most of the time spent on those reefs was dedicated to finding corals that were alive; coral cover, especially in Xiaodonghai, was very low because most corals had already died. Hughes et al. (2013) quantitative analyses determined that nearly 80% of the coral cover on fringing reefs along the Chinese mainland and around Hainan Island has been destroyed by human activities since the 1980s. Human impacts on coral reefs have been previously discussed in detail and have been implicated in coral disease (Hughes et al., 2013). Both sites on Hainan Island were off Sanya. In the 1950s, Sanya was a fishing village of ~2000 people; by 2010 Sanya had become a city with more than 600,000 people (Zhang, 2001; Hughes et al., 2013). By 2009, more than 6 million domestic tourists were visiting Sanya each year, which is 10 times the resident population! The fringing reefs closest to the city now have coral cover close to zero as a result of coastal development, increased pollution from sewage and industrial waste, and intensified food production from aquaculture and market gardens (Huang et al., 2003; Zhao et al., 2008; Hughes et al., 2013).

5.2 Carbon-Source Utilization

Previous studies, have documented differences between the water column, apparently healthy, and diseased samples, and it is commonly accepted that each has its own microbial community and quantity of microbes (Ritchie and Smith, 1995; Breitbart et al., 2005; George, 2011; Meyer et al., 2014). Biolog EcoPlate™ analyses were successfully conducted on samples only from Bitou and Yeliu from Taiwan (Table 6). Carbon utilization was significantly different between water samples and coral-mucus samples, whether from apparently healthy or lesioned corals. There were only three carbon sources utilized within the water column: glycogen, N-acetyl D-glucosamine, and pyruvic methyl ester. The comparison of mucus from apparently healthy and lesioned areas also revealed statistically significantly differences, more than twice as many positive utilization records were found in the mucus from lesioned areas. This may indicate that similar microbes were present in the apparently healthy and lesioned section of the coral, and, the quantity of the microbes in the lesioned areas had increased.

The low carbon utilization by the microbes in the water column from my samples appeared to show low microbial diversity and low abundances of microbes present that would use those particular carbon sources. Low microbial diversity within the water column when compared to microbial communities in coral mucus layers is not uncommon. Moreover, my water samples may not have been of sufficient volumes to effectively sample the bacterial community; Chiou et al. (2010) recommended filtering at least two liters of seawater. This may have contributed to the low positives observed on the EcoPlate™ for the water column samples.

Corals exhibiting pink discoloration lesions had a significantly different carbon utilization pattern than corals with growth anomalies or tissue loss. This indicates that the pink discoloration

has a distinct microbial community. Comparisons between the carbon sources utilized by the different afflictions revealed that the main carbon sources that are responsible for driving the differences were d-galacturonic acid, d-mannitol, and alpha-cyclodextrin. D-galacturonic acid was not utilized in the pink discoloration samples, only in the growth-anomaly samples. However, d-mannitol, and alpha-cyclodextrin were used in almost all lesioned samples exhibiting pink discoloration and a few of the samples in the healthy area.

D-mannitol is a naturally occurring six-carbon sugar alcohol and it is the most abundant polyol in nature, occurring in bacteria, yeasts, fungi, algae, and lichens (Wisselink et al., 2002). It can be industrially produced (Makkee et al., 1985), produced by the manna ash tree *Fraxinus ornus* (Soetaert, 1990), and by Mannitol-producing lactic acid bacteria (Wisselink et al., 2002). Mannitol has been reported to accumulate in response to environmental stresses and has been observed to protect bacteria during oxidative stress (Chaturvedi et al., 1997). D-mannitol has been implicated in coral disease previouslyand is known to be utilized by bacteria that have been implicated in coral disease (Krediet et al., 2009; George, 2011). Ritchie and Smith (1995b) found that D-mannitol was utilized more frequently in mucus samples from *A. cervicornis* with signs of white-band disease (80%) compared to water (61%) and healthy mucus samples (67%). I found that D-mannitol was utilized more frequently in mucus samples from lesions (9 of 14) compared to water (0 of 2) and apparently healthy mucus samples (5 of 14), which indicates a microbe or group of microbes within some of the diseased samples that could utilize D-mannitol that were less abundant in healthy mucus samples. Ben-Haim et al. (2003) applied six strains of *Vibrio coralliilyticus*, which are bacteria associated with bleaching and tissue lysis of *Pocillopora damicornis*, to Biolog GN plates and found that five out of six strains utilized D-mannitol. My data are consistent with the observation of Ben-Haim et al. I found *Vibrio* spp. primarily at Bitou (a site

where carbon utilization was assessed) (Table 33). Although the *Vibrio* were found at Bitou in the water column, apparently healthy areas of the corals, and lesioned areas of corals exhibiting pink discoloration and tissue loss, more D-mannitol was used within the lesioned areas, indicating more *Vibrio* were present within the lesions.

KJ577059.1	*Vibrio fortis*																																	■	■	■	■	■	■	■		■	■						■
KT626460.1	*Vibrio fortis*																										■	■	■	■				■	■	■	■	■	■	■										
LN832981.1	*Vibrio pelagius*																										■	■	■	■					■	■	■	■	■	■	■	■	■	■						
JX173559.1	*Vibrio pelagius*		■	■	■	■																																												
HQ290092.1	*Vibrio* sp.																										■	■		■				■	■	■	■	■	■	■	■	■	■	■						
DQ917857.1	*Vibrio* sp.			■																																														
LOC		T	T	T	T	T	T	T	T	T	T	T	T	T	T	T	T	T	T	T	T	T	T	T	T	T	T	T	T	T	T	T	T	T	T	T	T	T	T	T	T	T	T	T	T	T	T	T	T	T
Site		K	K	K	K	K	K	C	C	C	C	C	C	S	S	S	S	Y	Y	Y	Y	Y	Y	Y	Y	Y	B	B	B	B	B	B	B	B	B	B	B	B	B	B	B	B	B	B	G	G	G	G	G	B
HDW		H	H	H	D	H	D	H	H	D	D	H	D	H	D	H	D	H	D	H	H	H	H	D	H	D	H	D	H	D	H	D	H	D	D	H	H	D	H	D	H	D	H	D	H	H	D	H	D	W

Table 33. Summary of BLAST analysis of the 16S rRNA sequences most related to *Vibrio* by location, site, sample type (water, apparently healthy, disease), taxa and lesion type. LOC: T = Taiwan, C = China. Site: K = Kihau, C = Chaikou, S = Shanyuang, Y = Yeliu, B = Bitou, G = Gonguan, L = Luhuitou, X = Xiaodonghai. HDW: H = healthy, D = diseased, W = water. Black rectangle indicates that the carbon source was utilized.

No significant difference in carbon-source utilization was found between sites. Similarly, Daniels et al. (2011) noted that microbial communities within coral species do not vary much spatially and that water column communities do not vary much if samples are taken close to one another. Because Bitou and Yeliu shared many of the same coral species and the locations were relatively close, significant differences were not anticipated between the two sites.

5.3 DGGE Analysis

The DGGE analysis was incorporated into this study to characterize the bacterial communities in the water column, apparently healthy samples, and lesions. DGGE only profiles the dominant microbes within a community (Muyzer and Smalla, 1998). The results from DGGE showed that diversity of bacterial populations was slightly higher in the water samples, and that

significant differences were not seen between healthy and diseased corals. The lower bacterial diversity in diseased corals may be due to a shift in the bacterial community structure from the equilibrium state and the reduction of the immunity of the host, which may lead to colonization by opportunistic pathogens (Closek et al., 2014; Lin et al., 2016). The DGGE results compliment what was observed in the EcoPlate™ analysis. Bacterial communities are known to vary among water column, apparently healthy corals, and diseased corals, as noted previously.

Bacterial communities identified using DGGE varied significantly among all sites (Table 19). A similar spatial variability was previously reported by Daniels et al. (2011). Bacterial communities have also been linked to environmental and anthropogenic factors, which may have contributed to the significant differences among sites (Ritchie and Smith, 2004; Rosenberg et al., 2007; Ainsworth and Hoegh-Guldberg, 2009; Miller et al., 2015).

DGGE also showed similar results to carbon-utilization analysis by showing that pink discoloration was significantly different from all other afflictions, and all afflictions were significantly different from the water column. As noted previously, Corals are known to hold very specific bacterial communities that are commonly distinct from bacterial communities in the surrounding water. Recently, a study was conducted to determine the bacterial communities of *Porites* exhibiting pink-spot syndrome in southern Taiwan (Lin et al., 2016). The overall bacterial assemblages of this coral were composed mainly of Alphaproteobacteria, Gammaproteobacteria, Acidobacteria, Chloroflexi, Betaproteobacteria, Deltaproteobacteria, Firmicutes, Actinobacteria, Gemmatimonadetes, Bacteroidetes, Chloroflexi, Nitrospira, Verrucomicrobia, and unclassified Proteobacteria. I also recorded Alphaproteobacteria and Bacteroidetes in coral samples exhibiting pink discoloration, as well as in corals exhibiting other diseases, though I did not see higher diversities of bacteria in samples from lesions. Lin et al. (2016) also noted a higher diversity in the

bacterial communities associated with diseased or bleached corals and this pattern has been documented in several studies previously (Sekar et al., 2006; Pantos and Bythell, 2006; Chimetto et al., 2008; Bourne et al., 2008; Sunagawa et al., 2009; Kimes et al., 2013; Closek et al., 2014).

Clostridium spp., a gram-positive, obligate anaerobic bacterium, has also been identified as a human pathogen (Pasquale et al., 2011) and has been implicated in coral diseases including white plague and black-band disease (Frias-Lopez et al., 2002; Jones et al., 2004, Weynberg et al., 2015). *Clostridium* spp. was identified as being the nearest phylogenetic match to several of the sequences found in my study. The reservoir of bacterial pathogens possible in seafood is also well underlined by the FAO (2004), which listed among other pathogenic bacteria, the spore-forming *C. botulinum* and *C. perfringens*. *Clostridium difficile* was first described by Hall and O'Toole (1935) as part of the normal intestinal flora in newborn infants. Currently, *C. difficile*-associated diarrhea is one of the most common hospital infections worldwide, but has been also isolated from feces of asymptomatic humans (Oozaki et al., 2004). *Clostridium* spp. were found on corals exhibiting tissue loss and pink discoloration, and, in most cases, were found in both apparently healthy and diseased areas. Recently, *Clostridium* spp. was one of the dominant ribotypes identified in white syndrome lesions of affected *Echinopora lamellosa* in aquaria (Smith et al., 2015). Further investigation is needed to determine if *Clostridium* spp. is a pathogen associated with white syndromes. The presence of *Clostridium* spp. may also indicate sewage pollution.

Vibrio spp. were identified as being the nearest phylogenetic match to several of the sequences found in my study. *Vibrio* is a gram-negative, facultative anaerobe that is common in seawater ecosystems and is the main bacterial causative agent of many marine animal diseases, including coral (Kushmaro et al., 1997; Arboleda and Reichardt, 2008; Zhenyu et al., 2013). Of eight identified coral bacterial pathogens, six belong to the genus *Vibrio* (*V. alginolyticus, V.*

shilonii, V. coralliilyticus, V. natriengens, V. parahaemolyticus, and *V. harveyi*) (Rosenberg et al., 2007; Arboleda and Reichardt, 2008; Luna et al., 2010; Zhenyu et al., 2013). I found sequences related to *V. pelagius, V. fortis*, and an unidentified *Vibrio* sp. *Vibrio fortis* also occurred in several corals in both healthy and lesioned areas. *Vibrio pelagius* was only identified in lesioned areas and in the water column, and was not identified as being present in apparently healthy coral areas. This species was identified in lesioned areas of two coral colonies, one exhibiting pink discoloration and the other exhibiting tissue loss. Because *Vibrio* has been implicated in many marine diseases, and I found *V. pelagius* only in lesioned areas, further studies should be done to determine if *V. pelagius* is an unidentified coral pathogen.

Although *Vibrio* spp. have been implicated in coral disease, other studies have shown that *Vibrio* spp. can be a normal constituent of coral microbial assemblages, and opportunistically proliferate if holobiont health is compromised (Bourne and Munn, 2005; Bourne et al., 2008). This complements my findings, as *Vibrio* spp. were also identified in several apparently healthy sections of the corals. Munn (2015) suggested that most, if not all, *Vibrio* spp. should be considered opportunistic pathogens, which given the right environmental conditions can overwhelm an organism's defense mechanisms and lead to rapid microbial growth and host tissue destruction.

Although I found bacteria present that have been implicated previously in coral disease, I could not determine if these bacteria were causing the lesions, opportunistically taking advantage of the compromised nature of the coral, or were a part of the corals' normal microbial assemblage. Some studies have even hypothesized that many coral diseases are polymicrobial and opportunistic pathogens attack corals when their defenses are compromised or their normal microbiota is destabilized (Lesser et al., 2007; Muller and Woesik, 2012; Meyer et al., 2014), as noted above for *Vibrio* spp.

5.4 Histological Analysis

Histological examination of corals can be utilized to assess tissue damage associated with disease and to understand the role diseases play holistically on corals. Several previous studies have focused on histological examinations of tissue loss of corals, and tissue loss was the most commonly documented lesion found in my study. Histological examination was particularly important in this study because there has been the assumption that tissue loss (white syndrome) is caused by bacteria, although the absence of histological evidence for the presence of bacteria associated with cell death in white syndrome-affected coral has been pointed out elsewhere (Ainsworth et al., 2007; Work et al., 2012). Moreover, more than one causal agent may be associated with this suite of disease signs (Work et al. 2012; Bourne et al., 2015a,b; Raymundo et al., 2016). Additionally, other organisms, including ciliates, have been directly implicated in causing tissue loss in corals (Sweet and Bythell, 2012, 2015).

Several histological features that I observed in corals exhibiting tissue loss matched observations documented in the literature. The most common features in my samples were discharged spirocysts, atrophied gastrodermis, zooxanthellae released from the gastrodermis, fragmentation of the epidermis and gastrodermis, endolithic organisms, amoebocytes containing melanin-like granules and presence of extracellular brown granular material. Work and Aeby (2011) reported that *Acropora* in Hawaii, which exhibited white syndrome with acute tissue loss, manifested microscopic evidence of necrosis sometimes associated with ciliates, helminths, fungi, algae, sponges, or cyanobacteria, whereas those with subacute tissue loss manifested mainly wound repair. A previous histological study of *Porites* exhibiting bleaching with tissue loss revealed a 65% reduction in symbiont density, melanin-containing granular cells, tissue

fragmentation and necrosis in affected areas (Sudek et al., 2012). Discussions of the role of filamentous endolithic organisms on calcium carbonate-secreting organisms cite both positive and negative effects on the host (Tribollet, 2008). Fungi penetrate and dissolve coral skeleton and attack both endolithic algae and coral polyps (Bentis et al., 2000).

The loss of *Symbiodinium* cells also may have contributed to the observed atrophy in affected samples, which is indicative of a stressed coral colony. Atrophy has also been observed in bleached corals (Glynn et al., 1985) and corals that are affected by sediment stress (Vargas-Angel et al., 2007). Melanin has been documented in invertebrates (Cerenius et al., 2008) including corals (Palmer et al., 2010, 2011) and can encapsulate pathogens. Palmer et al. (2010) suggested that the presence of melanin within coral cells may be able to regulate shading of photosynthetic symbionts (zooxanthellae) by movement and re-orientation of the melanized cells. That study documented melanin in 15 scleractinian species on the Great Barrier Reef during a thermal bleaching event.

Color loss was a type of lesion observed in this study. Complete color loss is sometimes confused with tissue loss macroscopically. Additionally, color loss and tissue loss can coexist on a coral adjacent to one another and make it difficult to distinguish the two or recognize that both are present. The most common histological features in tissue loss samples that I observed were fragmented gastrodermis, necrotic and lysing gastrodermal cells, and zooxanthellae released from the gastrodermis. These features have been reported previously in corals exhibiting color loss. For example, a study of coral lesions at Palmyra Atoll found that, of the species exhibiting discoloration (color loss), 67% of cases showed evidence of necrosis (Williams et al., 2011). That study reported tissue fragmentation in one colony of *A. digitifera*, while one colony of *Lobophytum* sp. had lost zooxanthellae from its gastrodermal cells. In a study from Micronesia, gross and

microscopic lesions were examined that showed similar characteristics. The depletion of zooxanthellae from the gastrodermis, often associated with atrophy of tissues, made up a majority of microscopic diagnoses (Work et al., 2015). *Symbiodinium* cells can contribute more than 90% of the coral's energy requirements through photosynthesis (Muscatine et al., 1984). A loss of *Symbiodinium*, therefore, results in reduced energy being available for growth and other life processes, such as reproduction and repair.

Few studies have used histology to document pink discoloration, so histological characteristics of pink discoloration vary and are still being determined. Many of the previous histological studies focused on identifying trematodes to verify that the lesion was pink-line syndrome. The most common histological feature that I observed was brown granular material present throughout the tissues. Recently, Work et al. (2015) reported that lesions with pink discoloration were among the most common lesions found during surveys in Micronesia. That study found that corals with pink discoloration had filaments of algae surrounded by hypereosinophilic fragmented tissues and marked adjacent infiltrates of granular brown cells. They also noted that, in previous studies, the brown granular cells have stained positive for melanin. One of the most important observations of Work et al. (2015) was that they did not find trematodes. This is consistent with my observations, indicating that pink spots are not always associated with trematode larvae.

5.5 Future Work

Future coral disease surveys should incorporate percent cover of coral species affected and percentages of corals affected to determine the overall effect disease has on each species. Additionally, if at all possible, surveys should monitor the corals over time to gain insight on lesion progression.

Biolog EcoPlate™ can be utilized to gain insight on the different sources of carbon source utilized by bacteria so that fingerprints of bacteria implicated in coral disease can be identified. Carbon source utilization of bacteria may give insight to why certain bacteria are present, based on the composition of the mucus.

Sequencing is an essential tool to help identify potential pathogens. Future studies should also try to identify 'beneficial' bacteria that help corals thwart disease. Laboratory experiments should be set up to test the pathogenicity of particular bacteria of interest identified in this study, including *Clostridium* sp. and *Vibrio pelagius*.

Coral histology should continue to be used to characterize coral diseases. Future studies should examine coral lesions using both light microscopy and electron microscopy, which will allow for observation at higher magnification and resolution, and may even allow for identification of bacteria and viruses. Additional stains may also help with identification of the microbes present throughout the coral. The source of the brown granular material should be determined, as it has been reported in several studies. The species of ciliates involved in coral tissue loss should also be identified to gain insight on disease progression and the role of ciliates as agents of disease or opportunists taking advantage of an available food source.

5.6 Conclusions

1. At sites on Taiwan, lesions were encountered twice as often at the sites near Taipei and Taitung than at Green Island. The few lesions encountered on the reefs on Hainan Island, can be attributed to very sparse coral cover.
2. *Porites* was the genus most commonly observed with coral lesions. Tissue loss was the most common lesion found and was observed at all sites.
3. Microbes in the mucus from lesioned areas utilized most of the same carbon sources as in the healthy areas, but utilized those more than twice as often, indicating that similar microbes were present but increased in quantity in lesions.
4. Sequences related to coral disease were identified, including *Bacillus* sp., *Clostridium* sp., and *Vibrio* sp., as well as sequences related to anthropogenic sources, including *Bacillus* sp. (sewage sludge) and *Geobacillus thermolevorans* (irritable bowel syndrome within humans).
5. *Vibrio* were found at Bitou in the water column, apparently healthy areas of the corals, and lesioned areas of corals exhibiting pink discoloration and tissue loss, and there was more carbon source utilization of D-mannitol within the lesioned areas, indicating that the corals may have had greater quantities of *Vibrio* present within the lesions.
6. Tissue loss samples histologically revealed fragmentation and detachment of the gastrodermis and epidermis, presence of extracellular brown granular material and, in some samples, possible ciliates.
7. Color loss samples histologically revealed gastrodermal anomalies including necrosis and sloughing as well as released zooxanthellae.

8. Fifty percent of samples showed gastrodermal anomalies and some of these samples contained bacteria closely related to *Clostridium* spp. and *Vibrio* spp., which have been known to impact the digestive system in other organisms
9. Based on the DGGE analysis, the variety of significant differences between bacterial communities found on corals among sites, types of samples, afflicted taxa, and types of samples indicate that the diversity of microbes far exceeds the limitations of tools and resources currently available to study diseases in marine organisms.

6. References

Aeby, G.S., 2003. Corals in the genus *Porites* are susceptible to infection by a larval trematode. Coral Reefs 22: 216.

Aeby, G.S., 2009. Baseline levels of coral disease in the Northwestern Hawaiian Islands. Coral Health and Disease in the Pacific: Vision for Action, p.168.

Aeby, G. S., G. J. Williams, E. C. Franklin, J. Haapkyla, C. D. Harvell, S. Neale, C. A. Page, L. Raymundo, B. Vargas-Angel, B. L. Willis, T. M. Works, and S. K. Davy, 2011. Growth anomalies on the coral genera *Acropora* and *Porites* are strongly associated with host density and human population size across the Indo-Pacific. PLoS One 6: e16887.

Aeby, G.S., S. Callahan, E.F. Cox, C. Runyon, A. Smith, F.G. Stanton, B. Ushijima and T.M. Work, 2016. Emerging coral diseases in Kāneʻohe Bay, Oahu, Hawaii (USA): two major disease outbreaks of acute *Montipora* white syndrome. Diseases of Aquatic Organisms 119: 189–198.

Ainsworth, T. D. and O. Hoegh-Guldberg, 2009. Bacterial communities closely associated with coral tissues vary under experimental and natural reef conditions and thermal stress. Aquatic Biology 4: 289–296.

Ainsworth, T.D., E.C. Kvennefors, L.L. Blackall, M. Fine and O. Hoegh-Guldberg, 2007. Disease and cell death in white syndrome of acroporid corals on the Great Barrier Reef. Marine Biology 151: 19–29.

Anthony, K., S.R. Connolly, and O. Hoegh-Guldberg, 2007. Bleaching, energetics, and coral mortality risk: Effects of temperature, light, and sediment regime. Limnology and Oceanography 52: 716–726.

Antonius, A., 1981. The "band" diseases in coral reefs. Proceedings of the Fourth International Coral Reef Symposium 2: 7–14.

Antonius, A., 1985. Coral diseases in the Indo-Pacific: a first record. PSZN I: Marine Ecology 6: 197–218.

Antonius, A., 1999. *Halofolliculina corallasia*, a new coral-killing ciliate on Indo-Pacific reefs. Coral Reefs 18: 30.

Arbodela M.D.M. and W. Reichardt, 2008. *Vibrio* sp. causing *Porites* ulecrative white spot disease. Diseases of Aquatic Organisms 90: 93–104.

Bak, R.P.M., 1983. Neoplasia, regeneration and growth in the reef-building coral *Acropora palmata*. Marine Biology 77: 221–227.

Banin, E., T. Israely, A. Kushmaro, Y. Loya, E. Orr and E. Rosenberg, 2000. Penetration of the coral-bleaching bacterium *Vibrio shiloi* into *Oculina patagonica*. Applied Environmental Microbiology 66: 3031–3036.

Becker, C., B.D. Dalziel, M.F. Kersch-Becker, M.G. Park, and M. Mouchka, 2013. Indirect effects of human development along the coast on coral health. Biotropica, 45: 401–407.

Beeden, R., J.A. Maynard, P.A. Marshall, S.F. Heron, and B.L. Willis, 2012. A framework for responding to coral disease outbreaks that facilitates adaptive management. Environmental management 49: 1–13.

Beeden, R., B. Willis, L. Raymundo, et al. 2008. Underwater cards for assessing coral health on Indo-Pacific reefs, Coral Reef Targeted Research and Capacity Building for Management Program, Currie Communications, Melbourne.

Bellantuono, A.J., O. Hoegh-Guldberg and M. Rodriguez-Lanetty, 2011. Resistance to thermal stress in corals without changes in symbiont composition. Proceedings of the Royal Society of London B: Biological Sciences, p.rspb20111780.

Bellwood, D.R., T.P. Hughes, C. Folke, and M. Nyström, 2004. Confronting the coral reef crisis. Nature 429:827–833.

Ben-Haim, Y. and E. Rosenberg, 2002. A novel *Vibrio* sp. pathogen of the coral *Pocillopora damicornis*. Marine Biology 141: 47–55.

Ben-Haim, Y., F.L. Thompson, C.C. Thompson, M.C. Cnockaert, B. Hoste, J. Swings and E. Rosenberg, 2003. *Vibrio coralliilyticus* sp. nov., a temperature-dependent pathogen of the coral *Pocillopora damicornis*. International Journal of Systematic and Evolutionary Microbiology 53:309–315.

Bentis, C.J., L. Kaufman, and S. Golubic, 2000. Endolithic fungi in reef-building corals (Order:Scleractinia) are common, cosmopolitan, and potentially pathogenic. Biological Bulletin (Woods Hole) 198: 254−260.

Benzoni, F., P. Galli, and M. Pichon, 2010. Pink spots on *Porites*: not always a coral disease. Coral Reefs 29:153.

Bettarel, Y., Bouvier, T., Nguyen, H.K. and Thu, P.T., 2015. The versatile nature of coral-associated viruses. Environmental Microbiology 17: 3433−3439.

Biolog, 2004a. MicroLog™ System. Release 4.2. User guide. Biolog Inc., Hayward, CA, USA.

Biolog, 2004b. Tips on running marine microbes on Biolog microplates. Release 4.2. User

guide. Biolog Inc., Hayward, CA, USA.

Borneman, E. H., 2001. Aquarium Corals: Selection, Husbandry, and Natural History. Microcosm Ltd., Charlotte, VT, 463 pp.

Bourne, D., Y. Iida, S. Uthicke and C. Smith-Keune, 2008. Changes in coral-associated microbial communities during a bleaching event. Journal of International Society for Microbial Ecology 2: 350–363.

Bourne, D.G., T.D. Ainsworth, F. J. Pollock and B. L. Willis, 2015b. Towards a better understanding of white syndromes and their causes on Indo-Pacific coral reefs. Coral Reefs 34: 233–242.

Bourne, D.G., T.D. Ainsworth and B.L. Willis, 2015a. White syndromes of Indo-Pacific corals. In Woodley, C.M. et al. (eds), Diseases of Coral. Wiley-Blackwell, Boston, MA. p. 300–315.

Bourne, D.G. and C.B. Munn, 2005. Diversity of bacteria associated with the coral *Pocillopora damicornis* from the Great Barrier Reef. Environmental Microbiology 7: 1162–1174.

Bourne, D.G., M. Garren, T.M. Work, E. Rosenberg, G.W. Smith, and C.D. Harvell, 2009. Microbial disease and the coral holobiont. Trends in Microbiology 17: 554–562.

Boyett, H., D. Bourne, and B. Willis, 2007. Elevated temperature and light enhance progression and spread of black band disease on stag-horn corals of the Great Barrier Reef. Marine Biology 151: 1711–1720.

Breitbart, M., R. Bhagooli, S. Griffin, I. Johnston, and F. Rohwer, 2005. Microbial communities associated with skeletal tumors on *Porites compressa*. FEMS Microbiology Letters 243:431–436.

Brown, B.E. and J.C. Bythell, 2005. Perspectives on mucus secretion in reef corals. Marine Ecology Progress Series 296: 291–309.

Brown, B.E. and R.P. Dunne, 2016. Coral bleaching. In Woodley, C.M. et al. (eds), Diseases of Coral. Wiley-Blackwell, Boston, MA. p. 266–283.

Bruckner, A., 2016. History of coral disease research. In Woodley, C.M. et al. (eds), Diseases of Coral. Wiley-Blackwell, Boston, MA. p. 52–84.

Bruno, J.F. and E.R. Selig, 2007. Regional decline of coral cover in the Indo-Pacific: timing, extent, and subregional comparisons. PLoS One 2: e711.

Budd, A.F., H. Fukami, N.D. Smith, and N. Knowlton, 2012. Taxonomic classification of the reef coral family Mussidae (Cnidaria: Anthozoa: Scleractinia). Zoological Journal of the Linnean Society 166: 465–529.

Bythell, J., O. Pantos, and L. Richardson. 2004. White plague, white band, and other 'white' diseases. In Coral Health and Disease. Loya, Y., and Rosenberg, E. (eds). New York: Springer, pp. 351–365.

Bythell, J.C. and C. Wild, 2011. Biology and ecology of coral mucus release. Journal of Experimental Marine Biology and Ecology 408: 88–93.

Cerenius, L., B.L. Lee, K. Söderhäll, 2008. The proPO-system: pros and cons for its role in invertebrate immunity. Trends in Immunology 29: 263–271.

Chaturvedi, V., A. Bartiss, and B. Wong, 1997. Expression of bacterial mtlD in *Saccharomyces cerevisiae* results in mannitol synthesis and protects a glycerol-deficient mutant from high-salt and oxidative stress. Journal of Bacteriology 179: 157–162.

Chen, S. L., K.F. Yu, Q. Shi, S. Li, R. Wang, and M.X. Zhao, 2007. Distribution and status of scleractinian coral communities in the Daya Bay, Guangdong. Tropical Geography 27: 493–498.

Cheng, Y. and D. Dai, 2009. The infection process of the reef coral *Stylophora pistillata* by the parasitic copepod, *Xarifia obesa*. Coral Reefs 28: 681.

Cheng, Y. and D. Dai, 2010. Endosymbiotic copepods may feed on zooxanthellae from their coral host, *Pocillopora damicornis*. Coral Reefs 29: 13–18.

Cheng, J., B. Thapa and J.J. Confer, 2005. Research note: environmental concern and behaviors among coral reef tourists at Green Island, Taiwan. Tourism in Marine Environments 2: 39–43.

Chimetto, L.A., M. Brocchi, C.C. Thompson, R.C. Martins, H.R. Ramos and F.L. Thompson, 2008. *Vibrios* dominate as culturable nitrogen-fixing bacteria of the Brazilian coral *Mussismilia hispida*. Systematic and Applied Microbiology 31: 312–319.

Chiou, S., J. Kuo, T. Wong, T. Fan, K. Tew and J. Lui, 2010. Analysis of the coral associated bacterial community structures in healthy and diseased corals from off-shore of southern Taiwan. Journal of Environmental Science and Health 45: 408–415.

Closek, C.J., S. Sunagawa, M.K. DeSalvo, Y.M. Piceno, T.Z. DeSantis, E.L. Brodie, M.X. Weber, C.R. Voolstra, G.L. Andersen and M. Medina, 2014. Coral transcriptome and bacterial community profiles reveal distinct Yellow Band Disease states in *Orbicella faveolata*. Journal of International Society for Microbial Ecology 8: 2411–2422.

Coles, S. L., 1994. Extensive coral disease outbreak at Fahl Island Gulf of Oman Indian Ocean. Coral Reefs 13: 242.

Cooney, R.P., O. Pantos, M.D.A. Le Tissier, M.R. Barer, A.G. O'Donnell, and J.C. Bythell, 2002. Characterization of the bacterial consortium associated with black band disease in coral using molecular microbiological techniques. Environmental Microbiology 4:401–413.

Correa, A.M., Welsh, R.M. and Thurber, R.L.V., 2013. Unique nucleocytoplasmic dsDNA and+ ssRNA viruses are associated with the dinoflagellate endosymbionts of corals. ISME Journal 7: 13–27.

Costanza, R., R. dArge, R. de Groot, S. Farber, M. Grasso, B. Hannon, K. Limburg, S. Naeem, R.V. Oneill, J. Paruelo, R.G. Raskin, P. Sutton, and M. van den Belt, 1997. The value of the world's ecosystem services and natural capital. Nature 387: 253–260.

Cróquer, A., C. Bastidas, A. Elliott and M. Sweet, 2013. Bacterial assemblages shifts from healthy to yellow band disease states in the dominant reef coral *Montastraea faveolata*. Environmental Microbiology Reports 5: 90–96.

Dai, C. F., K. Soong, C. A. Chen, T. Y. Fan, H. J. Hsieh, M. S. Jeng, C. H. Chen, and S. Horng, 2004. Status of Coral Reefs of Taiwan. P. 153–164.

Daniels, C. A., Zeifman, A., Heym, K., Ritchie, K. B., Watson, C. A., Berzins, I., and M. Breitbart, 2011. Spatial heterogeneity of bacterial communities in the mucus of *Montastraea annularis*. Marine Ecology Progress Series 46: 29–40.

De Groot, R., L. Brander, S. Van Der Ploeg, R. Costanza, F. Bernard, L. Braat, M. Christie, N. Crossman, A. Ghermandi, L. Hein and S. Hussain, 2012. Global estimates of the value of ecosystems and their services in monetary units. Ecosystem Services 1:50–61.

Domart-Coulon, I. J., N. Traylor- Knowles, E. Peters, D. Elbert, C. A. Downs, K. Price, J. Stubbs, S. McLaughlin, E. Cox, G. Aeby, P. R. Brown and G. K. Ostrander, 2006. Comprehensive characterization of skeletal tissue growth anomalies of the finger corals *Porites compressa*. Coral Reefs 25: 531–543.

Ducklow, H. W. and R. Mitchell, 1979. Bacterial populations and adaptations in the mucus layers on living corals. Limnology and Oceanography 24: 715–725.

Dustan, P., 1977. Vitality of reef coral populations off Key Largo Florida: recruitment and mortality. Environmental Geology 2: 51–58.

Frade, P.R., Schwaninger, V., Glasl, B., Sintes, E., Hill, R.W., Simó, R. and Herndl, G.J., 2016. Dimethylsulfoniopropionate in corals and its interrelations with bacterial assemblages in coral surface mucus. Environmental Chemistry 13: 252–265.

Frette, L., A. Winding, and N. Kroer, 2010. Genetic and metabolic diversity of Arctic bacterioplankton during the post-spring phytoplankton bloom in Disko Bay, western Greenland. Aquatic Microbial Ecology 60: 29–41.

Frias-Lopez, J., Zerkle, A.L., Bonheyo, G.T., and B.W. Fouke, 2002. Partitioning of bacterial communities between seawater and healthy, black band diseased, and dead coral surfaces. Applied and Environmental Microbiology 68: 2214–2228.

Garland, J. L. and A. L. Mills, 1991. Classification and characterization of heterotrophic microbial communities on the basis of patterns of community-level sole-carbon source utilization. Applied and Environmental Microbiology 57: 2351–2359.

Garren, M., L. Raymundo, J. Guest, C. D. Harvell, and F. Azam, 2009. Resilience of coral-associated bacterial communities exposed to fish farm effluent. PLoS One 4: e7319. doi:10.1371/journal.pone.0007319.

Garren M, Son K, Raina J-B, Rusconi R, Menolascina F, Shapiro OH et al., 2014. A bacterial pathogen uses dimethylsulfoniopropionate as a cue to target heat stressed corals. ISME Journal 8: 999–1007.

George, A., 2011. Cataloguing coral diseases and pest in public aquaria. Proquest Theses and Dissertations. 126 pp. http://scholarcommons.usf.edu/etd/3115/

Gil-Agudelo, D. L., C. Myers, G. W. Smith and K. Kim, 2006a. Changes in the microbial communities associated with *Gorgonia ventalina* during *Aspergillosis* infection. Diseases of Aquatic Organisms 69: 89–94.

Gil-Aguedlo, D. L., L. Ali-Hassan, K. Kim and G. W. Smith, 2006b. Characterization of coral surface microbiota using metabolic profiling. Proceedings of the 10th International Coral Reef Symposium 1: 149–152.

Glasl, B., Herndl, G.J. and Frade, P.R., 2016. The microbiome of coral surface mucus has a key role in mediating holobiont health and survival upon disturbance. ISME Journal 10: 2280–2292.

Glynn, P.W., 1991. Coral reef bleaching in the 1980s and possible connections with global warming. Trends of Ecology and Evolution 6:175–179.

Glynn, P. W., 1993. Coral reef bleaching: ecological perspectives. Coral Reefs 12: 1–17.

Glynn, P. W., 1996. Coral reef bleaching: Facts, hypotheses and implications. Global Change Biology 2: 495–509.

Glynn, P.W., E.C. Peters and L. Muscatine, 1985. Coral tissue microstructure and necrosis: relation to catastrophic coral mortality in Panama. Diseases of Aquatic Organisms 1: 29–37.

Goldstein, R.J., 2007. Marine Reef Aquarium Handbook. Barron's Educational Series, Hauppauge, NY, 199 p.

Gu, M., and P.P. Wong, 2008. Coastal zone management focusing on coastal tourism in a transitional period of China. Ocean & Coastal Management 51:1–24.

Haapkylä, J., R. Unsworth, and A. Seymour, 2009. Spatio-temporal coral disease dynamics in the Wakatobi Marine National Park, South-East Sulawesi, Indonesia. Diseases of Aquatic Organisms 87: 105–115.

Hall, I.C., and E. O'Toole, 1935. Intestinal flora in new-born infants. American Journal of Diseases of Children 49: 390–402.

Hallock, P., 2000. Symbiont-bearing foraminifera: harbingers of global changes? Micropaleontology 46: 95–104.

Harvell, D., E. Jordán-Dahlgren, and S. Merkel, 2007. Coral disease, environmental drivers, and the balance between coral and microbial associates. Oceanography 20: 172–195.

Hoegh-Guldberg, O. and Fine, M., 2004. Low temperatures cause coral bleaching. Coral Reefs 23: 444.

Hormansdorfer, S., H. Wentges, K. Neugebaur-Buchler and J. Bauer, 2000. Isolation of *Vibrio alginolyticus* from seawater aquaria. International Journal of Hygiene and Environmental Health 203: 169–175.

Huang, H., D. Wang, C. Hu, and J. Lian, 2009. Current resources of the Xisha Islands, China. South China Sea Institute of Oceanology and Chinese Academy of Science, Guangzhou. Huang, H., C. Zhang, J. Yang, F. You, J. Lian, and Y. Tan. 2011. Scleractinian coral community characteristics in Zhubi coral reef (Nansha Island). Journal of Oceanography in Taiwan Strait 31: 79–84

Huang, L. M., Y. H. Tan, X. Y. Song, X. P. Huang, H. K. Wang, S. Zhang, J. D. Dong, and R. Y. Chen, 2003. The status of the ecological environment and a proposed protection strategy in Sanya Bay, Hainan Island, China. Marine Pollution Bulletin 47:180–186.

Hughes, T.P., A.H. Baird, D.R. Bellwood, M. Card, S.R. Connolly, C. Folke, R. Grosberg, O. Hoegh-Guldberg, J.B.C. Jackson, J. Kleypas, J.M. Lough, P. Marshall, M. Nystrom, S.R. Palumbi, J.M. Pandolfi, B. Rosen, and J. Roughgarden, 2003. Climate change, human impacts and the resilience of coral reefs. Science. 301: 929–933.

Hughes, T.P., H.U.I. Huang and M.A. Young, 2013. The wicked problem of China's disappearing coral reefs. Conservation Biology 27: 261–269.

Humes, A.G., 1985. Cnidarians and copepods: a success story. Transactions of the American Microscopical Society: 313–320.

Hutchings, P.A., and B. L. Wu, 1987. Coral reefs of Hainan Island, South China Sea. Marine Pollution Bulletin 18: 25–26.

Ivanenko, V. N. and A. V. Smurvov, 1996. About finding of bacteria on symbiotic copepod *Scottomyzon gibberum* (Siphonostomatoida: Asterocheridae), a possible transporter of pathogenic microorganisms. Doklady Akademii Nauk 346: 573–575.

Jones, R.J., J. Bowyer, O. Hoegh-Guldberg and L.L. Blackall, 2004. Dynamics of a temperature-related coral disease outbreak. Marine Ecology Progress Series 281: 63–77.

Kaczmarsky, L., 2006. Coral disease dynamics in the central Philippines. Diseases of Aquatic Organisms 69: 9–21.

Kellogg, C. A., Y. M. Piceno, L. M. Tom, T. Z. DeSantis, D. G. Zawada, and G. L. Andersen, 2012. PhyloChip™ microarray comparison of sampling methods used for coral microbial ecology. Journal of Microbiological Methods 88: 103–109.

Kimes, N.E., W.R. Johnson, M. Torralba, K.E. Nelson, E. Weil and P.J. Morris, 2013. The *Montastraea faveolata* microbiome: ecological and temporal influences on a Caribbean reef-building coral in decline. Environmental Microbiology 15: 2082-2094.

Kline, D., N. M. Kuntz, M. Breitbart, N. Knowlton and F. Rohwer, 2006. Role of elevated organic carbon levels and microbial activity in coral mortality. Marine Ecology Progress Series 314: 119–125.

Kooperman, N., E. Ben-Dov, E. Kramasky-Winter, Z. Braak and A. Kushmaro, 2007. Coral mucus-associated bacterial communities from natural and aquarium environments. FEMS Microbiology Letters 276: 106–113.

Korrubel, J. and B. Riegl, 1998. A new coral disease from the southern Arabian Gulf. Coral Reefs 17: 22.

Krediet, C.J., K.B. Ritchie, M. Cohen, E.K. Lipp, K.P. Sutherland and M. Teplitski, 2009. Utilization of mucus from the coral *Acropora palmata* by the pathogen *Serratia marcescens* and by environmental and coral commensal bacteria. Applied and Environmental Microbiology 75:3851–3858.

Kushmaro, A. and E. Kramarsky-Winter, 2004. Bacteria as a source of coral nutrition. Coral Health and Disease. Springer-Verlag, New York, NY, p. 231–241.

Kushmaro, A., Y. Loya, M. Fine and E. Rosenberg, 1996. Bacterial infection and coral bleaching. Nature 380: 396.

Kushmaro, A., E. Rosenberg, M. Fine and Y. Loya, 1997. Bleaching of the coral *Oculina patagonica* by *Vibrio* AK-1. Marine Ecology Progress Series 147: 159–165.

Kushmaro, A., E. Rosenberg, M. Fine, Y. Ben-Haim and Y. Loya, 1998. Effect of temperature on bleaching of the coral *Oculina patagonica* by *Vibrio shiloi* AK-1. Marine Ecology Progress Series 171: 131–137.

Lawrence, S.A., J.E. Davy, W.H. Wilson, O. Hoegh-Guldberg, and S.K. Davy, 2015. *Porites* white patch syndrome: associated viruses and disease physiology. Coral Reefs 34: 249–257.

Lesser M.P., J.C. Bythell, R.D. Gates, R.W. Johnstone, O. Hoegh-Guldberg, 2007. Are infectious diseases really killing corals? Alternative interpretations of the experimental and ecological data. Journal of Experimental Marine Biology and Ecology 346: 36–44.

Li, S., K-F. Yu, Q. Shi, T. Chen, M. Zhao, and J. Zhao, 2008. Interspecies and spatial diversity in the symbiotic zooxanthellae density in corals from northern South China Sea and its relationship to coral reef bleaching. Chinese Science Bulletin 53: 295–303.

Liao, M., S. Tang, C. Hsu, K. Wen, H. Wu, W. Chen, J. Wang, P. Meng, W. Twan, C. Lu, C. Dai, K. Soong and A. Chen, 2007. The "Black Disease" of reef-building corals at Green Island, Taiwan – Outbreak of a Cyanobacteriosponge, *Terpios hosinota* (Suberitidae; Hadromerida). Zoological Studies 46: 520.

Lin, C.H., C.H. Chuang, W.H. Twan, S.F. Chiou, T. Wong, J. Liu and J. Kuo, 2016. Seasonal changes in bacterial communities associated with healthy and diseased *Porites* coral in Southern Taiwan. Canadian Journal of Microbiology.

Liu, R.Y., 1998. The effects of human activities on benthos diversity. Symposium on Coastal Ocean Resources and Environment '97: Proceedings of the Sustainable Consumption Research Exchange '97 (Hong Kong, China, SCORE): 39–46.

Luna, G.M., F. Biavasco, and R. Danovaro, 2010. *Vibrio harveyi* as a causative agent of the White Syndrome in tropical stony corals. Environmental Microbiology 2: 120–127

Makkee, M., A.P.G. Kieboom, and H. Van Bekkum, 1985. Production methods of D-mannitol. Starch 37: 136–141.

Mao-Jones, J., K.B. Ritchie, L.E. Jones, and S.P. Ellner, 2010. How microbial community composition regulates coral disease development. PLoS Biology 8: e1000345.

Meikle, P., G. N. Richards and D. Yellowlees, 1988. Structural investigations on the mucus from six species of coral. Marine Biology 99: 187–193.

Meron, D., E. Atias, L. I. Kruh, H. Elifantz, D. Minz, M. Fine and E. Banin, 2011. The impact of reduced pH on the microbial community of the coral *Acropora eurystoma*. ISME Journal 5: 51–60.

Meyer, J.L., V.J Paul and M. Teplitski, M, 2014. Community shifts in the surface microbiomes of the coral *Porites astreoides* with unusual lesions. PloS One 9: p.e100316.

Miller, A.W. and L.L. Richardson, 2015. Emerging coral diseases: a temperature-driven process? Marine Ecology 36: 278–291.

Miller, J., M.J. Sweet, E. Wood and J. Bythell, 2015. Baseline coral disease surveys within three marine parks in Sabah, Borneo. PeerJ 3: e1391.

Mitchell, R. and I. Chet, 1975. Bacterial attack of corals in polluted water. Microbial Ecology 2: 227–233.

Morton, B., and G. Blackmore, 2001. South China Sea. Marine Pollution Bulletin 42:1236–1263.

Mosby's Medical Dictionary, 2009. Elsevier, Amsterdam, 1998 p .

Muller, E.M. and R.van Woesik, 2012. Caribbean coral diseases: primary transmission or secondary infection? Global Change Biology 18: 3529–3535

Munn, C.B., 2015. The role of *Vibrios* in diseases of corals. Microbiology Spectrum 3: 1–10.

Muscatine, L., P.G. Falkowski, J.W. Porter, and Z. Dubinsky, 1984. Fate of photosynthetic fixed carbon in light-adapted and shade-adapted colonies of the symbiotic coral *Stylophora pistillata*. Proceedings of Royal Society London Series B. Biological Sciences 222: 181–202.

Muyzer G. and K. Smalla. 1998. Application of denaturing gradient gel electrophoresis (DGGE) and temperature gradient gel electrophoresis (TGGE) in microbial ecology. Antonie van Leeuwenhoek 73: 127–141.

Muyzer, G., E. C. D. Waal, and A. G. Uitterlinden, 1993. Profiling of complex microbial populations by denaturing gradient gel electrophoresis analysis of polymerase chain reaction-amplified genes coding for 16S rRNA. Applied and Environmental Microbiology 59: 695–700.

Muyzer, G., A. Teske, C. O. Wirsen, and H. W. Jannasch, 1995. Phylogenetic relationships of *Thiomicrospira* species and their identification in deep-sea hydrothermal vent samples by denaturing gradient gel electrophoresis of 16S rDNA fragments. Archives of Microbiology 164: 165–172.

Myers, J. and L. Raymundo, 2009. Coral disease in Micronesian reefs: a link between disease prevalence and host abundance. Diseases of Aquatic Organisms 87: 97–104.

Nie, B., T. Chen, M. Liang, Y. Wang, J. Zhong, and Y. Zhu, 1997. Relationship between coral growth rate and sea surface temperature in the northern part of South China Sea during the past 100. Science in China Series D: Earth Sciences 40: 173–182.

Ng, J.C., Y. Chan, H.M. Tun, F.C. Leung, P.K. Shin and J.M. Chiu, 2015. Pyrosequencing of the bacteria associated with *Platygyra carnosus* corals with skeletal growth anomalies reveals differences in bacterial community composition in apparently healthy and diseased tissues. Frontiers Microbiology 6: 1142.

Nguyen-Kim, H., Y. Bettarel, T. Bouvier, C. Bouvier, H. Doan-Nhu, L. Nguyen-Ngoc, T. Nguyen-Thanh, H. Tran-Quang and J. Brune, 2015. Coral mucus is a hot spot for viral infections. Applied and Environmental Microbiology 81: 5773–5783.

Nugues, M. M. and R. P. M. Bak, 2009. Brown-band syndrome on feeding scars of the crown-of-thorn starfish *Acanthaster planci*. Coral Reefs 28: 507–510.

Oozaki, E., H. Kato, H. Kita, T. Karasawa, T. Maegawa, Y. Koinov, K. Matsamoto, T. Takada et al, 2004. *Clostridium difficile* colonization in healthy adults: transient colonization and correlation with enterococcal colonization. Journal of Medical Microbiology 53:167–172.

Palmer, C. V., C. K. Modi, and L. D. Mydlarz, 2009a. Coral fluorescent proteins as antioxidants. PLoS ONE 4:e7298 doi: 10.1371/journal.pone.0007298

Palmer, C. V., M. S. Roth, and R. D. Gates, 2009b. Red fluorescent protein responsible for pigmentation in trematode-infected *Porites compressa* tissues. Biological Bulletin 216: 68–74.

Palmer, C.V., J.C. Bythell, and B.L. Willis, 2010. Levels of immunity parameters underpin bleaching and disease susceptibility of reef corals. The FASEB Journal, 24: 1935–1946.

Palmer, C.V., J.C. Bythell, and B.L. Willis, 2011. A comparative study of phenoloxidase activity in diseased and bleached colonies of the coral *Acropora millepora*. Developmental & Comparative Immunology 35: 1098–1101.

Pan, Z. F., Z. C. Huang, S.Z. Yang, Z.C. Xu, L.J. Lao, B.Z. Fu, J.M. Wu, and S.F. Xiong, 1983. Modern coral reefs and environment in Hainan Island and the Xisha Islands. Beijing: Chinese Society for Mineralogy, Petrology and Geochemistry, Summary report on Scientific Investigation of Modern Carbonate Sediment in Hainan Island and Xisha islands. p. 15–26.

Pantos, O., and J.C. Bythell, 2006. Bacterial community structure associated with white band disease in the elkhorn coral *Acropora palmata* determined using culture-independent 16S rRNA techniques. Diseases of Aquatic Organisms 69: 79–88.

Pantos, O., R. P. Cooney, M. D. A. Le Tissier, M. R. Barer, A.G. O'Donnell and J.C. Bythell, 2003. The bacterial ecology of a plague-like disease affecting the Caribbean coral *Montastraea annularis*. Environmental Microbiology 5: 370–382.

Pasquale, V., V.J. Romano, M. Rupnik, S. Dumontet, I. Čižnár, F. Aliberti, F. Mauri, V. Saggiomo, and K. Krovacek, 2011. Isolation and characterization of *Clostridium difficile* from shellfish and marine environments. Folia Microbiologica 56: 431-437.

Patton, J. S., S. Abraham and A. A. Benson, 1977. Lipogenesis in the intact coral *Pocillopora clapitata* and its isolated zooxanthellae: evidence for a light-driven carbon cycle between symbiont and host. Marine Biology 44: 235–247.

Peters, E.C., 2004. Histotechniques and histology of the Anthozoans. Unpublished short course handouts.

Peters, E.C., 2016. Anatomy. In Woodley, C.M. et al. (eds), Diseases of Coral. Wiley-Blackwell, Boston, MA. p. 85–107.

Peters, E.C. and M.E. Pilson, 1985. A comparative study of the effects of sedimentation on symbiotic and asymbiotic colonies of the coral Astrangiadanae Milne Edwards and Haime 1849. Journal of Experimental Marine Biology and Ecology 92: 215–230.

Peters, E.C., J. C. Halas and H. B. McCarty, 1986. Calicoblastic neoplasms in *Acropora palmata*, with a review of reports on anomalies of growth and form in corals. Journal of the National Cancer Institute 76: 895–912.

Pollock, F.J., Morris, P.J., Willis, B.L. and D.G. Bourne, 2011. The urgent need for robust coral disease diagnostics. PLoS Pathology 7: e1002183.

Qui, D., L. Huang, H. Huang, J. Yang, and S. Lin, 2010. Two functionally distinct ciliates dwelling in *Acropora* corals in the South China Sea near Sanya, Hainan Province, China. Applied and Environmental Microbiology 76: 5639–5643.

Randall, C.J., A.G. Jordan-Garza, R. van Woesik, 2015. Ciliates associated with signs of disease on two Caribbean corals. Coral Reefs. 34: 243–247.

Ravindran, J., and C. Raghukumar, 2002. Pink line syndrome (PLS) in the scleractinian coral *Porites lutea*. Coral Reefs 21: 252.

Ravindran, J., C. Raghukumar, and S. Raghukumar, 2001. Fungi in *Porites lutea*: association with healthy and diseased corals. Diseases of Aquatic Organisms 47: 219–228.

Ravindran, J., C. Raghukumar, and B. Manikandan, 2016. Pink-line syndrome. In Woodley, C.M. et al. (eds), Diseases of Coral. Wiley-Blackwell, Boston, MA. p. 391–395.

Raymundo, L., C. Harvell, and T. Reynolds, 2003. *Porites* ulcerative white spot disease: description, prevalence, and host range of a new coral disease affecting Indo-Pacific reefs. Diseases of Aquatic Organisms 56: 95–104.

Raymundo, L.J., C.S. Couch, and C.D. Harvell, 2008. Coral disease handbook: guidelines for assessment, monitoring & management. Coral Reef Targeted Research and Capacity Building for Management Program, Melbourne. p. 122.

Raymundo, L.J., T.M. Work, R. L. Miller and P.L. Lozada-Misa, 2016. Effects of *Coralliophila violacea* on tissue loss in the scleractinian corals Porites spp. depend on host response. Diseases of Aquatic Organisms 119: 75–83.

Richardson, L.L., K.G. Kuta, and S. Schnell, 1997. Ecology of the black band disease microbial consortium. Proceedings from the 8th International Coral Reef Symposium 1:597–600.

Richardson, L. L., 1998. Coral diseases: what is really known? Trends in Ecology and Evolution 13: 438–443.

Richardson, L.L., R. Sekar, J.L. Myers, M. Gantar, J.D. Voss, L. Kaczmarsky, E.R. Remily, G.L. Boyer, and P.V. Zimba, 2007. The presence of the cyanobacterial toxin microcystin in black band disease of corals. FEMS Microbiology Letters 272: 182–187.

Riddle, D., 2010. Aquarium corals: stony coral parasites: part one: copepods, not just red bugs. Advanced Aquarists 9: http://www.advancedaquarist.com/2010/1/corals#section-5.

Riegl, B., 2002. Effects of the 1996 and 1998 positive sea-surface temperature anomolies on corals, coral diseases and fish in the Arabian Gulf (Dubai, UAE). Marine Biology 140: 29–40.

Ritchie, K. B., 2006. Regulation of microbial populations by coral surface mucus and mucus-associated bacteria. Marine Ecology Progress Series 322: 1–14.

Ritchie, K. B. and G. W. Smith, 1995a. Carbon-source utilization of coral-associated marine heterotrophs. Journal of Marine Biotechnology 3:107–109.

Ritchie, K. B. and G. W. Smith, 1995b. Preferential carbon utilization by surface bacterial communities from water mass, normal, and white-band diseased *Acropora cervicornis*. Molecular Marine Biology and Biotechnology 4: 345–352.

Ritchie, K. B. and G. W. Smith, 2004. Microbial communities of coral surface mucopolysaccharide layers. Coral Health and Disease. New York, Springer-Verlag, p. 259–264.

Ritchie, K. B., R.A. Holley, T. McGrath and G. W. Smith, 1996. INT-linked dehydrogenase activity in the surface mucopolysaccharide layers of Bahamian scleractinian corals. Proceedings of the Symposium Natural History Bahamas 6: 18–27.

Rohwer, F., M. Breitbart, J. Jara, F. Azam, and N. Knowlton, 2001. Diversity of bacteria associated with the Caribbean coral *Montastraea franksi*. Coral Reefs 20: 85–91.

Rohwer, F., V. Seguritan, F. Azam and N. Knowlton, 2002. Diversity and distribution of coral-associated bacteria. Marine Ecology Progress Series 243: 1–10.

Rosenberg, E., O. Koren, L. Reshef, R. Efrony and I. Zilber-Rosenberg, 2007. The role of microorganisms in coral health, disease and evolution. Nature Reviews Microbiology 5: 355–362.

Rützler, K. and D. Santavy, 1983. The black band disease of Atlantic reef corals. I. Description of the cyanophyte pathogen. PSZNI: Marine Ecology 4: 301–319.

Ruetzler, K., and K. Muzik, 1993. *Terpios hoshinota*, a new cyanobacteriosponge threatening Pacific reefs. Scientia Marina 57: 395–403.

Sekar, R., D.K. Mills, E.R. Remily, J.D. Voss and L.L. Richardson, 2006. Microbial communities in the surface mucopolysaccharide layer and the black band microbial mat of black band-diseased *Siderastrea siderea*. Applied Environmental Microbiology 72: 5963–5973.

Séré, M.G., P. Chabanet, J. Turquet, J.P. Quod and M.H. Schleyer, 2015. Identification and prevalence of coral diseases on three Western Indian Ocean coral reefs. Diseases of Aquatic Organisms 114: 249–261.

Shi, Q., G.H. Lui, H.Q. Yan, and H.L. Zhang, 2012. Black disease (*Terpios hoshinota*): a probable cause for the rapid coral mortality at the northern reef of Yongxing Island in the South China Sea. AMBIO 41: 446–455.

Smith, D., P. Leary, J. Craggs, J. Bythell and M. Sweet, 2015. Microbial communities associated with healthy and white syndrome-affected *Echinopora lamellosa* in aquaria and experimental treatment with the antibiotic ampicillin. PloS One 10: e0121780.

Snieszko, S.F., 1974. The effects of environmental stress on outbreaks of infectious diseases of fishes. Journal of Fish Biology 6: 197–208.

Soetaert, W., 1990. Production of mannitol with *Leuconostoc mesenteroides*. Mededelingen van de Faculteit Landbouwwetenschappen Rijksuniversiteit Gent 55: 1549–1552.

Soong, K., C. Dai, and C. Lee, 2002. Status of Pratas Atoll in South China Sea. In H. Tsai, (ed.), Proceedings of the 4th Conference on the Protected Areas of East Asia. IUCN/WCPA/EA-4, Taipei. p. 739–742.

Sorokin, Y. I., 1973. On the feeding of some scleractinian corals with bacteria and dissolved organic matter. Limnology and Oceanography 18: 380–385.

Squires, D., 1965. Neoplasia in a coral? Science 148: 503–505.

Stafford-Smith, M.G., 1993. Sediment-rejection efficiency of 22 species of Australian scleractinian corals. Marine Biology 115: 229–243.

Stanić, D., S. Oehrle, M. Gantar, and L.L. Richardson, 2011. Microcystin production and ecological physiology of Caribbean black band disease cyanobacteria. Environmental Microbiology 13: 900–910.

Sudek, M., T.M. Work, G.S. Aeby, and S.K. Davy, 2012. Histological observations in the Hawaiian reef coral, *Porites compressa*, affected by *Porites* bleaching with tissue loss. Journal of Invertebrate Pathology 111:121–125.

Sunagawa, S., T.Z. DeSantis, Y.M. Piceno, E.L. Brodie, M.K. DeSalvo, C.R. Voolstra, E. Weil, G.L. Andersen and M. Medina, 2009. Bacterial diversity and White Plague Disease-associated community changes in the Caribbean coral *Montastraea faveolata*. Journal of International Society for Microbial Ecology 3: 512–521.

Sussman, M., D. Bourne, and B. Willis, 2006. A single cyanobacterial ribotype is associated with both red and black bands on diseased corals from Palau. Diseases of Aquatic Organisms 69: 111–118.

Sussman, M., B.L. Willis, S. Victor and D.G. Bourne, 2008. Coral pathogens identified for white syndrome (WS) epizootics in the Indo-Pacific. PLoS One 3: e2393.

Sutherland, K. P., J. W. Porter and C. Torres, 2004. Disease and immunity in Caribbean and Indo-Pacific zooxanthellate corals. Marine Ecology Progress Series 266: 273–302.

Sweet, M. and J. Bythell, 2012. Ciliate and bacterial communities associated with White Syndrome and Brown Band Disease in reef-building corals. Environmental Microbiology 14: 2184–2199.

Sweet, M. and J. Bythell, 2015. White Syndrome in *Acropora muricata*: Nonspecific bacterial infection and ciliate histophagy. Molecular Ecology 24:1150–1159.

Townend, J., 2002. Practical Statistics for Environmental and Biological Scientists. John Wiley and Sons, New York, NY, 276 pp.

Tribollet, A., 2008. The boring microflora in modern coral reef ecosystems: a review of its roles. In Current Developments in Bioerosion, Wisshak, M. and L. Tapanila (eds.), Springer, Berlin, p. 67–94.

Ulstrup, K. E., M. Ku¨hl and D. G. Bourne, 2007. Zooxanthellae harvested by ciliates associated with brown band syndrome of coral remain photosynthetically competent. Applied Environmental Microbiology 73: 1968–1975.

Upton, S.J. and E.C. Peters, 1986. A new and unusual species of coccidium (Apicomplexa: Agamococcidiorida) from Caribbean scleractinian corals. Journal of Invertebrate Pathology 47: 184–193.

Vadas, R.L., 1979. Abiotic disease in seaweeds: Thermal effluents as causal agents. Cellular and Molecular Life Sciences 35: 435–437.

Vargas-Angel, B., E.C. Peters, E. Kramarsky-Winter, D.S. Gilliam, and R.E. Dodge, 2007. Cellular reactions to sedimentation and temperature stress in the Caribbean coral *Montastraea cavernosa*. Journal of Invertebrate Pathology 95: 140–145.

Walker, D.I. and R.F.G. Ormond, 1982. Coral death from sewage and phosphate pollution at Aqaba, Red Sea. Marine Pollution Bulletin 13: 21–25.

Wang, Y. S., Z. P. Lou, C. C. Sun, M. L. Wu, and S. H. Han, 2006. Multivariate statistical analysis of water quality and phytoplankton characteristics in Daya Bay, China, from 1999 to 2002. Oceanologia 48: 193–211.

Weil, E. and A. J. Hooten, 2008. Underwater Cards for Assessing Coral Health on Caribbean Reefs. Australia, GEF-CRTR-Currie Comm.

Weynberg, K.D., C.R. Voolstra, M.J. Neave, P. Buerger. and M.J. van Oppen, 2015. From cholera to corals: viruses as drivers of virulence in a major coral bacterial pathogen. Scientific Reports 5: 17889.

Williams, G. J., T. M. Work, G. S. Aeby, I. S. Knapp and S. K. Davy, 2011. Gross microscopic morphology of lesions in Cnidaria from Palmyra Atoll, Central Pacific. Journal of Invertebrate Pathology 106: 165–173.

Willis, B. L., C. A. Page and E. A. Dinsdale, 2004. Coral disease on the Great Barrier Reef. In: Rosenberg E, Loya Y (eds), Coral Disease and Health. Springer, Berlin, p. 69–104.

Willis, B. L., C. Page, D. Bourne, L. Owens, S. Anthony, H. Boyett, E. Dinsdale, D. Harvell, D. Jacobson, C. Lonergan, S. Neale, C. Palmer, L. Raymundo, and M. Sussman, 2009. Coral Disease on the Great Barrier Reef and in the Western Pacific. In: Galloway, S.B., Bruckner, A.W. and Woodley, C.M. (eds.), 2009. *Coral Health and Disease in the Pacific: Vision for Action.* NOAA Technical Memorandum NOS NCCOS 97 and CRCP 7 National Oceanic and Atmospheric Administration, Silver Spring, MD. p. 234-241.

Wisselink, H.W., R.A. Weusthuis, G. Eggink, J. Hugenholtz, and G.J. Grobben, 2002. Mannitol production by lactic acid bacteria: a review. International Dairy Journal 12: 151-161.

Work, T. M. and G. S. Aeby, 2006. Systematically describing gross lesions in corals. Diseases of Aquatic Organisms 70: 155–160.

Work, T.M. and G.S. Aeby, 2011. Pathology of tissue loss (white syndrome) in *Acropora* sp. corals from the Central Pacific. Journal of Invertebrate Pathology 107: 127–131.

Work, T. and C. Meteyer, 2014. To understand coral disease, look at coral cells. EcoHealth 11:610–618.

Work, T. M. and R. A. Rameyer, 2005. Characterizing lesions in corals from American Samoa. Coral Reefs 24: 384–390.

Work, T.M., G.S. Aeby and S.L. Coles, 2008. Distribution and morphology of growth anomalies in *Acropora* from the Indo-Pacific. Diseases of Aquatic Organisms 78: 255–264.

Work, T.M., G.S. Aeby, and K.A. Hughen, 2016. Gross and microscopic lesions in corals from Micronesia. Veterinary Pathology 53: 153-162.

Work, T.M., G.S. Aeby, G. Lasne and A. Tribollet, 2014. Gross and microscopic pathology of hard and soft corals in New Caledonia. Journal of Invertebrate Pathology 120:50–58.

Work, T.M., R. Russell and G.S. Aeby, 2012. Tissue loss (white syndrome) in the coral *Montipora capitata* is a dynamic disease with multiple host responses and potential causes. Proceedings of the Royal Society B: rspb20121827.

Yang, R.T. and C.F. Dai, 1980. Community structure and species diversity of reef corals at Nanwan Bay, Taiwan. Acta Oceanographica Taiwanica 11: 238–251.

Yang, H., J. Shen, F. Fu, Y. Wang, and N. Zhao, 2014. Black band disease as a possible factor of the coral decline at the northern reef-flat of Yongxing Island, South China Sea. Science China Earth Sciences 57: 569–578.

Yarden, O., T. D. Ainsworth, G. Roff, W. Leggat, M. Fine and O. Hoegh-Guldberg, 2007. Increased prevalence of ubiquitous ascomycetes in an acroporid coral (*Acropora formosa*) exhibiting symptoms of brown band syndrome and skeletal eroding band. Applied Environmental Microbiology 73: 2755-2757.

Yevich, P. P. and C. A. Barszcz, 1983. Histopathology as a monitor for marine pollution: results of the histopathologic examination of the animals collected for the U.S. 1976 Mussel Watch Program. Rapports et Proces-verbaux des Réunions. Conseil International pour l'Éxploration de la Mer 182: 96–102.

Yu, K-F., J-X. Zhao, M.G. Lawrence, and Y. Feng, 2010. Timing and duration of growth hiatuses in mid Holocene massive *Porites* corals from the northern South China Sea. Journal of Quaternary Science 25: 1284–1292.

Zhang, Q., 2004. Coastal Bio-Geomorphologic Zonation of Coral Reefs and Mangroves and Tide Level Control. Journal of Coastal Research 43: 202–211.

Zhang, Q. M. 2001. On biogeomorphology of Luhuitou fringing reef of Sanya City, Hainan Island, China. Chinese Science Bulletin 46:97–102.

Zhang, Q.M., Q. Shi, G. Chen, T.C.W. Fong, D.C.C. Wong, H. Huang, H.K. Wang, and M.X. Zhao, 2006. Status monitoring and health assessment of Luhuitou fringing reef of Sanya, Hainan, China. China Science Bulletin 51: 81–88.

Zhao, M., K. Yu, Q. Zhang, and Q. Shi. 2008. Spatial pattern of coral diversity in Luhuitou fringing reef Sanya, China. Acta Ecologica Sinica 28:1419–1428.

Zhao, M.X., K.F. Yu, Q.M. Zhang, and Q. Shi, 2010. Long-term dynamics of coral cover in Luhuitou fringing reef, Sanya. Oceanologia et Limnologia Sinica 6: 440–447.

Zhao, M.X., K.F. Yu, Q.M. Zhang, Q. Shi, and G.J. Price, 2012. Long-term decline of a fringing coral reef in the northern South China Sea. Journal of Coastal Research 28: 1088-1099.

Zhenyu, X., K. Shaowen, H. Chaoqun, Z. Zhixiong, W. Shifeng and Z. Yongcan, 2013. First characterization of bacterial pathogen, *Vibrio alginolyticus*, for *Porites andrewsi* white syndrome in the South China Sea. PloS one 8:e75425.

Zou, R. L., S. W. Song, and J. H. Ma, 1975. Hermatypic Scleractinia in Shallow Waters of Hainan Island. Beijing: Science Press, pp. 1–66.

Appendix 1. Ciliates and Their Relationship with Coral Health and Disease

1.5.1 Abstract

In recent years, the prevalence of ciliate-related coral diseases has increased, yet their implications for coral health are typically overshadowed by studies of bacteria as coral pathogens. The purpose of this paper is to review literature documenting coral diseases that are associated with ciliates. Currently, there are four coral diseases in which ciliates are directly implicated: skeletal eroding band disease with the ciliate *Halofolliculina corallasia*, Caribbean ciliate infection with *Halofolliculina* sp., brown band disease with *Philaster guamensis*, and brown jelly disease with *Philaster* sp. (taxonomic assignments vary). Brown jelly syndrome occurs primarily in aquarium settings and may be the same disease as brown band, only manifesting somewhat differently in the absence of natural predators on the ciliates. Environmental factors that appear to influence ciliate prevalence include injury, elevated temperature and proximity to fresh water. Climate change will likely increase ciliate prevalence by increasing stress to the coral hosts.

1.5.2 Introduction

Research on coral disease has primarily focused on microbial diseases with emphasis on bacteria as pathogens (Peters et al. 1983; Ritchie and Smith, 1995; Kellogg et al 2014; Arotsker et al. 2015; Sere et al. 2015). Meiofauna have been implicated in coral disease but have received less attention (Antonius 1999; Haapkyla et al. 2007; Bourne et al. 2008; Rawlinson et al. 2011). Although overshadowed, attention on ciliates, a group of protozoans, has grown in recent years. Ciliates have been implicated in numerous diseases affecting aquatic organisms including

flounder (Harikrishnan et al. 2012), lobster (Acorn et al. 2011), fresh water fish (Dickerson and Clark 1998; Coyne et al. 2011), and river crabs (Jun 2011). Ciliates were first implicated in coral disease in the early 2000s when they were reported to be associated with skeletal eroding band, the first coral disease known to be caused by a protozoan (Antonius and Lipscomb 2001). Since then, ciliates have been directly implicated in a variety of coral syndromes including brown band syndrome (Bourne et al. 2008), brown jelly syndrome (Borneman 2001), Caribbean ciliate infections (Croquer et al. 2006), white syndrome (Work and Aeby 2011), and white band disease (Sweet and Bythell 2012) (Table 1). Excellent images of coral diseases, including those caused by ciliates, can be viewed at http://coraldisease.org/diseases.

The objective of this paper is to provide a review of reports and studies of coral diseases directly related to ciliates, discuss ciliate interactions with other organisms, and summarize the effects of ciliates on coral health and disease. The following questions will be explored: (1) What genera and species of ciliates are implicated in coral disease? (2) Are brown band and brown jelly the same disease? (3) What environmental factors influence ciliate prevalence? (4) Why have ciliate infections become more documented in recent years? (5) How might climate change influence ciliate prevalence?

1.5.3 The Ciliate-Associated Diseases

1.5.3.1 Skeletal Eroding Band Disease

Skeletal eroding band was the first coral disease known to be caused by a protozoan (Antonius 1999; Antonius and Lipscomb 2001). This disease has been noted as being widespread throughout the Indo-Pacific since its discovery in 1988 (Page and Willis 2008). Locations of coral reefs affected by skeletal eroding band include the Red Sea, South Africa and Mauritius in the Indian Ocean, the Great Barrier Reef and the Solitary Islands of Australia, and Pacific Islands

including Papua New Guinea, the Philippines, Palau, and the Marshall Islands (Antonius 1999; Antonius and Lipscomb 2001; Page and Willis 2008; Palmer and Gates 2010; Sere et al. 2015). In 2010, the first report of skeletal eroding band in Hawaii involved colonies of *Montipora capitata* and *Pocillopora* spp. (Palmer and Gates 2010). This disease is most prevalent in corals of the Acroporidae and Pocilloporidae families and has been reported to affect at least 31 species (Willis et al. 2004) and 22 genera (Winkler et al. 2004).

In reports from field surveys, the prevalence of skeletal eroding band compared to other coral diseases has been extremely high (Page and Willis 2008). A 2002-2003 survey showed that it was the most prevalent disease on two of three reefs studied on the Great Barrier Reef, affecting 5.4% of all corals (Willis et al. 2004). Skeletal eroding band was found on up to 38% of corals in Red Sea surveys (Winkler et al. 2004), and accounted for 40–60% of disease cases recorded in each year (2004–2006) in coral disease surveys conducted on the Great Barrier Reef (Page and Willis 2008).

Skeletal eroding band has been characterized as a lesion with a speckled black band (~1–10 cm wide) composed of empty loricae (shell-like housings) of the folliculinid ciliate, *Halofolliculina corallasia* (Winkler et al. 2004). The ciliates disrupt and lyse coral tissues through spinning and secreting chemicals while simultaneously embedding their loricae within the skeletal matrix (Willis et al. 2004). Similar to Caribbean ciliate infection, the clusters of ciliates create the appearance of the band, although the coloration is black. While superficially similar to black-band disease, skeletal eroding band differs because it leaves behind a speckled skeleton with empty black loricae instead of the stark white skeleton found in black band disease.

Skeletal eroding band exhibits a relatively slow progression rate, sometimes as slow as 1 mm per week, in contrast to black band disease, which can progress as rapidly as 1 cm per day

(Rutzler et al. 1983; Antonius and Lipscomb 2001). Skeletal eroding band has also been linked to Caribbean ciliate infection; both infections are occupied by a ciliate from the genus *Halofolliculina*. However, it appears that two different species are responsible (Croquer et al. 2006a; Croquer et al. 2006b).

Yarden et al. (2007) previously noted the prevalence of fungi on *Acropora formosa* exhibiting signs of skeletal eroding band on the Great Barrier Reef. In particular, they found a fungus, *Fusarium* sp., only on *A. formosa* samples exhibiting signs of eroding band disease.

Coral injuries also are often associated with the development of skeletal eroding band. Page and Willis (2008) found that up to 100% of artificially created injuries were colonized within 10 days in two of the three experimental coral species. In some cases, injured corals were colonized by *H. corallasia* in as little as 6 hours! Lamb et al. (2014) found that the prevalence of skeletal eroding band at high-use dive sites was 2-fold greater than at low-use dive sites. Additionally, they found that corals with physical injury were four times more susceptible to skeletal eroding band disease compared to colonies without injury at high-use sites.

1.5.3.2 Caribbean Ciliate Infection

Caribbean ciliate infection was initially characterized in 2006 as a dark band separating healthy tissue on one side from skeleton on the other. Croquer et al. (2006b) found ciliates of the genus*Halofolliculina* infecting 26 species of stony coral from six families (Acroporidae, Agaricidae, Astrocoeniidae, Faviidae, Meandrinidae, and Poritidae). Samples were observed and collected off the coasts of Venezuela, Panama, Mexico, Curacao, and Puerto Rico.

Upon collection, Croquer et al. (2006b) used microscopy to identify the prevalence of ciliates, which were responsible for creating the dark band. This study initially proposed that the

ciliate infection may have originated from an invasion of ciliates from the Indo-Pacific region. However, further examination revealed that Caribbean ciliates and the Indo-Pacific ciliates were two different species (D. Lipscomb et al. unpublished data). At the time of the study, the mechanism of transmission and the rate of tissue mortality could not be determined. The authors suggested that transmission occurs directly through the water column or by direct contact of infected tissue with susceptible colonies. Susceptibility may be linked to the presence of previous injury to the colony.

In 2009, Rodriguez et al. conducted a study on Caribbean ciliate infection affecting *Agaricia tenuifolia* corals in Bocas del Toro, Panama. During their field studies, they found ciliate-infected colonies lost tissue 10 times faster than healthy control colonies, and 84% of healthy colonies recovered from artificial wounds while only 11% ciliate-infected colonies recovered. Proximity to an infected colony was the most important factor affecting host susceptibility. During their laboratory experiments, 86% of healthy colonies became infected by ciliates after 10 days of exposure, 90% of colonies kept in 30°C water became infected while 70% of colonies kept in 26°C water became infected. The number of ciliates increased by 357% after 8 days, and population growth of ciliates was higher in colonies taken at deeper depths than at shallower depths (Rodriguez et al. 2009).

1.5.3.3 Brown Band Disease

Brown band disease was first noted in the northern and southern sectors of the Great Barrier Reef affecting three major coral families: Acroporidae, Pocilloporidae, and Faviidae (Willis et al. 2004; Bourne et al. 2008). Brown band was characterized as a brown zone bordered by healthy coral tissue, leaving behind exposed white skeleton as the band progressed over the colony (Willis et al. 2004). The white zone may be either bleached tissue or denuded

skeleton. The brown coloration in the band is derived from dense populations of ciliates containing zooxanthellae from the coral tissue consumed. The 'brown' coloration can range from brown to white based on the quantity of ciliates present, which has led to ciliates being implicated in the white syndromes (Work and Aeby 2011; Randall et al. 2015; Sweet and Bythell 2015).

Sweet and Bythell (2012) found, when comparing white syndrome and brown band disease on *Acropora* corals from the Great Barrier Reef, that two ciliate morphotypes were consistently present in lesions of both diseases. Both types were identified morphologically and genetically to be closely related to *Philaster digitformis* and *Porpostoma guamensis*; however, the authors propose the proper generic designation should be *Philaster guamensis* not *Porpostoma guamensis*.

It was originally proposed that brown band disease may be caused by the same ciliate that causes brown jelly in aquarium corals, *Helicostoma nonatum* (Borneman 2001; Willis et al. 2004). However, the ciliate responsible for brown band disease has recently been named as *Philaster* (*Porpostoma) guamensis* (Lobban et al. 2011).

Yarden et al. (2007) reported a link between the prevalence of brown band disease and skeletal eroding band with the occurence of fungi. Fungi were isolated from only 12% of healthy samples of *Acropora formosa*, and from more than 63% of *A. formosa* exhibiting disease. The fungi, *Humicola fuscoatra* and *Penicillium citrinum*, were found on *A. formosa* colonies exhibiting signs of brown band disease. It is unclear whether the fungi are beneficial, detrimental, or opportunistic invaders of the diseased area (Yarden et al. 2007). However, the fungal genera present produce a variety of antibacterial, antifungal, antiviral, and antiprotozoan compounds (Maio and Qian 2005; Bhadury et al. 2006). Yarden et al. (2007) suggest that the

fungal species identified in their study may be involved in maintaining an ecological balance within the coral colony.

Coral injuries as a result of predation have also been linked to brown band disease (Nugues and Bak 2009; Nicolet et al. 2013; Katz et al. 2014). Brown band disease was first linked to feeding scars on the coral reefs of Derawan Island, Indonesia, when colonies of *Acropora cyntherea* preyed upon by *Acanthaster planci* (crown-of-thorns starfish) showed a high incidence of brown band disease (Nugues and Bak 2009). Nicolet et al. (2013) found that the feeding of *Drupella* sp. (gastropod) on *Acropora muricata* was a highly effective vector of brown band disease, resulting in the feeding scars of *Drupella* sp. being the origin of brown-band infections on more than 40% of their experimental colonies. Katz et al. (2013) found that the feeding of *Acanthaster planci* on *Acropora hyacinthus* provided an opportunity for *Porpostoma guamense* ciliates to colonize the compromised coral host, proliferate, form brown-band lesions, and ultimately kill the coral host.

1.5.3.4 Brown Jelly Disease

Brown jelly disease is the second most common coral disease within the aquarium trade (Danovaro and Luna 2008). This disease has only been documented in corals kept in aquaria and it is characterized by tissue death associated with a widespread brown mucoid substance (Borneman and Lowrie 2001; Hunt 2008). *Helicostoma nonatum*, a ciliate, is often found within the brown jelly; however, other ciliates such as *Euplotes* spp. have also been observed (Delbeek and Sprung 1994; Hunt 2008). Most reports of brown jelly exist in the grey literature and aquarists hold most of the knowledge about the disease.

Although the name *Helicostoma nonatum* is most often associated with the ciliate pathogen associated with brown jelly disease, there is much confusion as to the identity of the ciliate pathogen. Most of the confusion lies within the nomenclature of *Helicostoma nonatum* and its limited descriptions in the literature. *Porpostoma natatum* is related taxonomically to *H. nonatum* (Kahan et al. 1982; Kuhlman et al. 1996; Song 2000) and has been officially recorded in the Australian Antarctica Data Centre as being synonymous (Sweet et al. 2011). Hummon (2008) considered the proper moniker for *H. nonatum* to be *Paraturbanella stradbroki*. Sweet et al. (2011) suggested, based on a paper from Zhang et al. (2011), that the proper name for the brown-jelly ciliate is *Philaster* sp., which is closely related to *Philaster digitiformis*.

Brown jelly syndrome can infect a wide variety of corals. Stony corals from the genus *Euphyllia* and newly imported, damaged *Goniopora* spp. and *Acropora* spp. are commonly affected (Delbeek and Sprung 1994). This infection often occurs after trauma, such as physical damage, sudden changes in environmental conditions, or stinging by neighboring corals (Hunt 2008). Brown jelly infections are particularly prevalent when aquarium water temperatures exceed 27°C (Delbeek and Sprung 1994).

1.5.3.5 White Syndromes

In recent years, ciliates have been implicated in the white syndromes (Work and Aeby 2011; Sweet and Bythell 2012; Sweet and Bythell 2015; Randall et al. 2015). White syndromes are visibly characterized by an advancing full-depth tissue lesion with a sharp demarcation between apparently normal tissues and the exposed coral exoskeleton (Willis et al. 2004). The term white syndrome (WS) collectively refers to white plague, white band disease (WBD), and other diseases which macroscopically show signs of denuded skeleton (Bythell et al. 2004).

Most recently, ciliate were associated with white syndromes on coral colonies of *Acropora muricata* in Fiji. Bacterial pathogenic candidates were observed; however, in all samples the histophagous ciliate *Philaster lucinda* was found. The ciliate infection is said to be the secondary infection, and only able to take place after the primary infection of bacteria weakens the defenses of the coral host. *Philaster lucinda*, has been consistently observed in all cases of the disease we have investigated to date, including n = 67 cases of WS and n = 36 WBD, in the Indo-Pacific and the Caribbean, respectively (Sweet and Bythell 2012; Sweet et al. 2014; Sweet and Bythell 2015).

1.5.4 Discussion

1.5.4.1 Distribution of Ciliates Infections

To date, ciliate infections in corals have been documented on many coral reefs in both the Indo-Pacific and Atlantic-Caribbean. The most common issue that has been found to promote ciliate diseases in the wild is physical injury. Experimental studies have consistently found higher incidence of ciliate disease in injured corals than in uninjured colonies.

Another trend that has been noted is a source of freshwater near the corals. For example, brown band diseased corals were found in Tumon Bay, Guam, which is subjected to groundwater seepage (Lobban et al. 2011). Many aquaria in the United States use freshwater to make artificial seawater and brown jelly is the second most common disease found in corals kept in aquaria. Only a few aquaria, like the Florida Aquarium and the Waikiki Aquarium, pump in seawater to fill their exhibits (Ringelspaugh, pers. comm.). Many ciliates, in particular ones associated with disease, have been found in freshwater sources (Dickerson and Clark 1998; Coyne et al. 2011; Nematollahi et al. 2014).

Ishida and Ishibashi (2006) found *Helicostoma* (the ciliate implicated in brown jelly syndrome) located in Lake Nakaumi, which is a stratified, brackish-water lake in which has the salinity of its lower and upper layers are about 10‰ and 30‰, respectively (Ishitobi et al. 1993). This indicates that *Helicostoma* can survive in low salinity and may even be able to survive in or have origins in freshwater. Ishida and Ishibashi (2206) also documented that when testing environmental factors (i.e., water temperature, salinity, and pH), salinity showed the strongest influence on the species composition of ciliates.

Freshwater runoff or subsurface intrusion may provide a source of ciliates to coral reefs. Ciliate infections in corals appear to be more prevalent in the Indo-Pacific than in the Atlantic-Caribbean. Interestingly, salinity in much of the Indo-Pacific is typically about 2‰ lower in Pacific waters (Talley, 2002). However, skeletal eroding band has been reported from the Red Sea (Winkler et al. 2004), where salinities exceed 36‰.

1.5.4.2 Brown Band vs. Brown Jelly: The Same Disease?

Because the nomenclature associated with the ciliate found in brown jelly diseased corals has been inconsistent and confusing, it is hard to confirm or dismiss the possibility that brown band and brown jelly may be the same affliction (Sweet et al. 2012). If the ciliates are found to be the same, some researchers may still be skeptical due to the difference in the visibly recognizable signs of each disease. Brown jelly and brown band differ because the former is characterized as an amorphous brown mucoid substance while the latter is characteristically a distinct brown band. One possibility is that the "brown jelly" may result from the accumulation of ciliates and their wastes in the absence of predators of the ciliates, a situation that is likely more common in aquaria than in nature. Because many aquaria rely on exhibit appearance and not what is found in nature (e.g., mixing Indo-Pacific and Atlantic-Caribbean coral species),

many exhibits may lack predators or detritus feeders that would reduce the amorphous brown cluster to a brown band.

1.5.4.3 Ciliates, the Environment, Climate Change and Anthropogenic Impact

Climate change and anthropogenic impacts have long been predicted to increase disease prevalence and an organism's susceptibility to disease (Harvell et al. 2002; Altizer et al. 2013). Corals are more susceptible to ciliate infections when they are stressed, in particular by temperature and injury and possibly by reduced salinity (Croquer et al. 2006; Hughes 1994; Hughes et al. 2003; Santavy et al. 2005; Lamb et al. 2015). Previous studies have also documented that ciliates can become more prevalent in corals that exhibit bleaching or are exposed to eutrophication, which is usually associated with anthropogenically influenced freshwater runoff. (Delbeek and Sprung 1994; Rodriguez et al. 2009; Page and Willis 2008; Katz et al. 2014). Ciliates that ingest coral tissue are very likely opportunistic and therefore tend to increase in prevalence when provided a resource of weakened corals that have limited energy to repair wounds and to regenerate cnidocysts to fend off predation.

Based on the information available, ciliate-associated infections on corals will likely increase with climate change. As the corals are increasingly exposed to environmental stressors, opportunistic ciliates will predictably increase their exploitation of the weakened corals.

1.5.4.4 Future Research

1. To date, most studies of ciliate infection have utilized direct observations. Although each ciliate infection has a likely culprit, none have been tested to satisfy Koch's postulates, the four

criteria established to identify the causative agent of a particular disease. Studies are needed to identify an official causal agent in each ciliate infection.

2. Because ciliate species are difficult to identify microscopically, studies should utilize molecular genetics to identify ciliate species.

3. Studies should examine how climate change and anthropogenic activities affect ciliates and their relationship with coral disease. Such studies should include parameters such as temperature, depth, salinity, nutrient enrichment, and sedimentation.

1.5.5 References

Acorn, A.R., Fraser Clark, K., Jones, S., Després B.M., Munro, S., Cawthorn, R.J., Greenwood, S.J., 2011. Analysis of expressed sequence tags (ESTs) and gene expression changes under different growth conditions for the ciliate *Anophryoides haemophila*, the causative agent of bumper car disease in the American lobster (*Homarus americanus*). J. Invertebr. Pathol. 107, 146–154.

Altizer, S., Ostfeld, R.S., Johnson, P.T., Kutz, S., Harvell, C.D., 2013. Climate change and infectious diseases: from evidence to a predictive framework. Science. 341, 514–519.

Antonius, A., 1999. *Halofolliculina corallasia*, a new coral-killing ciliate on Indo-Pacific reefs. Coral Reefs. 18, 300.

Antonius, A., Lipscomb, D., 2001. First protozoan coral killer identified in the Indo-Pacific. Atoll Res. Bull. 481, 1–23.

Ben-Haim, Y., Rosenberg, E., 2002. A novel *Vibrio* sp pathogen of the coral *Pocillopora damicornis*. Mar. Biol. 141**,** 47–55.

Bhadury, P., Mohammad, B.T., Wright, P.C., 2006. The current status of natural products from marine fungi and their potential as anti-infective agents. J. Ind. Microbiol. Biotechnol. 33, 325–337.

Borneman, E.H., 2001. Aquarium corals: selection, husbandry, and natural history.

Microcosm Ltd., Charlotte, VT.

Borneman, E.H., Lowrie, J., 2001. Advances in captive husbandry and propagation: an easily utilized reef replenishment means from the private sector? Bull. Mar. Sci. 69, 897–913.

Bourne, D.G., Boyett, H.V., Henderson, M.E., Muirhead, A., Willis, B.L., 2008. Identification of a ciliate (Oligohymenophorea:Scuticociliatia) associated with brown band disease on corals of the Great Barrier Reef. Appl. Environ. Microbiol. 74, 883–888.

Coyne, R.S., Hannick, L., Shanmugam, D., Hostetler, J.B., Brami, D., Joardar, V.S., Clark, T.G., 2011. Comparative genomics of the pathogenic ciliate *Ichthyophthirius multifiliis*, its free-living relatives and a host species provide insights into adoption of a parasitic lifestyle and prospects for disease control. Genome Biol. 12, 100.

Croquer, A., Bastidas, C., Lipscomb, D., 2006a. Folliculinid ciliates: a new threat to Caribbean corals? Dis. Aquat. Organ. 69, 75–78.

Croquer, A., Bastidas, C., Lipscomb, D., Rodriguez-Martinez, R.E., Jordan-Dahlgren, E., Guzman, H.M., 2006b. First report of folliculinid ciliates affecting Caribbean scleractinian corals. Coral Reefs. 25, 187–191.

Danovaro, D., Luna, G., 2008. Italian Consortium for Marine Sciences (CoNISMa): Research Unit—Coral Zoo. http://www.coralzoo.org/home/

Delbeek, J.C., Sprung, J., 1994. The reef aquarium. Ricordea Publishing, Miami, FL.

Dickerson, H., Clark, T., 1998. *Ichthyophthirius multifiliis*: a model of cutaneous infection and immunity in fishes. Immunol. Rev. 166, 377–384.

Haapkyla, J., Seymour, A.S., Trebilco, J., Smith, D., 2007. Coral disease prevalence and coral health in the Wakatobi Marine Park, south-east Sulawesi, Indonesia. J. Mar. Biol. Assoc. U.K. 87, 403–414.

Harikrishnan, R., Jin, C.N., Kim, J.S., Balasundaram, C., Heo, M.S., 2012. *Philasterides dicentrarchi*, a histophagous ciliate causing scuticociliatosis in olive flounder, *Philasterides dicentrarch*–Histopathology investigations. Exp. Parasitol. 130, 239–245.

Harvell, C.D., Kim, K., Burkholder, J.M., Colwell, R.R., Epstein, P.R., Grimes, D.J., Hofmann, E.E., Lipp, E.K., Osterhaus, A., Overstreet, R.M., Porter, J.W., Smith, G.W., Vasta, G.R., 1999. Emerging marine diseases: climate links and anthropogenic factors. Science. 285, 1505–1510.

Hughes, T.P., 1994. Catastrophes, phase shifts, and large-scale degradation of a Caribbean coral reef. Science. 265, 1547–1551.

Hughes, T.P., Baird, A.H., Bellwood, D.R., Card, M., Connolly, S.R., Folke, C., Grosberg, R., Hoegh-Guldberg, O., Jackson, J.B.C., Kleypas, J., Lough, J.M., Marshall, P., Nystrom, M., Palumbi, S.R., Pandolfi, J.M., Rosen, B., Roughgarden, J., 2003. Climate change, human impacts and the resilience of coral reefs. Science. 301, 929–933.

Hummon, W., 2008. Biodiversity, morphology and ecology of small benthic organisms. Meiofauna Marina. 16.

Hunt, P., 2008. The marine reef aquarium. Barron's Educational Series, Inc., New York, NY.

Ishida, H., Ishibashi, M., 2006. Seasonal changes in species composition of ciliate in the Lake Nakaumi. J. Protozool. Res. 39, 29–35.

Ishitobi, Y., Kamiya, H., Itogawa, H., 1993. Tidal, meteorological and hydrological effects on the water level variation in a lagoon, Lake Shinji. J. Limnol. 54, 69–79.

Jun, L., 2011. Diagnosis and Treatment Technology of Ciliates in River Crab Aquaculture. Value Engineering. 3, 253.

Kahan, D., Wilbert, N., Vit, G., Barel, T., 1982. Feeding-behaviour of *Porpostoma notatum* (Ciliata). J. Protozool. 29, 535.

Katz, S.M., Pollock, F.J., Bourne, D.G., Willis, B.L., 2014. Crown-of-thorns starfish predation and physical injuries promote brown band disease on corals. Coral Reefs. 33, 705–716.

Kuhlmann, H.W., Braeucker, R., Schepers, A.G., 1996. *Porpostoma notatum*, a marine scuticociliate with a conspicuous organelle, shows phototactic orientation. J. Eukaryot. Microbiol. 43, 15A.

Lamb, J.B., Williamson, D.H., Russ, G.R., Willis, B.L., 2015. Protected areas mitigate diseases of reef-building corals by reducing damage from fishing. Ecology. 96, 2555–2567.

Lamb, J.B., True, J.D., Piromvaragorn, S., Willis, B.L., 2014. Scuba diving damage and intensity of tourist activities increases coral disease prevalence. Biol. Conserv. 178, 88–96.

Lobban, C.S., Raymundo, L., Montagnes, D.J.S., 2011. *Porpostoma guamensis* n. sp., a Philasterine Scuticociliate associated with brown-band disease of corals. J. Eukaryot. Microbiol. 58, 103–113.

Miao, L., Qian, P.Y., 2005. Antagonistic antimicrobial activity of marine fungi and bacteria isolated from marine biofilm and seawaters of Hong Kong. Aquat. Microb. Ecol. 38, 231–238.

Nematollahi, A., Jaberi, S., Helan, J.A., Sheikhzadeh, N., 2014. Histopathological study on parasites in freshwater ornamental fishes in Iran. J. Parasit. Dis. DOI 10.1007/s12639-014-0573-9.

Nicolet, K.J., Hoogenboom, M.O., Gardiner, N.M., Pratchett, M.S., Willis, B.L., 2013. The corallivorous invertebrate *Drupella* aids in transmission of brown band disease on the Great Barrier Reef. Coral Reefs. 32, 585–595.

Nugues, M.M., Bak, R.P.M., 2009. Brown-band syndrome on feeding scars of the crown-of-thorn starfish *Acanthaster planci*. Coral Reefs. 28, 507–510.

Page, C.A., Willis, B.L., 2008. Epidemiology of skeletal eroding band on the Great Barrier Reef and the role of injury in the initiation of this widespread coral disease. Coral Reefs. 27, 257–272.

Palmer, C.V., Gates, R.D., 2010. Skeletal eroding band in Hawaiian corals. Coral Reefs. 29, 469.

Peters, E.C., Oprandy, J.J., Yevich, P.P., 1983. Possible causal agent of white band disease in Caribbean acroporid corals. J. Invertebr. Pathol. 41, 394–396.

Porter, J.W., Dustan, P., Jaap, W.C., Patterson, K.L., Kosmynin, V., Meier, O.W., Patterson, M.E., Parsons, M., 2001. Patterns of spread of coral disease in the Florida Keys. Hydrobiologia. 460, 1–24.

Randall, C.J., Jordan-Garza, A.G., van Woesik, R., 2015. Ciliates associated with signs of disease on two Caribbean corals. Coral Reefs. 34, 243–247.

Rawlinson, K.A., Gillis, J.A., Billings, R.E.J., Borneman, E.H., 2011. Taxonomy and life history of the *Acropora*-eating flatworm *Amakusaplana acroporae* nov. sp. (Polycladida: Prosthiostomidae). Coral Reefs. DOI 10.1007/s00338-011-0745-3.

Ritchie, K.B., Smith, G.W., 1995. Preferential carbon utilization by surface bacterial communities from water mass, normal, and white-band diseased *Acropora cervicornis*. Mol. Mar. Biol. Biotechnol. 4, 345–352.

Rodríguez, S., Cróquer, A., Guzmán, H.M., Bastidas, C., 2009. A mechanism of transmission and factors affecting coral susceptibility to *Halofolliculina* sp. infection. Coral Reefs. 28, 67–77.

Rützler, K., Santavy, D., Antonius, A., 1983. The black band diseases of Atlantic reef corals, III: Distribution, ecology, and development. PSZNI Marine Ecology 4, 329–358

Santavy, D.L., Summers, J.K., Engle, V.D., Harwell, L.C., 2005. The condition of coral reefs in South Florida (2000) using coral disease and bleaching as indicators. Environ. Monit. Assess. 100, 129–152.

Sere, M.G., Tortosa, P., Chabanet, P., Quod, J.P., Sweet, M.J., Schleyer, M.H., 2015. Identification of a bacterial pathogen associated with Porites white patch syndrome in the Western Indian Ocean. Mol. Ecol. 24, 4570–4581.

Song, W.B., 2000. Morphological and taxonomical studies on some marinemscuticociliates from China Sea, with description of two new species, *Philasterides armatalis* sp. n., and *Cyclidium varibonneti* sp. n. (Protozoa: Ciliophora: Scuticociliatida). Acta. Protozool. 39, 295–322.

Sweet, M., Bythell, J., 2012. Ciliate and bacterial communities associated with White Syndrome and Brown Band Disease in reef-building corals. Environ. Microbiol. 14, 2184–2199.

Sweet, M., Bythell, J., 2015. White Syndrome in *Acropora muricata*: Nonspecific bacterial infection and ciliate histophagy. Mol. Ecol. 24, 1150–1159.

Sweet, M., Jones, R., Bythell, J., 2012. Coral diseases in aquaria and in nature. J. Mar. Biol. Assoc. U.K. 92, 791–801.

Talley, L.D., 2002. Salinity Patterns in the Ocean. Enc. Glob. Enviro. Ch. 2, 629–640.

Willis, B., Page, C., Dinsdale, E., 2004. Coral disease on the Great Barrier Reef. In: Rosenberg, E. and Loya, Y. (Ed.), Coral disease and health. Springer-Verlag, Berlin and Heidelberg, pp. 69–104.

Winkler, R., Antonius, A., Renegar, D.A., 2004. The skeleton eroding band disease on coral reefs of Aqaba, Red Sea. Mar. Ecol. 25, 129–144.

Work, T.M., Aeby, G.S., 2011. Pathology of tissue loss (white syndrome) in *Acropora* sp. corals from the Central Pacific. J. Invertebr. Pathol. 107, 127–131.

Yarden, O., Ainsworth, T.D., Roff, G., Leggat, W., Fine, M., Hoegh-Guldberg, O., 2007. Increased prevalence of ubiquitous *Ascomycetes* in an acropoid coral (*Acropora formosa*) exhibiting symptoms of brown band syndrome and skeletal eroding band disease. Appl. Environ. Microbiol. 73, 2755–2757.

Zhang, Q., Miao, M., Struder-Kypke, M.C., Al-Rasheid, K.A.S., Al-Farraj, S.A., Song, W., 2011. Molecular evolution of Cinetochilum and Sathrophilus (Protozoa, Ciliophora, Oligohymenophorea), two genera of ciliates with morphological affinities to scuticociliates. Zoologica Scripta. 40:317–325.

Appendix 2. Complete Table 29

Full Table 29. Pair-wise multivariate analysis of variance (PW_MANOVA) on the basis of Bray-Curtis dissimilarities for bacterial assemblages based on affliction (1=*Porites*, 2=*Millepora*, 3=*Lobophyllia*, 4=*Platygyra*, 5=*Turbinaria*, 6=*Montipora*, 7=*Coeloseris*, 8=*Isopora*, 9=*Cyphastrea*, 10=*Palythoa*, 11=*Stylophora*, 12=*Heliopora*).

```
------------------------------------------------------------
Results of pair-wise comparisons between each factor level:
============================================================
          t:     p:     p_bon: p_ds:  p_holm:
1 vs. 2: 1.4507 0.0300 1.0000 0.8661 1.0000
1 vs. 3: 2.4813 0.0010 0.0660 0.0639 0.0660
1 vs. 4: 0.9935 0.4680 1.0000 1.0000 1.0000
1 vs. 5: 1.3791 0.0470 1.0000 0.9583 1.0000
1 vs. 6: 1.2505 0.0860 1.0000 0.9974 1.0000
1 vs. 7: 1.1988 0.1390 1.0000 0.9999 1.0000
1 vs. 8: 1.1999 0.0650 1.0000 0.9882 1.0000
1 vs. 9: 1.0696 0.3980 1.0000 1.0000 1.0000
1 vs. 10: 1.0831 0.3520 1.0000 1.0000 1.0000
1 vs. 11: 1.5750 0.0050 0.3300 0.2817 0.3100
1 vs. 12: 1.8127 0.0030 0.1980 0.1799 0.1920
2 vs. 3: 4.4467 0.0280 1.0000 0.8465 1.0000
2 vs. 4: 4.5826 0.3130 1.0000 1.0000 1.0000
2 vs. 5: 1.5457 0.0110 0.7260 0.5181 0.6710
2 vs. 6: 1.5076 0.1150 1.0000 0.9997 1.0000
2 vs. 7: 1.5076 0.1120 1.0000 0.9996 1.0000
2 vs. 8: 1.6627 0.3690 1.0000 1.0000 1.0000
2 vs. 9: 3.9050 0.3480 1.0000 1.0000 1.0000
2 vs. 10: 7.4515 0.3240 1.0000 1.0000 1.0000
2 vs. 11: 6.5809 0.3640 1.0000 1.0000 1.0000
2 vs. 12: 1.8998 0.0150 0.9900 0.6312 0.8850
3 vs. 4: 3.2169 0.1190 1.0000 0.9998 1.0000
3 vs. 5: 2.5185 0.0040 0.2640 0.2324 0.2520
3 vs. 6: 2.4649 0.0170 1.0000 0.6775 0.9860
3 vs. 7: 2.4649 0.0120 0.7920 0.5492 0.7200
3 vs. 8: 2.6366 0.0310 1.0000 0.8749 1.0000
3 vs. 9: 4.0871 0.0310 1.0000 0.8749 1.0000
3 vs. 10: 4.6319 0.0290 1.0000 0.8566 1.0000
3 vs. 11: 4.5633 0.0170 1.0000 0.6775 0.9860
3 vs. 12: 2.9278 0.0010 0.0660 0.0639 0.0660
4 vs. 5: 1.0782 0.6890 1.0000 1.0000 1.0000
4 vs. 6: 1.0000 1.0000 1.0000 1.0000 1.0000
4 vs. 7: 1.0000 1.0000 1.0000 1.0000 1.0000
4 vs. 8: 1.0000 1.0000 1.0000 1.0000 1.0000
4 vs. 9: 2.6317 0.3270 1.0000 1.0000 1.0000
4 vs. 10: 12.6886 0.3280 1.0000 1.0000 1.0000
4 vs. 11: 6.9041 0.3400 1.0000 1.0000 1.0000
4 vs. 12: 1.2548 0.2670 1.0000 1.0000 1.0000
```

```
5 vs. 6: 0.8557 0.7180 1.0000 1.0000 1.0000
5 vs. 7: 0.9789 0.3680 1.0000 1.0000 1.0000
5 vs. 8: 1.0890 0.2920 1.0000 1.0000 1.0000
5 vs. 9: 1.4834 0.0720 1.0000 0.9928 1.0000
5 vs. 10: 1.5740 0.0530 1.0000 0.9725 1.0000
5 vs. 11: 1.1520 0.1500 1.0000 1.0000 1.0000
5 vs. 12: 1.0701 0.2200 1.0000 1.0000 1.0000
6 vs. 7: 0.8660 0.7680 1.0000 1.0000 1.0000
6 vs. 8: 1.0000 0.9520 1.0000 1.0000 1.0000
6 vs. 9: 1.4306 0.1020 1.0000 0.9992 1.0000
6 vs. 10: 1.5436 0.0540 1.0000 0.9744 1.0000
6 vs. 11: 1.5305 0.1050 1.0000 0.9993 1.0000
6 vs. 12: 1.4565 0.0650 1.0000 0.9882 1.0000
7 vs. 8: 1.0000 0.3430 1.0000 1.0000 1.0000
7 vs. 9: 1.4306 0.1200 1.0000 0.9998 1.0000
7 vs. 10: 1.5436 0.1000 1.0000 0.9990 1.0000
7 vs. 11: 1.3677 0.1810 1.0000 1.0000 1.0000
7 vs. 12: 1.2217 0.1170 1.0000 0.9997 1.0000
8 vs. 9: 1.5425 0.3220 1.0000 1.0000 1.0000
8 vs. 10: 1.7226 0.3340 1.0000 1.0000 1.0000
8 vs. 11: 1.7006 0.3390 1.0000 1.0000 1.0000
8 vs. 12: 1.4106 0.1040 1.0000 0.9993 1.0000
9 vs. 10: 1.1476 0.2520 1.0000 1.0000 1.0000
9 vs. 11: 4.2328 0.3160 1.0000 1.0000 1.0000
9 vs. 12: 1.8027 0.0280 1.0000 0.8465 1.0000
10 vs. 11: 10.4872 0.1570 1.0000 1.0000 1.0000
10 vs. 12: 1.8272 0.0190 1.0000 0.7181 1.0000
11 vs. 12: 1.2252 0.1100 1.0000 0.9995 1.0000
-------------------------------------------------------------
```

Appendix 3. Figures (A-F) and Tables (A-F)

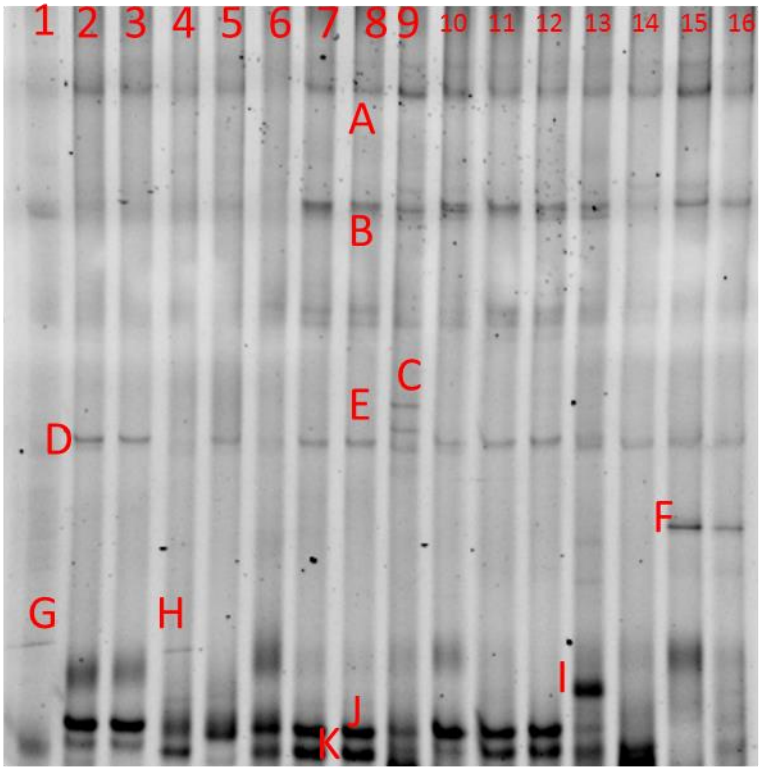

Figure A. Denaturing gradient gel electrophoresis (DGGE) (45-80% gradient at 60° C for 830 minutes with a constant voltage (115V)) profiles of 16S rRNA gene showing that coral associated bacteria vary between coral tissue in an apparently healthy area and abnormal area and their surrounding water column. Lane 1: Bitou water sample. Lane 2 and 3: *Porites* sp. Exhibiting pink discoloration (apparently healthy and abnormal). Lane 4 and 5: *Palythoa* sp. exhibiting a growth anomaly. Lane 6: *Porites* sp. exhibiting pink discoloration (abnormal). Lane 7 and 8: *Porites* sp. Exhibiting tissue loss (apparently healthy and abnormal). Lane 9 and 10: *Stylophora* sp. Exhibiting tissue loss (apparently healthy and abnormal). Lane 11 and 12: *Porite*s sp. Exhibiting pink discoloration (apparently healthy and abnormal). Lane 13 and 14: *Porites* sp. Exhibiting pink discoloration (apparently healthy and abnormal). Lane 15 and 16: *Porites* sp. Exhibiting pink discoloration (apparently healthy and abnormal).

Table A. BLAST analysis of the 16S rRNA bands from Figure A.

Band Letter	Accession no.	Nearest phylogenetic relative	% similarity
A	LN832981.1	Vibrio pelagius partial 16S rRNA gene, isolate 96-274	94
B	KJ577059.1	Vibrio fortis strain H064 16S ribosomal RNA gene, partial sequence	91
C	AF544931.1	Uncultured Firmicutes bacterium clone 1-7-3 16S ribosomal RNA gene, partial sequence	90
D	HQ290092.1	Vibrio sp. GHt1-4 16S ribosomal RNA gene, partial sequence	85
E	GU576953.1	Vibrio sp. SWB9 16S ribosomal RNA gene, complete sequence	76
F	JX844663.1	Bacillus amyloliquefaciens strain DK_TN01 16S ribosomal RNA gene, partial sequence	94
G	FJ002199.1	Minutocellus sp. CCMP1701 16S ribosomal RNA gene, partial sequence; chloroplast	83
H	JF721990.1	Cytophaga sp. HQYD1 16S ribosomal RNA gene, partial sequence	85
I	KT185187.1	Marinifilum sp. R-52652 16S ribosomal RNA gene, partial sequence	97
J	KT626460.1	Vibrio fortis strain PA1 16S ribosomal RNA gene, partial sequence	94
K	HQ662960.1	Alcanivorax sp. ALC-TC3 16S ribosomal RNA gene, partial sequence	84

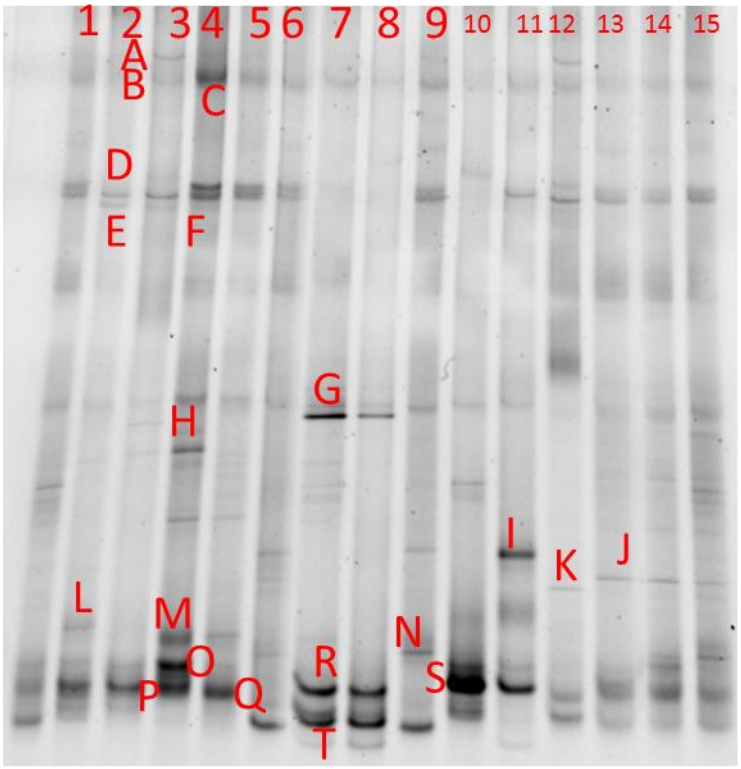

Figure B. Denaturing gradient gel electrophoresis (DGGE) (45-80% gradient at 60° C for 830 minutes with a constant voltage (115V)) profiles of 16S rRNA gene showing that coral associated bacteria vary between coral tissue in an apparently healthy area and abnormal area and their surrounding water column. Lane 1: Shanyuang water sample. Lane 2 and 3: *Montipora* sp. Exhibiting tissue loss (apparently healthy and abnormal). Lane 4 and 5: *Heliopora* sp. Exhibiting color loss (apparently healthy and abnormal). Lane 6: Chaikou water sample. Lane 7 and 8: *Porite*s sp. Exhibiting tissue loss (apparently healthy and abnormal). Lane 9: Gonguan water sample. Lane 10: *Coeloseris* sp. Exhibiting tissue loss (apparently healthy). Lane 11: *Isopora* sp. Exhibiting tissue loss (apparently healthy). Lane 12: *Porite*s sp. Exhibiting pink discoloration (abnormal). Lane 13: Bitou water sample. Lane 14: Yeliu water sample. Lane 15: Kihau water sample.

Table B. BLAST analysis of the 16S rRNA bands from Figure B.

Band Letter	Accession no.	Nearest phylogenetic relative	% similarity
A	HF952772.1	Thermovum composti partial 16S rRNA gene, isolate 16-2-VM-3	87
B	JF344173.1	Uncultured alpha proteobacterium clone PET-049 16S ribosomal RNA gene	87
C	JN679964.1	Uncultured bacterium clone FB2_27 16S ribosomal RNA gene, partial	77
D	JN672323.1	Uncultured bacterium clone GBL1046d01 16S ribosomal RNA gene, partial sequence	88
E	JN672323.1	Uncultured bacterium clone GBL1046d01 16S ribosomal RNA gene, partial sequence	88
F	GU576930.1	Uncultured marine bacterium clone 23-B14 16S ribosomal RNA gene, partial	80
G	FJ930362.1	Uncultured bacterium clone C2D5-2 16S small subunit ribosomal RNA	99
H	KF146466.1	Arenicalla sp.	86
I	JQ516550.1	Sphingobacteriales bacterium clone 0907_Mf_HT3_B34 16S ribosomal RNA gene, partial sequence	96
J	JF948820.1	Uncultured gamma proteobacterium clone Pa26e10 16S ribosomal RNA gene	80
K	CU917964.1	Alpha proteobacterium	91
L	KF146513.1	Thioclava pacifica strain DL5-4 16S ribosomal RNA gene, partial sequence	85
M	JQ347359.1	Uncultured bacterium clone AP67 16S ribosomal RNA gene, partial sequence	95
N	KM520644.1	Uncultured bacterium clone 155S8Bb06U 16S ribosomal RNA gene, partial	80
O	GU576930.1	Uncultured marine bacterium clone 23-B14 16S ribosomal RNA gene, partial	81
P	AM913948.1	Rhodospirillales bacterium L96 partial 16S rRNA gene, isolate L96	89
Q	NR_042903.2	Thalassobius aestuarii strain JC2049 16S ribosomal RNA gene, partial sequence	96
R	AB034902.1	Geobacillus thermoleovorans	86
S	KF180034.1	Uncultured bacterium clone RSAE3C53 16S ribosomal RNA gene, partial sequence	99
T	KT266806.1	Geobacillus thermoparaffinivorans strain TH1 16S ribosomal RNA gene, partial sequence	99

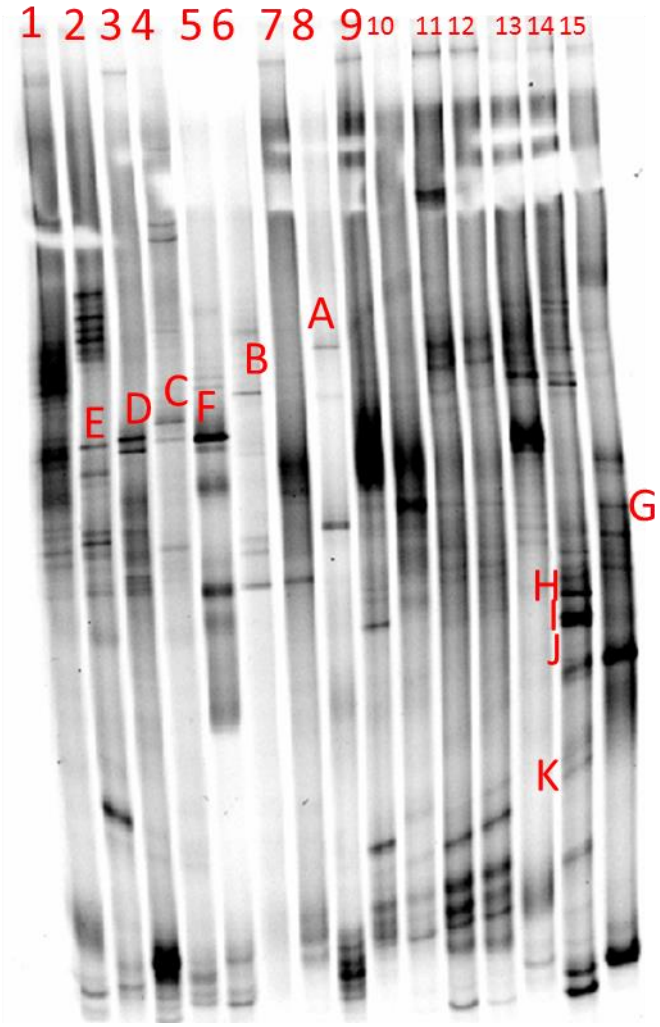

Figure C. Denaturing gradient gel electrophoresis (DGGE) (45-80% gradient at 60° C for 830 minutes with a constant voltage (115V)) profiles of 16S rRNA gene showing that coral associated

bacteria vary between coral tissue in an apparently healthy area and abnormal area and their surrounding water column. Lane 1: Chaikou water sample. Lane 2 and 3: *Montipora* sp. Exhibiting tissue loss (apparently healthy and abnormal). Lane 4 and5: *Coeloseris mayeri* exhibiting color loss (apparently healthy and abnormal). Lane 6: Bitou water sample. Lane 7 and 8: *Porite*s sp. Exhibiting tissue loss (apparently healthy and abnormal). Lane 9 and 10: *Porite*s sp. Exhibiting pink discoloration (apparently healthy and abnormal). Lane 11 and 12: *Porite*s sp. Exhibiting tissue loss (apparently healthy and abnormal). Lane 13: Gonguan water sample. Lane 14 and 15: *Isopora palifera* exhibiting tissue loss (apparently healthy and abnormal).

Table C. BLAST analysis of the 16S rRNA bands from Figure C.

Band Letter	Accession no.	Nearest phylogenetic relative	% similarity
A	HM213005.1	Elphidium albiumbilicatum isolate 10029.87 small subunit ribosomal RNA (SSU) gene, partial sequence; plastid	83
B	GU940749.1	Uncultured bacterium clone N201B_354 16S ribosomal RNA gene, partial sequence	97
C	JF896595.1	Uncultured cyanobacterium isolate DGGE gel band ZNZ-D5 16S ribosomal RNA gene, partial sequence	83
D	GU118822.1	Uncultured bacterium clone Mfra_A03 16S ribosomal RNA gene, partial sequence	99
E	GU118164.1	Uncultured bacterium clone Dstr_N15 16S ribosomal RNA gene, partial sequence	89
F	GU118164.1	Uncultured bacterium clone Dstr_N15 16S ribosomal RNA gene, partial sequence	98
G	EU372890.1	Bacillus sp. CJNY56 16S ribosomal RNA gene, partial sequence	100
H	KJ095000.1	Anoxybacillus flavithermus strain Gecek13 16S ribosomal RNA gene, partial sequence	99
I	AB969726.1	Uncultured gamma proteobacterium gene for 16S ribosomal RNA, partial sequence, clone: TK10S-62	98
J	AB470961.1	Clostridium sp. r53 gene for 16S rRNA, partial sequence	99
K	LN875493.1	Endozoicomonas sp. Acr-14 partial 16S rRNA gene, strain Acr-14, isolate Sea coral	95

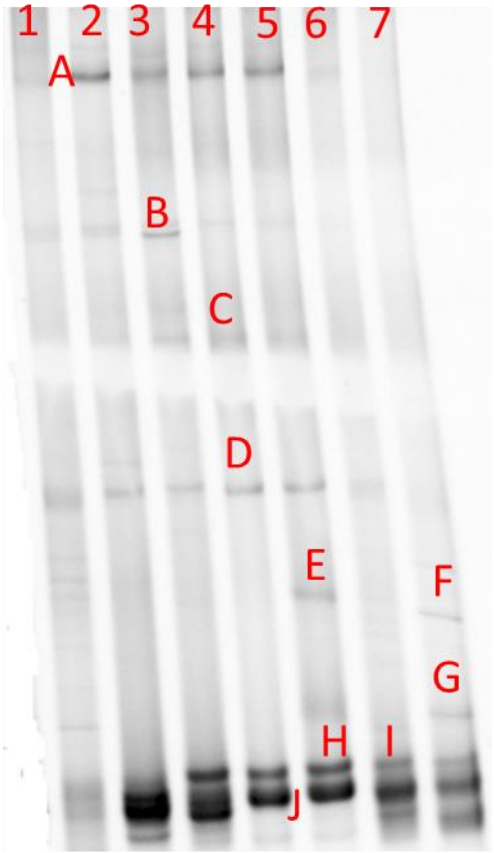

Figure D. Denaturing gradient gel electrophoresis (DGGE) (45-80% gradient at 60° C for 830 minutes with a constant voltage (115V)) profiles of 16S rRNA gene showing that coral associated bacteria vary between coral tissue in an apparently healthy area and abnormal area and their

surrounding water column. Lane 1: Kihau water sample. Lane 2 and 3: *Millepora tenera* exhibiting tissue loss (apparently healthy and abnormal). Lane 4 and 5: *Porites* sp. Exhibiting pink discoloration (apparently healthy and abnormal). Lane 6 and 7: *Porites* sp. Exhibiting pink discoloration (apparently healthy and abnormal). Red letters indicate DGGE bands that have been cut and sent for sequencing.

Table D. BLAST analysis of the 16S rRNA bands from Figure D.

Band Letter	Accession no.	Nearest phylogenetic relative	% similarity
A	KC668734.1	Uncultured bacterium clone P2-F08 16S ribosomal RNA gene, partial sequence	95
B	HQ288601.1	Uncultured bacterium clone H66 16S ribosomal RNA gene, partial sequence	95
C	DQ917857.1	Uncultured Vibrio sp. clone ME2 16S ribosomal RNA gene, partial sequence	88
D	KF180129.1	Uncultured bacterium clone RSAE6C40 16S ribosomal RNA gene, partial sequence	99
E	KC107830.1	Chryseobacterium sp. A5 16S ribosomal RNA gene, partial sequence	90
F	GU119626.1	Uncultured organism clone Dstr_E19 16S ribosomal RNA gene, partial sequence; chloroplast	88
G	FJ205226.1	Uncultured Bacteroidetes bacterium clone A11B 16S ribosomal RNA gene, partial sequence	86
H	JX173559.1	Vibrio pelagius strain ZR035 16S ribosomal RNA gene, partial sequence	97
I	JN675194.1	Uncultured bacterium clone B1_19 16S ribosomal RNA gene, partial sequence	92
J	KF180115.1	Uncultured bacterium clone RSAE6C25 16S ribosomal RNA gene, partial sequence	99

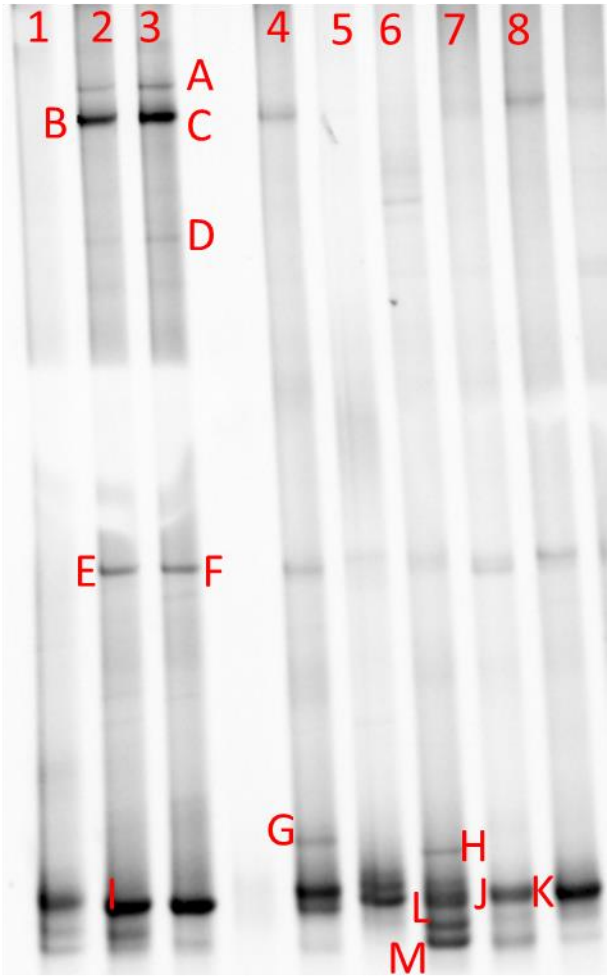

Figure E. Denaturing gradient gel electrophoresis (DGGE) (45-80% gradient at 60° C for 830 minutes with a constant voltage (115V)) profiles of 16S rRNA gene showing that coral associated

bacteria vary between coral tissue in an apparently healthy area and abnormal area and their surrounding water column. Lane 1: Luhuitou water sample. Lane 2 and 3: *Porites* sp. Exhibiting pink discoloration (apparently healthy and abnormal) Lane 4: *Turbinaria* sp. (abnormal from a colony exhibiting tissue loss). Lane 5: *Porites* sp. (abnormal from a colony exhibiting tissue loss). Lane 6 and 7: *Porite*s sp. Exhibiting tissue loss (apparently healthy and abnormal). Lane 8: *Porite*s sp. Exhibiting tissue loss (abnormal).

Table E. BLAST analysis of the 16S rRNA bands from Figure E.

Band Letter	Accession no.	Nearest phylogenetic relative	% similarity
A	KF180115.1	Uncultured bacterium clone RSAE6C25 16S ribosomal RNA gene, partial sequence	100
B	KF180115.1	Uncultured bacterium clone RSAE6C25 16S ribosomal RNA gene, partial sequence	99
C	KF180115.1	Uncultured bacterium clone RSAE6C25 16S ribosomal RNA gene, partial sequence	99
D	KF180115.1	Uncultured bacterium clone RSAE6C25 16S ribosomal RNA gene, partial sequence	99
E	KF180115.1	Uncultured bacterium clone RSAE6C25 16S ribosomal RNA gene, partial sequence	99
F	KF180115.1	Uncultured bacterium clone RSAE6C25 16S ribosomal RNA gene, partial sequence	100
G	KF180034.1	Uncultured bacterium clone RSAE3C53 16S ribosomal RNA gene, partial	93
H	LN823958.1	Rhizobium sp. RhS-3 partial 16S rRNA gene, strain RhS-3	86
I	KF180115.1	Uncultured bacterium clone RSAE6C25 16S ribosomal RNA gene, partial sequence	97
J	KF282423.1	Rhodobacteraceae bacterium GUDS980 16S ribosomal RNA gene, partial sequence	99
K	KF180129.1	Uncultured bacterium clone RSAE6C40 16S ribosomal RNA gene, partial sequence	95
L	HQ754673.1	Uncultured organism clone ELU0036-T191-S-NIPCRAMgANb_000092 small subunit ribosomal RNA gene, partial sequence	97
M	HQ754673.1	Uncultured organism clone ELU0036-T191-S-NIPCRAMgANb_000092 small subunit ribosomal RNA gene, partial sequence	100

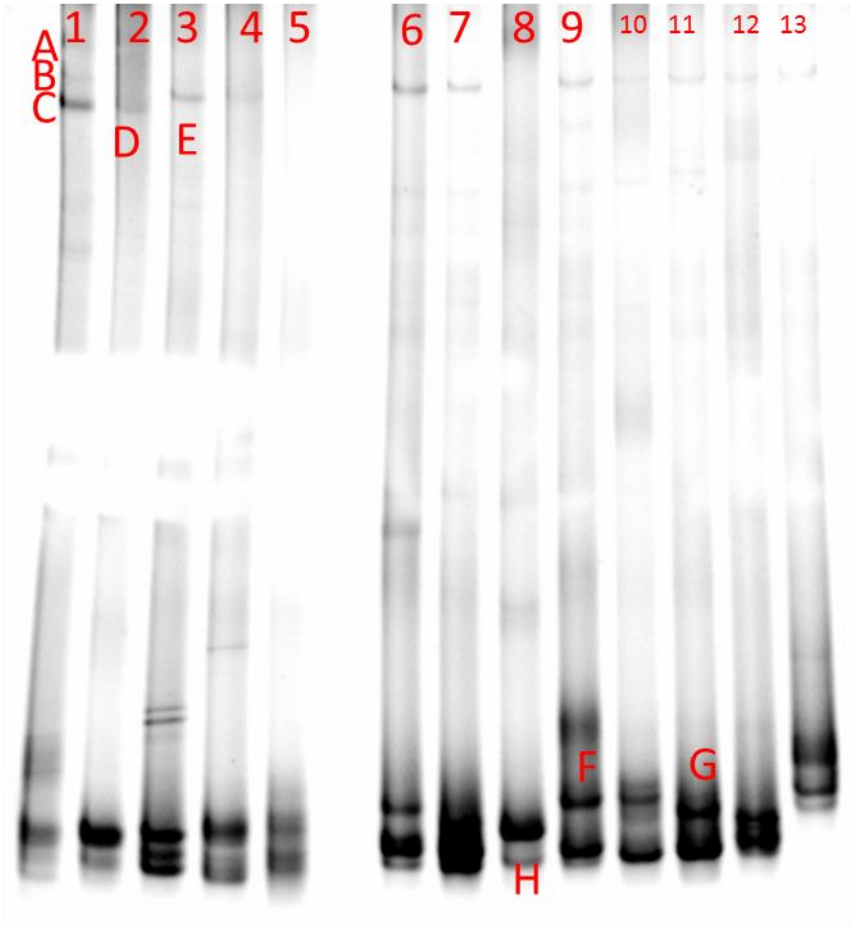

Figure F. Denaturing gradient gel electrophoresis (DGGE) (45-80% gradient at 60° C for 830 minutes with a constant voltage (115V)) profiles of 16S rRNA gene showing that coral associated bacteria vary between coral tissue in an apparently healthy area and abnormal area and their surrounding water column. Lane 1: Xiaodonghai water sample. Lane 2 and 3: *Porites* sp. Exhibiting color loss (apparently healthy and abnormal). Lane 4 and 5: *Lobophyllia* sp. exhibiting tissue loss. Lane 6: *Porites* sp. exhibiting pink discoloration (abnormal). Lane 6: *Platygyra* sp. Exhibiting color loss (abnormal). Lane 7 and 8: *Platygyra* sp. Exhibiting color loss (apparently healthy and abnormal). Lane 9 and 10: *Platygyra* sp. Exhibiting color loss (apparently healthy and abnormal). Lane 11 and 12: *Platygyra* sp. Exhibiting color loss (apparently healthy and abnormal). Lane 13: *Platygyra* sp. Exhibiting color loss (abnormal).

Table F. BLAST analysis of the 16S rRNA bands from Figure F.

Band Letter	Accession no.	Nearest phylogenetic relative	% similarity
A	KF036053.1	Uncultured bacterium clone MWL-62 16S ribosomal RNA gene, partial sequence	86
B	KF373144.1	Uncultured bacterium clone SPHAL-26 16S ribosomal RNA gene, partial sequence	93
C	KF373144.1	Uncultured bacterium clone SPHAL-26 16S ribosomal RNA gene, partial sequence	99
D	HE574879.1	Uncultured bacterium partial 16S rRNA gene, clone ANGII_5	98
E	KP100327.1	Bacillus sp. VITPGPR01 16S ribosomal RNA gene, partial sequence	94
F	KP844953.1	Neisseria sp. HMSC06F02 clone WUSC-06_f02_2 16S ribosomal RNA gene, partial sequence	100
G	KP975317.1	Uncultured bacterium clone OTU61 16S ribosomal RNA gene, partial sequence	100
H	HM598135.1	Uncultured bacterium clone SCS_HX21_57 16S ribosomal RNA gene, partial sequence	78